

# A Deffuant–Weisbuch Model of Opinion Dynamics with Adaptive Confidence Bounds

Max Collins

*Department of Mathematics, Harvey Mudd College, Claremont, California 91711, USA*

Zhuying Gong

*Department of Mathematics, University of California, Los Angeles, California 90095, USA*

Arie Ogranovich

*Department of Mathematics, Rice University, Houston, Texas 77005, USA*

Nicholas White

*Department of Mathematics, University of Nebraska-Lincoln, Lincoln, Nebraska 68588, USA*

Mentors: Sarah Tymochko and Mason A. Porter

*Department of Mathematics, University of California, Los Angeles, California 90095, USA*

(Dated: August 11, 2023)

Agent-based models of opinion dynamics have enabled researchers to examine how opinions spread and interact on a network. One popular agent-based model is the Deffuant–Weisbuch (DW) bounded-confidence model (BCM), in which two neighboring agents update their opinion at each discrete time step if the opinions of the two agents are sufficiently close to each other. Researchers have also developed mean-field equations to approximate the agent-based DW models on an infinite-size network. The standard DW model fixes a specific confidence bound for all agents; however, in real life, people with different opinions tend to possess different amounts of tolerance towards opinions that differ from theirs. One can imagine that individuals with extreme opinions tend to listen less to others, while people with moderate opinions may be more open-minded and willing to accept different opinions. To explore this possibility, we incorporate an adaptive confidence bound into the standard DW model. In our model, each agent’s willingness to listen to others is a function of its current opinion. We call such a function a “confidence-bound function.” We prove that our DW model with adaptive confidence bounds reaches a limit state in 3 cases, and we simulate both agent-based and mean-field dynamics with our model for various graphs and confidence-bound functions. In our agent-based simulations, we explore how changes in one or two parameters affect a limit state’s behavior and how long it takes the model to terminate. For our mean-field approximation, we adapt an partial integro-differential equation from Fennell et al. [1] and solve for the density function that approximates the agent-based density distribution in the opinion space at different time steps.

## I. INTRODUCTION

Living in a world with a plethora of information, individuals in a social network often update their opinions while interacting with the world. In reality, an individual’s opinion is difficult to model, as it can change based on new information, media sources, one’s emotions, family and friends, and many other factors. Using a network, we are able to simplify the situation and simulate how agents communicate with one another, assuming one’s opinion only changes based on interactions.

In light of this, there is growing interest in mathematical models that study opinion dynamics on networks [2–4]. Some key components of opinion dynamics include opinion spaces, opinion update rule, network, agents (i.e. nodes), connections (i.e. edges), and time [4]. Opinion spaces can be discrete or continuous. For continuous opinion spaces in one dimension, one can represent them with an interval, such as  $[0, 1]$ . Opinion update rules define how agents’ opinions change when they interact. Time can be discrete or contin-

uous, but we will focus on discrete time steps in this paper.

One class of opinion dynamics models are bounded-confidence models (BCMs), which incorporate the idea that agents may only be willing to change their opinion when interacting with another agent who has a sufficiently similar opinion [5]. This is done by incorporating the concept of a confidence bound. Assuming the opinion space is a one-dimensional interval, a confidence bound gives an agent an interval that any other agents they interact with must fall into in order for the agent to update its opinion. Within this class of models, there are many choices to be made about how the agents in the model update. For example, a confidence bound can be symmetric or asymmetric. In the symmetric case, the confidence interval is centered around the opinion. In the asymmetric case, the confidence interval of an agent may not be centered around its opinion. A confidence bound can also be homogeneous or heterogeneous. In the homogeneous case, all agents have the same size confidence bound. In the heterogeneous case, they have intervals of the same or different sizes. Another choice to be made is if agents will

take all of their neighbors into consideration during their update (synchronous) or if at each time step, one pair of agents with an edge between them uses each other to update (asynchronous). These choices are reflected in two popular variants of BCM models: the Hegelman–Krauss (HK) model updates synchronously [6] and the Deffaunt–Weisbuch (DW) model updates asynchronously [7]. While many researchers have considered homogeneous and heterogeneous confidence bounds, less research has involved opinion-dependent confidence bounds [8–11].

In this paper, we focus on incorporating confidence-bound functions that depends on agents’ opinions. Through our theoretical and numerical results, we explore the effect of different confidence-bound functions on the final limit state of opinion dynamics and convergence time.

### A. Prior Work

Some existing work has incorporated heterogeneous and adaptive confidence bounds into BCMs.

#### 1. Changes to Confidence Bounds

Adaptive confidence bounds were considered in Li et al. [12]. Li et al. extend the HK and DW models such that the confidence bounds are defined to exist between each pair of agents and to update with interactions between that pair of agents. They prove limiting behavior of these adaptive confidence-bound functions and numerically explored the limit state behavior of their model.

The idea of a heterogeneous confidence bound was first considered in Lorenz [8]. In this model, agents are assigned their own confidence bound from an arbitrary distribution before the updates begin. Lorenz demonstrated numerically that heterogeneity in confidence bounds can help a population achieve consensus. Moreover, Lorenz showed that populations can drift to the extremes of the opinion space with low numbers of initial extreme agents. Chen et al. [10] proved that the heterogeneous DW model reaches a limit state with high probability for certain compromise parameter values. The addition of media influence to the heterogeneous DW model is considered in Pineda et al. [9]. They showed that in the presence of media, the limit state behavior is very sensitive to the initial conditions of the model.

#### 2. Changes to the Compromise Parameter

Another relevant extension of the DW model is the introduction of compromise function, such as the sigmoidal compromise function considered in Brooks et al. [13] and the relative agreement model proposed in Deffaunt [14] where agents update both their opinions and their compromise parameter at the same time step. Adaptivity can also be in-

corporated into the network structure, as is done in Kozma et al. [15]. In this model, if a pair of agents in a randomly chosen edge have opinions outside of each other’s confidence bound, then their edge is broken with some probability. Otherwise, the agents update their opinions. They demonstrate numerically that fragmentation and consensus occur for a small range of confidence bound values than the standard DW model.

#### 3. Mean-Field Theories

Many tools employed in the study of homogeneous DW are also relevant to our model. Specifically, mean-field theories are useful to analyze the DW model when the size of a network tends to infinity. In Fennell et al. [1], a mean-field theory is developed for networks where one can partition the network into classes. They develop a degree-based mean-field theory and a more general class-based mean-field theory.

### B. Our Contribution

In this paper, we present a new adaptive-confidence model in which an agent’s confidence bound is a function of its current opinion. We start by introducing background information on networks and BCMs in Section II. We then introduce our model in Section III. In Section IV, we provide theoretical results proving existence of limiting behavior for our model under certain conditions regarding graph topology and properties of the confidence-bound function (see Section III). In Section V, we present numerical evidence that supports the existence of a limit state. In addition, we present the results of simulations on a range of networks with various confidence-bound functions. In Section VII, we adapt the degree-based mean-field model from [1] to our model. Through agent-based and mean-fields simulations, we demonstrate the behavior of our adaptive-confidence model.

## II. BACKGROUND

### A. Networks

A network (i.e., a graph) is a set of vertices (i.e., nodes) and a set of edges that connect the nodes. One can define a graph  $G = (V, E)$ , where  $V$  is a set of nodes and  $E$  is a set of edges. There are undirected and directed graphs. In undirected graphs, an edge  $\{x, y\}$ , between node  $x$  and node  $y$ , is the same as  $\{y, x\}$ . In directed graphs, however, edges are ordered pairs. Therefore, an edge  $(x, y)$  from  $x$  to  $y$  is not equivalent to the edge  $(y, x)$  from  $y$  to  $x$ . Throughout this paper, we will use the terms network and graph interchangeably, and assume all graphs are undirected unless stated otherwise.

We say that a directed graph  $G = (V, E)$  is weakly connected if, for any nontrivial partition  $\{H, V \setminus H\}$  of  $V$ , there exists a directed edge in  $E$  either from  $H$  to  $V \setminus H$  or vice versa.

### B. The Standard DW Model

The standard DW model is an asynchronous BCM with a continuous opinion space where the population is homogeneous in confidence bound [7]. The standard setting involves a graph  $G = (V, E)$ . For a node  $i \in V$ , we denote the opinion of node  $i$  as  $x_i$  and denote the vector of opinions of all agents at time  $t$  as  $\mathbf{x}(t) = [x_1(t), x_2(t), \dots, x_N(t)]$ . We assign all opinions uniformly at random from an opinion space  $[0, 1]$ . Equations (1) and (2) are a mathematical representation of the update rule.

$$x_i(t+1) = \begin{cases} x_i(t) + \mu\Delta_{ji}(t), & \text{if } |\Delta_{ij}(t)| < c \\ x_i(t), & \text{otherwise,} \end{cases} \quad (1)$$

$$x_j(t+1) = \begin{cases} x_j(t) + \mu\Delta_{ij}(t), & \text{if } |\Delta_{ij}(t)| < c \\ x_j(t), & \text{otherwise,} \end{cases} \quad (2)$$

where  $c \in [0, 1]$  is the confidence bound,  $\mu \in (0, 1)$  the compromise parameter, and  $\Delta_{ij} = x_i - x_j$  is the discordance between agents  $i$  and  $j$ . At each time step  $t$ , we uniformly randomly selects an edge from the network. If the pair of nodes in the selected edge have opinions whose difference is less than the confidence bound, the agents update their opinion by the product of the compromise parameter and the discordance. We could equivalently check that each agent is within the *confidence interval* of the other, that is  $j \in [x_i(t) - c, x_i(t) + c]$  and  $i \in [x_j(t) - c, x_j(t) + c]$ . For  $\mu > 0.5$ , agents  $i$  and  $j$  over-compromise; the standard choice of  $\mu$  is in the range  $(0, 0.5]$ .

### III. OUR MODEL

Suppose that an agent's opinion influences its openness to consider opinions that differ from its own. This relaxation allows flexibility in the model and a feedback loop between an individual's opinion and their willingness to listen.

To incorporate this idea into the DW model, we propose the following model. Consider a graph  $G = (V, E)$ . We assign each agent an opinion randomly from some distribution. In the numerical section, we will consider only a uniform distribution for assigning initial opinions. However, for the analysis in the limit states section, we will need to consider arbitrary initial distributions. Once the opinions are assigned, each agent's confidence bound is determined by a function  $c(x_i) : [0, 1] \rightarrow [0, 1]$ , which we call a *confidence-bound function*. The confidence-bound function maps the

opinion of an agent to a confidence bound. The update rule then becomes

$$x_i(t+1) = \begin{cases} x_i(t) + \mu\Delta_{ji}(t), & \text{if } |\Delta_{ij}(t)| < c(x_i(t)) \\ x_i(t), & \text{otherwise,} \end{cases} \quad (3)$$

$$x_j(t+1) = \begin{cases} x_j(t) + \mu\Delta_{ij}(t), & \text{if } |\Delta_{ij}(t)| < c(x_j(t)) \\ x_j(t), & \text{otherwise,} \end{cases} \quad (4)$$

where  $\mu \in (0, 1)$  and  $\Delta_{ij} = x_i - x_j$  are defined as in the standard DW model. At each time step, we select an edge  $e = \{i, j\}$  uniformly at random from  $E$ . As with the standard DW, we then check that agent  $j$  holds an opinion that is within agent  $i$ 's confidence interval and update the opinion of node  $i$  according to Equation (3). We then repeat the process for  $j$ , while checking if  $i$  has an opinion within the confidence interval of  $j$  and update the opinion of node  $j$  according to Equation (4). If the opinion of an agent has been updated, the confidence bound of the agent also changes.

In our model our opinion updates are not necessarily symmetric. We define an asymmetric update as an update where only one of the following occur:  $x_i(t) \neq x_i(t+1)$  or  $x_j(t) \neq x_j(t+1)$ . We define a symmetric update as an update where both  $x_i(t) \neq x_i(t+1)$  and  $x_j(t) \neq x_j(t+1)$  occur. We define the effective digraph  $G_{\text{eff}} = (V, E')$  as:

$$(i, j) \in E' \text{ if } \{i, j\} \in E \text{ and } |\Delta_{ij}| < c(x_j).$$

That is, the effective digraph contains an edge  $(i, j)$  if and only if node  $i$  can influence node  $j$ . In other words,  $(t) = (V, E_{\text{eff}}(t))$ , where  $E_{\text{eff}}(t) \subseteq E$  and for all  $i, j \in V$ . Note as well that

$$(i, j) \in E_{\text{eff}}(t) \Leftrightarrow |x_i(t) - x_j(t)| < c(x_i(t)) \text{ and } \{i, j\} \in E.$$

A cluster is then defined as a strongly connected component in  $G_{\text{eff}}$ .

More explicitly, we define our model as the following:

**Definition III.1.** Consider a graph  $G = (V, E)$  with  $n$  nodes, a confidence-bound function  $c : [0, 1] \rightarrow [0, 1]$ , and a convergence parameter  $\mu$ . For any  $i \in V$  and any non-negative integer  $t \in \mathbb{Z}_{\geq 0}$ , let  $x_i(t)$  denote the opinion of node  $i$  at time  $t$ . In addition, let  $\mathbf{x}(t) = (x_1(t), x_2(t), \dots, x_n(t))$  denote the vector of all opinions at time  $t$ . Finally, let  $D$  denote a probability distribution on the space  $[0, 1]^n$  of possible opinion vectors.

The adaptive-confidence DW model is defined as the following stochastic process: we randomly sample  $\mathbf{x}(0)$  from  $D$ , i.e.  $\mathbf{x}(0) \sim D$ . For any  $t \in \mathbb{Z}_{\geq 0}$ , at time  $t+1$ , an edge  $(i, j) \in E$  is selected uniformly at random, after which nodes  $i$  and  $j$  update their opinions according to Equation (3) and Equation (4).

#### IV. LIMIT STATES

In studying models of opinion dynamics, the limiting behavior of the model gives a great deal of parsable information such as whether or not the network reaches consensus or fragments into multiple opinion clusters. For many models in opinion dynamics, Lorenz [16] proved results that guarantee existence of a limit state for the model, including the standard DW model. For our adaptive DW model, we cannot use this result given the presence of asymmetric updates which breaks assumption (2) in Theorem (2) of [16].

In this section, we present results guaranteeing limiting behavior for certain cases of confidence functions for our adaptive DW model. However, we cannot guarantee existence of a limit state for general  $c(x)$ . Consider the confidence function:

$$c(x) = \begin{cases} 0, & \text{if } x \in \{0, 1\} \\ 1, & \text{otherwise.} \end{cases}$$

Let  $G$  be a complete graph with 3 nodes, with  $\mathbf{x}(0) = [0, 0.5, 1]$ . For these initial conditions we have  $P(\lim_{t \rightarrow \infty} \mathbf{x}(t) \text{ does not exist}) = 1$ .

We will present results for both complete graphs and for general graph topologies. For complete graphs, we guarantee existence of a limit state almost surely for any confidence function with  $c(x) > \frac{1}{2+\mu}$ . For general graph topologies, we guarantee existence of a limit state for monotone confidence functions and almost surely guarantee a limit state for confidence functions with  $\inf_{x \in [0, 1]} c(x) > 0$  and either  $x - c(x)$  or  $x + c(x)$  nondecreasing. We begin with some definitions.

**Definition IV.1.** For fixed graph topology,  $\mu$ ,  $c$ , and initial opinions  $\mathbf{x}$ , and edge choices, we say the adaptive DW model, on a graph with  $N$  nodes, **converges to a limit state** if

$$\text{there exists } \mathbf{x}^* \in [0, 1]^N \text{ such that } \lim_{t \rightarrow \infty} \mathbf{x}(t) = \mathbf{x}^* .$$

**Definition IV.2.** For fixed graph topology,  $\mu$ ,  $c$ , and initial opinions  $\mathbf{x}(0)$ , we say that the DW model, on a graph with  $N$  nodes, **converges to a limit state almost surely** if

$$P(\text{there exists } \mathbf{x}^* \in [0, 1]^N \text{ such that } \lim_{t \rightarrow \infty} \mathbf{x}(t) = \mathbf{x}^*) = 1 .$$

**Definition IV.3.** Let  $x_{\min}(t)$  denote the minimum opinion at time  $t$  and let  $i_{\min}(t)$  denote a node with the minimum opinion at time  $t$ . Analogously, let  $x_{\max}(t)$  and  $i_{\max}(t)$  denote the maximum opinion and the corresponding node at time  $t$ .

##### A. Complete Graphs

In this subsection we discuss results regarding sufficient conditions for a limit state to exist for the adaptive DW model on complete graphs. Lemma IV.1 and Lemma IV.2 will be used to show Theorem IV.1.

**Lemma IV.1.** Fix an edge sequence  $\{(i_t, j_t)\}_{t=0}^{\infty}$ . Then  $x_{\min}(t)$  is nondecreasing and  $x_{\max}(t)$  is nonincreasing, and both are convergent as  $t \rightarrow \infty$ .

*Proof.* Because  $\mu \in [0, 1]$ , we have that

$$\begin{aligned} \min\{x_{i_t}(t+1), x_{j_t}(t+1)\} &\geq \min\{x_{i_t}(t), x_{j_t}(t)\}, \\ \max\{x_{i_t}(t+1), x_{j_t}(t+1)\} &\leq \max\{x_{i_t}(t), x_{j_t}(t)\}. \end{aligned}$$

For each node  $v \in V \setminus \{i_t, j_t\}$ , we have that  $x_v(t) = x_v(t+1)$ . Therefore,  $x_{\max}(t)$  is nonincreasing and  $x_{\min}(t)$  is nondecreasing. Consequently, as both sequences are bounded in  $[0, 1]$ , we have that  $x_{\min}(t)$  and  $x_{\max}(t)$  converge as  $t \rightarrow \infty$ .  $\square$

**Lemma IV.2.** Let  $c(x) : [0, 1] \rightarrow [0, 1]$  with  $c(x) \geq b > 0$  for all  $x \in [0, 1]$ . Then, the probability of the following event is 0: there exists  $i \in V$  such that for all  $t \in \mathbb{N}$ , there exists  $s > t$  such that

$$\begin{aligned} x_i(s) &\notin [x_{\min}(s), x_{\min}(s) + b] \text{ and } x_i(s+1) \in [x_{\min}(s+1), x_{\min}(s+1) + b] \\ \text{or } x_i(s) &\notin (x_{\max}(s) - b, x_{\max}(s)] \text{ and } x_i(s+1) \in (x_{\max}(s+1) - b, x_{\max}(s+1)]. \end{aligned}$$

*Proof.* We restrict to the case that  $x_i(s) \notin (x_{\max}(s)-b, x_{\max}(s)]$  and that  $x_i(s+1) \in (x_{\max}(s+1)-b, x_{\max}(s+1)]$ . The proof for  $x_{\min}(t)$  is analogous. Suppose for sake of contradiction that there exists  $i \in V$  such that for all  $t \in \mathbb{N}$  there exists  $s > t$  such that  $x_i(s) \notin (x_{\max}(s)-b, x_{\max}(s)]$  and that  $x_i(s+1) \in (x_{\max}(s+1)-b, x_{\max}(s+1)]$ . Then, either  $x_{\max}(s) \neq x_{\max}(s+1)$  or  $x_i(s) \neq x_i(s+1)$ . One of these two cases must occur infinitely often.

**Case 1:** If  $x_{\max}(s) \neq x_{\max}(s+1)$  infinitely often, we label such time steps  $\{t_k\}_{k=0}^{\infty}$ . Given that  $x_{\max}(t)$  must remain within  $[0, 1]$ , we have that there exists  $k'$  such that for all  $k \geq k'$  we have  $x_{\max}(t_k) - x_{\max}(t_k+1) < \min\{(1-\mu)b\mu, b/2\}$ . Let  $k > k'$ . Therefore, at time  $t_k$ , it cannot be the case that  $i$  has a symmetric update with  $i_{\max}(t_k)$  because  $x_{\max}(t_k) - x_{\max}(t_k+1) < (1-\mu)b\mu$ . Therefore, because  $x_i(t_k) \notin (x_{\max}(t_k)-b, x_{\max}(t_k)]$ , we have that  $x_i(t_k+1) \in (x_{\max}(t_k+1)-b, x_{\max}(t_k+1)]$  and  $x_{\max}(t_k+1) - x_i(t_k+1) \geq b/2$ .

At time  $t_k+1$ , we label the set of all nodes with opinions in  $[x_i(t_k+1), x_{\max}(t_k+1)]$  as  $Q(t_k+1)$ . Then, with probability at least  $\frac{1}{E^{|Q(t_k+1)|}}$ , the following sequence of edge selections occurs:  $\{(i, i_{\max}(t_k+1)), (i_{\max}(t_k+1), j_i), \dots, (i_{\max}(t_k+1), j_{|Q(t_k+1)|})\}$  for all  $j_l \in Q(t_k+1)$ . Because the opinions of all of these nodes are within  $b$  of each other, all of these edge selections result in symmetric updates, which cannot increase the maximum opinion. Notice that the first edge selection makes the value of  $x_{i_{\max}(t_k+1)}$  decrease by at least  $(1-\mu)b\mu$ . Therefore, after the sequence of edge selections, we have that

$$x_{\max}(t_k+1) - x_{\max}(t_k+|Q|+2) \geq \frac{(\min\{1-\mu, \mu\})^{|Q(t_k+1)|} b\mu}{2}.$$

Because the probability that this occurs is at least  $\frac{1}{E^{|Q(t_k+1)|}}$ , we have that  $P(\lim_{t \rightarrow \infty} x_{\max}(t) < 0) = 1$ .

**Case 2:** If  $x_i(s) \neq x_i(s+1)$  infinitely often, denote such time steps  $\{t_k\}_{k=0}^{\infty}$ . We have already proven the case that  $x_{\max}(t_k) \neq x_{\max}(t_k+1)$ , (see Case 1) so we can assume that  $i$  and  $i_a(t_k)$  do not interact with a symmetric update at time  $t_k$ . We see that  $x_i(t_k+1) - x_{\max}(t_k+1) \geq \min\{1-\mu, \mu\}b$ .

At time  $t_k+1$ , we label the set of all nodes with opinions in  $[x_i(t_k+1), x_{\max}(t_k+1)]$  as  $Q(t_k+1)$ . Then, with probability at least  $\frac{1}{E^{|Q(t_k+1)|}}$ , the following sequence of edge selections occurs:  $\{(i, i_{\max}(t_k+1)), (i_{\max}(t_k+1), j_i), \dots, (i_{\max}(t_k+1), j_{|Q|})\}$  for all  $j_l \in Q(t_k+1)$ .

Notice that the first edge selection makes the value of  $x_{i_{\max}(t_k+1)}(t_k+1)$  decrease by at least  $(1-\mu)b\mu$ . Therefore, after the sequence of edge selections, we have that

$$x_{\max}(t_k+1) - x_{\max}(t_k+|Q(t_k+1)|+2) \geq (\min\{1-\mu, \mu\})^{|Q|} b\mu.$$

Because the probability that this occurs is at least  $\frac{1}{E^{|Q(t_k+1)|}}$ , we have that  $P(\lim_{t \rightarrow \infty} x_{\max}(t) < 0) = 1$ . Therefore,  $P(\text{there exists } i \in V \mid \text{for all } t \in \mathbb{N}, \text{ there exists } s > t \mid x_i(s) \notin (x_{\max}(s)-b, x_{\max}(s)], x_i(s+1) \in (x_{\max}(s)-b, a(s))) = 0$ .  $\square$

**Theorem IV.1.** For  $c(x) : [0, 1] \rightarrow [0, 1]$  with  $c(x) > \frac{1}{2+\mu}$  for all  $x \in [0, 1]$ , our adaptive DW model converges to a limit state almost surely.

*Proof.* We know that, if eventually only symmetric updates occur, by the work of Lorenz, [16] our model converges to a limit state. Therefore, we will show, almost surely, that asymmetric updates eventually stop occurring. Suppose that asymmetric updates never stop occurring. Therefore, there exists some  $i \in V$  such that  $i$  updates asymmetrically an infinite number of times. Denote the time steps where  $i$  updates asymmetrically as  $\{s\}_{s=0}^{\infty}$ . Let  $I_{\min}(t) = [x_{\min}(t), x_{\min}(t)+b)$ ,  $I_{\max}(t) = (x_{\max}(t)-b, x_{\max}(t)]$ , and  $I_{\text{mid}}(t) = [x_{\min}(t), x_{\max}(t)] \setminus (I_{\min}(t) \cup I_{\max}(t))$ . Note that for all  $t \in \mathbb{N}$   $[x_{\min}(t), x_{\max}(t)] = I_{\min}(t) \cup I_{\max}(t) \cup I_{\text{mid}}(t)$ . Note as well that  $x_i(t_k) \notin I_{\min}(t_k) \cap I_{\max}(t_k)$  for all  $k \in \mathbb{N}$  because a node must have opinion with distance at least  $b$  from a node in order to have an asymmetric update with it.

Let  $\{j_s\}_{s=0}^{\infty}$  be the sequence of nodes with which  $i$  updates with for each  $s \in \mathbb{Z}^+$ . For any  $s$ , if  $x_i(s) \in I_{\min}(s)$  then  $x_{j_s}(s) \in I_{\max}(s) \cup I_{\text{mid}}(s)$ . Also, if  $x_i(s) \in I_{\max}(s)$  then  $x_{j_s}(s) \in I_{\min}(s) \cup I_{\text{mid}}(s)$ . Finally, if  $x_i(s) \in I_{\text{mid}}(s)$  then  $x_{j_s}(s) \in I_{\min}(s) \cup I_{\max}(s)$ . We know as well that each asymmetric update causes  $x_i$  to change by at least  $\mu b$ . Suppose for sake of contradiction that  $x_i$  remains in one of these intervals forever. If  $x_i(s) \in I_{\text{mid}}(s)$  then  $x_i(s+1) \notin I_{\text{mid}}(s+1)$  as  $\text{len}(I_{\text{mid}}(t)) < \mu b$ , for all  $t \in \mathbb{N}$ .

Without loss of generality, suppose that there exists some  $T \in \mathbb{N}$  such that  $x_i(t) \in I_{\max}(t)$  for all  $t > T$ . The case for  $I_{\min}(t)$  is analogous. Then there exists  $s' \in \mathbb{N}$  such that  $s' > T$ . Then at time  $s'+1$ , as  $x_i(s')$  must have decreased, we have that  $x_{\max}(s'+1) - x_i(s'+1) \geq \mu b$ . Then, we label the set of all nodes with opinions in  $[x_i(s'+1), x_{\max}(s'+1)]$  by  $Q(s'+1)$ . Then with probability at least

$$\frac{1}{E^{|Q(s'+1)|}},$$

the following sequence of edge selections occurs:  $\{(i, i_{\max}(s'+1)), (i_{\max}(s'+1), j_i), \dots, (i_{\max}(s'+1), j_{|Q(s'+1)|})\}$  for all  $j_l \in Q(s'+1)$ .

Notice that the first edge selection makes the value of  $x_{i_{\max}(s+1)}(s+1)$  decrease by at least  $\min\{1-\mu, \mu\}b\mu$ . Therefore, after the sequence of edge selections, we have that

$$x_{\max}(s+1) - x_{\max}(s + |Q(s'+1)| + 2) \geq \min\{1-\mu, \mu\}^{|Q(s'+1)|} b\mu.$$

Because the probability that this occurs is at least  $\frac{1}{E^{|Q|}}$  and for each  $k \geq k'$  this choice of edge sequence has probability at least  $\frac{1}{E^{|Q(s+1)|}}$  of occurring, we have that  $P(\lim_{t \rightarrow \infty} x_{\max}(t) < 0) = 1$ .

Therefore,  $x_i$  stays within either  $I_{\max}$  or  $I_{\min}$  forever with probability 0. Thus, with probability 1  $x_i$  must alternate between  $I_{\max}$  and  $I_{\min}$  (as it cannot remain within  $I_{\text{mid}}$ ) which happens with probability 0 by Lemma IV.2. Therefore, the system converges to a limit state almost surely.  $\square$

**Corollary IV.2.1.** *For any  $c(x) : [0, 1] \rightarrow [0, 1]$  with  $c(x) \geq b > 0$ , for all  $x \in [0, 1]$ , if there exists  $t \in \mathbb{N}$  such that  $b(2 + \mu) > x_{\max}(t) - x_{\min}(t)$ , our adaptive DW model converges to a limit state almost surely.*

On complete graphs, we now have one class of functions, in addition to constant functions, [16] for which our model almost surely converges to a limit state.

## B. General Graphs With Monotone Confidence

For this subsection, we move to a more general case. First, let  $G = (V, E)$  be a graph. Lemma IV.3, Lemma IV.4, and Lemma IV.5 are used to show Theorem IV.2.

**Lemma IV.3.** *Suppose  $c : [0, 1] \rightarrow [0, 1]$  is a nondecreasing confidence function for our adaptive DW model. Then, if edge  $(i, j)$ , where  $x_i(t) \leq x_j(t)$  is selected at time  $t$ , then one of the following is true:*

1.  $x_i(t+1) = x_i(t)$ ,  
 $x_j(t+1) = x_j(t)$ ,
2.  $x_i(t+1) = x_i(t) + \mu(x_j(t) - x_i(t))$ ,  
 $x_j(t+1) = x_j(t) + \mu(x_i(t) - x_j(t))$ ,
3.  $x_i(t+1) = x_i(t)$ ,  
 $x_j(t+1) = x_j(t) + \mu(x_i(t) - x_j(t))$ .

*Proof.* If edge  $(i, j)$  is selected at time  $t$ , then either  $x_i(t+1) = x_i(t)$  or  $x_i(t+1) = x_i(t) + \mu(x_j(t) - x_i(t))$ . Similarly, either  $x_j(t+1) = x_j(t)$  or  $x_j(t+1) = x_j(t) + \mu(x_i(t) - x_j(t))$ . Therefore, if  $x_j(t+1) = x_j(t) + \mu(x_i(t) - x_j(t))$ , we have the desired result.

Now, we must show that if  $x_j(t+1) = x_j(t)$ , then  $x_i(t+1) = x_i(t)$ . Suppose that  $x_j(t+1) = x_j(t)$ , in which case we know that  $x_i(t)$  must lie outside the confidence bound of node  $j$  at time  $t$ . Therefore,  $x_i(t) \notin [x_j(t) - c(x_j(t)), x_j(t) + c(x_j(t))]$ , and because  $x_i(t) \leq x_j(t)$ , we conclude that  $x_i(t) < x_j(t) - c(x_j(t))$ . Additionally, because  $c$  is monotonically increasing,  $c(x_j(t)) \geq c(x_i(t))$ , so

$$x_i(t) < x_j(t) - c(x_j(t)) \leq x_j(t) - c(x_i(t)) \quad \text{or} \quad x_j(t) > x_i(t) + c(x_i(t)).$$

Therefore,  $x_j(t)$  lies outside the confidence bound of node  $i$  at time  $t$ . Based on Definition III.1, we conclude that  $x_i(t+1) = x_i(t)$ , as desired.  $\square$

Note that an analogous result is true for  $c(x)$  nonincreasing.

**Lemma IV.4.** *For a vector  $\mathbf{y} \in \mathbb{R}^n$ , let  $f(\mathbf{y}) = \sum_{1 \leq i < j \leq n} \max\{y_i, y_j\}$ . Suppose that  $c : [0, 1] \rightarrow [0, 1]$  is monotone, and fix the edge choices of the DW model as  $\{(i_t, j_t)\}_{t=0}^{\infty}$ . Then  $f(\mathbf{x}(t))$  is strictly decreasing with  $t$ . In particular, for  $\delta > 0$ , if at time  $t$ ,  $|x_{i_t}(t) - x_{j_t}(t)| \geq \delta$  and  $\mathbf{x}(t) \neq \mathbf{x}(t+1)$ , then*

$$f(\mathbf{x}(t+1)) \leq f(\mathbf{x}(t)) - m\delta,$$

where  $m := \min\{\mu, 1 - \mu\}$ .

*Proof.* There are two cases: asymmetric updates, and symmetric updates. For an asymmetric update, without loss of generality, say that  $x_{j_t}(t) \neq x_{j_t}(t+1)$ . Therefore,  $x_{j_t}(t) > x_{i_t}(t)$ . This implies that  $x_{j_t}(t+1) = x_{j_t}(t) + \mu(x_{i_t}(t) - x_{j_t}(t))$ . So  $x_{j_t}(t+1) \leq x_{j_t}(t) - \gamma\delta$ . Therefore,

$$\max\{x_{i_t}(t+1), x_{j_t}(t+1)\} \leq \max\{x_{i_t}(t), x_{j_t}(t)\} - m\delta.$$

Thus, as no other nodes changed their opinions at this time step, for all  $i, j \in V$ ,  $\max\{x_i(t+1), x_j(t+1)\} \leq \max\{x_i(t), x_j(t)\}$ . Therefore,  $f(\mathbf{x}(t+1)) \leq f(\mathbf{x}(t)) - m\delta$ .

For the symmetric update case, without loss of generality, assume that  $x_{i_t}(t) < x_{j_t}(t)$ . Then, the symmetric update causes  $x_{i_t}$  to increase and  $x_{j_t}$  to decrease. Let  $r = |x_{i_t}(t+1) - x_{i_t}(t)| = |x_{j_t}(t+1) - x_{j_t}(t)|$ . Note that  $r > m\delta$ . Let  $k \in V \setminus \{i_t, j_t\}$ . We have that

$$\begin{aligned} \max\{x_k(t+1), x_{i_t}(t+1)\} - \max\{x_k(t), x_{i_t}(t)\} &= \begin{cases} 0 & x_k(t+1) \geq x_{i_t}(t+1), \\ r & x_k(t) \leq x_{i_t}(t), \\ r - |x_k(t) - x_{i_t}(t)| & x_k(t) > x_{i_t}(t) \text{ and } x_k(t+1) < x_{i_t}(t+1), \end{cases} \\ \max\{x_k(t+1), x_{j_t}(t+1)\} - \max\{x_k(t), x_{j_t}(t)\} &= \begin{cases} 0 & x_k(t) \geq x_{j_t}(t), \\ -r & x_k(t) \leq x_{j_t}(t+1) \text{ and } x_k(t) \leq x_{j_t}(t+1), \\ -|x_k(t) - x_{j_t}(t)| & x_k(t) < x_{i_t}(t) \text{ and } x_k(t+1) > x_{i_t}(t+1). \end{cases} \end{aligned}$$

From these cases, we see that if

$$\max\{x_k(t+1), x_{i_t}(t+1)\} > \max\{x_k(t), x_{i_t}(t)\},$$

then either  $\max\{x_k(t+1), x_{i_t}(t+1)\} + \max\{x_k(t+1), x_{j_t}(t)\} = 0$  or

$$\begin{aligned} \max\{x_k(t+1), x_{i_t}(t+1)\} + \max\{x_k(t+1), x_{j_t}(t)\} &= r - |x_k(t) - x_{i_t}(t)| - |x_k(t) - x_{j_t}(t)| \\ &= r - |x_{i_t}(t) - x_{j_t}(t)| \\ &< 0. \end{aligned}$$

If  $\max\{x_k(t+1), x_{i_t}(t+1)\} \not> \max\{x_k(t), x_{i_t}(t)\}$ , we have that  $\max\{x_k(t+1), x_{i_t}(t+1)\} - \max\{x_k(t), x_{i_t}(t)\} = 0$  and  $\max\{x_k(t+1), x_{j_t}(t+1)\} - \max\{x_k(t), x_{j_t}(t)\} < 0$ . Therefore

$$\max\{x_k(t+1), x_{i_t}(t+1)\} + \max\{x_k(t+1), x_{j_t}(t+1)\} < \max\{x_k(t+1), x_{i_t}(t)\} + \max\{x_k(t+1), x_{j_t}(t)\}.$$

We also have that

$$\max\{x_{i_t}(t+1), x_{j_t}(t+1)\} < \max\{x_{i_t}(t), x_{j_t}(t)\} - m\delta.$$

Therefore,  $f(\mathbf{x}(t+1)) \leq f(\mathbf{x}(t)) - m\delta$ , as desired. □

**Lemma IV.5.** *Suppose the confidence function  $c : [0, 1] \rightarrow [0, 1]$  is nondecreasing. In addition, fix the edge choices of the DW model as  $\{(i_t, j_t)\}_{t=0}^{\infty}$ . Additionally, let  $\{(i_{t_k}, j_{t_k})\}_{k=0}^{\infty}$  denote the subsequence of edges where  $\mathbf{x}(t_k) \neq \mathbf{x}(t_k+1)$ . Let  $m := \min\{\mu, 1 - \mu\}$ . It then follows that,*

$$\sum_{k \geq 1} |x_{i_{t_k}}(t_k) - x_{j_{t_k}}(t_k)| \leq m^{-1} \cdot f(\mathbf{x}(t_1+1)) < \infty.$$

*Proof.* First, notice that  $\sum_{k \geq 1} |x_{i_{t_k}}(t_k) - x_{j_{t_k}}(t_k)|$  is either convergent to some quantity in  $[0, \infty)$  or diverges to  $\infty$  since it is a formal sum of nonnegative values. It remains to show that the sum converges to a finite value.

Define  $f : [0, 1]^n \rightarrow \mathbb{R}$  by  $f(\mathbf{y}) = \sum_{1 \leq i < j \leq n} \max\{y_i, y_j\}$ , and fix  $k \geq 2$ . We have by Lemma IV.4 that

$$f(\mathbf{x}(t_k + 1)) \leq f(\mathbf{x}(t_k)) - m|x_{i_{t_k}}(t_k) - x_{j_{t_k}}(t_k)|.$$

In addition,  $f$  is nonincreasing and  $t_k \geq t_{k-1} + 1$ , so  $f(\mathbf{x}(t_k)) \leq f(\mathbf{x}(t_{k-1} + 1))$ , so

$$f(\mathbf{x}(t_k + 1)) \leq f(\mathbf{x}(t_{k-1} + 1)) - m|x_{i_{t_k}}(t_k) - x_{j_{t_k}}(t_k)|.$$

Therefore, for  $k \geq 1$ , it follows that

$$f(\mathbf{x}(t_k + 1)) \leq f(\mathbf{x}(t_1 + 1)) - \sum_{q=0}^{k-1} m|x_{i_{t_q}} - x_{j_{t_q}}| = f(\mathbf{x}(t_1 + 1)) - m \sum_{q=0}^{k-1} |x_{i_{t_q}} - x_{j_{t_q}}|.$$

Recall that  $f$  is nonnegative, so for all  $k \geq 2$ ,  $f(\mathbf{x}(t_1 + 1)) - m \sum_{q=0}^{k-1} |x_{i_{t_q}} - x_{j_{t_q}}| \geq 0$ . This implies that

$$\sum_{q=0}^{k-1} |x_{i_{t_q}} - x_{j_{t_q}}| \leq m^{-1} \cdot f(\mathbf{x}(t_1 + 1)) \Rightarrow \sum_{k \geq 1} |x_{i_{t_k}}(t_k) - x_{j_{t_k}}(t_k)| \leq m^{-1} \cdot f(\mathbf{x}(t_1 + 1)),$$

as desired.  $\square$

**Theorem IV.2.** *Suppose the confidence function  $c : [0, 1] \rightarrow [0, 1]$  is monotone. In addition, fix the edge choices of the DW model as  $\{(i_t, j_t)\}_{t=0}^{\infty}$ , and let  $\{(i_{t_k}, j_{t_k})\}_{k=0}^{\infty}$  denote the subsequence of edges where  $\mathbf{x}(t_k) \neq \mathbf{x}(t_k + 1)$ . Then the adaptive DW model with given confidence and edge choices converges to a limit state  $\mathbf{x}^*$  as  $t \rightarrow \infty$ .*

*Proof.* Without loss of generality, let  $c(x)$  be nondecreasing. Recall from Lemma IV.5 that  $\sum_{k \geq 1} |x_{i_{t_k}}(t_k) - x_{j_{t_k}}(t_k)| = m^{-1} \cdot f(\mathbf{x}(t_1 + 1))$ . We will use this to show that  $\sum_{t \geq 1} |x_{i_t}(t) - x_{i_t}(t-1)| \leq d$  for any  $i \in V$ . We first show that  $|x_i(t) - x_i(t-1)| \leq |x_{i_t}(t-1) - x_{j_t}(t-1)|$ . There are two cases:

1. First, if  $i \neq i_t$  and  $i \neq j_t$ , then we immediately have  $|x_i(t+1) - x_i(t)| = 0 \leq |x_{i_t}(t) - x_{j_t}(t)|$ .
2. Second, suppose that  $i = i_t$  or  $i = j_t$ . Because  $\mu < 1$  we have

$$x_{i_t}(t+1), x_{j_t}(t+1), x_{i_t}(t), x_{j_t}(t) \in [x_{i_t}(t), x_{j_t}(t)],$$

so  $x_i(t+1), x_i(t) \in [x_{i_t}(t), x_{j_t}(t)]$ . It then follows that  $|x_i(t+1) - x_i(t)| \leq |x_{i_t}(t) - x_{j_t}(t)|$ .

Next, observe that  $\sum_{t \geq 1} |x_i(t+1) - x_i(t)|$  is a sum of nonnegative terms, and hence is either convergent to a value in  $[0, \infty)$  or diverges to  $\infty$ . We know that if  $t \neq t_k$  for any  $k \geq 1$  (i.e.  $\mathbf{x}(t+1) = \mathbf{x}(t)$ ) then  $|x_i(t+1) - x_i(t)| = 0$ . This allows us to drop terms with  $t \neq t_k$  for any  $k$ , yielding

$$\sum_{t \geq 1} |x_i(t+1) - x_i(t)| = \sum_{k \geq 1} |x_i(t_k + 1) - x_i(t_k)|.$$

Because  $|x_i(t_k + 1) - x_i(t_k)| \leq |x_{i_{t_k}}(t_k) - x_{j_{t_k}}(t_k)|$ , we have an analogous relation for the sums of these terms. That is,

$$\sum_{k \geq 1} |x_i(t_k + 1) - x_i(t_k)| \leq \sum_{k \geq 1} |x_{i_{t_k}}(t_k) - x_{j_{t_k}}(t_k)| \leq \gamma^{-1} \cdot f(\mathbf{x}(t_1 + 1)).$$

This implies that

$$\sum_{t \geq 1} |x_i(t+1) - x_i(t)| = \sum_{k \geq 1} |x_i(t_k + 1) - x_i(t_k)| \leq \gamma^{-1} \cdot f(\mathbf{x}(t_1 + 1))$$

is finite, so  $\{x_i(t)\}_{t=0}^{\infty}$  is a Cauchy sequence and therefore converges to some  $x_i^* \in \mathbb{R}$ .  $\square$

TABLE I: Defining notation used in Section IV C.

Notation	Definition
$m$	$\min\{\mu, 1 - \mu\}$
$\{A_i\}_{i=1}^k$	a sequence of statements
$\bigvee_{i=1}^k A_i$	statement that at least one of the $A_i$ is true, also known as the logical disjunction
$\neg A$	logical negation of the statement $A$
$\bigwedge_{i=1}^k A_i$	the statement that all of the $A_i$ are true, also known as the logical conjunction
The <i>possible graph</i> : $G_{\text{pos}}(t)$	the graph will all edges which ever appear within the effective graph at and after time $t$ ; formally, $(V, \bigcup_{t' \geq t} E_{\text{eff}}(t))$
$\{e_t\}_{t=0}^{\infty}$	the sequence of edges chosen in <b>DW</b>
The <i>observed graph</i> : $G_{\text{obs}}(t)$	the graph of all edges which are selected at and after time $t$ ; formally, $(V, \{e_{t'}   t' \geq t\})$
$\text{sep}(e, t)$	the statement that the graph intersection $G_{\text{obs}}(t) \cap G_{\text{pos}}(t)$ is not weakly connected
$e_t$ is <i>effective</i>	$e_t \in E_{\text{eff}}(t)$
$\text{sep}(e)$	the event that $\text{sep}(e, t)$ is true for some $t$ , formally $\text{sep}(e) := \bigvee_{t \geq 0} \text{sep}(e, t)$
$\text{conn}(e)$	$\text{conn}(e) = \neg \text{sep}(e) = \bigwedge_{t \geq 0} \neg \text{sep}(e, t)$
$f = \{f_t\}_{t=0}^{t_f}$	a sequence of edge selections which can be finite or infinite.
$\text{same}(f, s, e)$	the statement that the first $s$ edge choices $\{e_t\}_{t=0}^s$ of <b>DW</b> match the edges in $f$
$\text{stab}(e)$	the statement that every node in <b>DW</b> has a limit opinion
$\text{dif}(\epsilon, d, s_0, s, e)$	the event that after the edge selections $\{e_t\}_{t=0}^s$ , there are at least $d$ nodes at time $s$ whose opinions are at least $x_{\min}(s_0) + \epsilon$ and that there are fewer than $d$ such nodes at any time $s' < s$
$\text{DIF}(\epsilon, d, s, T, e)$	the event that there exists $t \leq T$ such that $\text{dif}(\epsilon, d, s, t, e)$
consensus	the event such that $\lim_{t \rightarrow \infty} x_i(t) = k$ for all $i \in V$

### C. General Graphs with Monotone Lower Bound

Let  $G = (V, E)$  be a graph. In this section, we consider an adaptive DW model **DW** as in Definition III.1, where we further assume that the function  $x - c(x)$  is nondecreasing with  $x$ . As mentioned before, we claim an analogous result for  $x + c(x)$  nondecreasing; for this case, see Remark IV.2. In Table I, we provide a list of definitions and notation which will be used throughout the section:

The approach in this section will be to treat randomness as a control protocol; the idea of this control protocol will be used in proving Lemma IV.6. This is inspired by previous work on other opinion dynamic models have used this approach to prove consensus or the existence of a limit state [10, 17].

**Lemma IV.6.** *Let  $\epsilon \in (0, mb]$ , time  $s_0, s \geq 0$  and  $0 < d < N$ . Then there exists a time  $T \geq s$  such that*

$$P_{\text{DW}}(\text{DIF}(m\epsilon, d + 1, s_0, T, e) | \text{dif}(\epsilon, d, s_0, s, e)) \geq \frac{1}{2|E|^v} \cdot P_{\text{DW}}(\text{conn}(e) | \text{dif}(\epsilon, d, s_0, s, e)),$$

where

$$v := \left\lceil \frac{\ln b}{\ln(1 - \mu)} \right\rceil.$$

*Proof.* Let  $H$  denote the set of nodes  $i \in V$  such that  $x_i(s) \geq x_{\min}(s_0) + \epsilon$ . Assume  $\text{dif}(\epsilon, d, s_0, s, e)$  and suppose there exists some minimum  $t \geq s$  for which  $e_t$  is an effective edge between a node  $i \in H$  and a node  $j \in V \setminus H$ . Note that this second statement would be implied by  $\neg \text{sep}(e, s)$ .

Because  $t$  is minimal, all previous effective edge choices  $e_{t'}$  with  $s < t' < t$  are either in  $H \times H$  or  $(V \setminus H) \times (V \setminus H)$ . An edge choice from either of these sets preserves the properties that  $\min_{l \in H} x_l(t') \geq \epsilon$  and  $\max_{l \in V \setminus H} x_l(t') < \epsilon$ . Thus,  $x_i(t) \geq \epsilon$  and  $x_j(t) < \epsilon$ . There are two cases:

- **Case 1:** We assume  $x_i(t) < x_j(t) + c(x_j(t))$ , so that node  $i$  is in the confidence interval of  $j$  at time step  $t$ . After edge  $e_t = (i, j)$  is selected we know that

$$\begin{aligned} x_j(t+1) &= (1-\mu)x_j(t) + \mu x_i(t) \\ &\geq (1-\mu)x_{\min}(t) + \mu x_i(t) \\ &\geq x_{\min}(t) + \mu\epsilon \geq x_{\min}(s_0) + \mu\epsilon, \end{aligned} \quad (5)$$

$$\begin{aligned} x_i(t+1) &= (1-\mu)x_i(t) + \mu x_j(t) \\ &\geq (1-\mu)x_i(t) + \mu x_{\min}(t) \\ &\geq x_{\min}(t) + (1-\mu)\epsilon \geq x_{\min}(s_0) + (1-\mu)\epsilon. \end{aligned} \quad (6)$$

Because no other elements of  $H$  change their opinions between time steps  $t$  and  $t+1$ , we conclude from (4) that all elements of  $H$  have opinions of at least  $x_{\min}(s_0) + (1-\mu)\epsilon$ . Because there are  $\geq d$  elements of  $H$ , there must be at least  $d+1$  nodes whose opinion at time  $t+1$  is at least

$$\min x_{\min}(s_0) + \mu\epsilon, x_{\min}(s_0) + (1-\mu)\epsilon = x_{\min}(s_0) + b\epsilon.$$

Therefore,  $\text{dif}(m\epsilon, d+1, s, t+1, e)$  is true, and therefore  $\text{DIF}(m\epsilon, d+1, s, t+1, e)$  is true.

- **Case 2:** We assume that  $x_i(t) \geq x_j(t) + c(x_j(t))$ , so that  $i$  is not in the confidence bound of  $j$  at time step  $t$ . Then, for  $t' > t$  such that  $x_i(t') \geq x_j(t') + c(x_j(t'))$ , we can repeatedly select edge  $(i, j)$   $t' - t$  times with probability  $1/|E|^{t'-t}$ . Because  $x - c(x)$  is an increasing function, we know that, during this selection, node  $j$  always remains inside the confidence bound of node  $j$ . This implies that

$$\begin{aligned} x_i(t') &= x_j(t' - 1) + (1-\mu) \cdot (x_i(t' - 1) - x_j(t' - 1)) \\ &= x_j(t) + (1-\mu)^{t'-t} (x_i(t) - x_j(t)). \end{aligned}$$

There is then some positive number  $u$  of selections of the edge  $(i, j)$ , where

$$u \leq \left\lceil \frac{\ln b - \ln(x_i(t) - x_j(t))}{\ln(1-\mu)} \right\rceil \quad (7)$$

such that  $x_i(t+u) \leq x_j(t) + b \leq x_j(t) + c(x_j(t)) = x_j(t+u) + c(x_j(t+u))$ . By construction, because  $x_i(t+u-1) > x_j(t) + b$ , we know  $x_i(t+u) > x_j(t) + b(1-\mu) \geq x_{\min}(t) + b(1-\mu) \geq x_{\min}(s_0) + \epsilon$ . By assumption, the first selection of  $(i, j)$  is given, so this happens with probability  $1/|E|^{u-1}$ .

From here, we use the work from Case 1 to see that, with a total probability of at least  $1/|E|^u$  we get  $\text{dif}(m\epsilon, d+1, s, t+u, e)$  is true. We also know that  $x_i(t) - x_j(t) \leq 1$ . Thus, substituting into (7) yields  $u \leq v$ . Finally, this lets us conclude  $\text{DIF}(m\epsilon, d+1, s, t+v, e')$  is true with probability at least  $1/|E|^v$ .

We see that, with probability at least  $1/|E|^v$ , at least one of  $\text{DIF}(m\epsilon, d+1, s, t+1, e)$  or  $\text{DIF}(m\epsilon, d+1, s, t+v, e)$  is true. Since  $\text{DIF}(m\epsilon, d+1, s, t+1, e) \Rightarrow \text{DIF}(m\epsilon, d+1, s, t+v, e)$ , we conclude that  $\text{DIF}(m\epsilon, d+1, s, t+v, e)$  is true with probability at least  $1/|E|^v$ .

Our initial assumption on  $e$  was that  $\text{dif}(\epsilon, d, s_0, s, e)$  is true and there exists some minimum  $t \geq s$  for which  $e_t$  is an effective edge between a node  $i \in H$  and a node  $j \in V \setminus H$ . We also noted that the second statement is implied by  $\neg \text{sep}(e, s)$ . For a fixed  $e$  satisfying  $\neg \text{sep}(e, s)$ , let  $t_e$  denote the minimum  $t \geq s$  for which  $e_t$  is an effective edge between a node in  $H$  and a node in  $V \setminus H$ . Letting  $t \geq s$  be given, we conclude that

$$P_{\text{DW}}(\text{DIF}(m\epsilon, d+1, s, t_e + v, e) | \text{dif}(\epsilon, d, s_0, s, e), \neg \text{sep}(e, s), t_e = t) \geq \frac{1}{|E|^v}. \quad (8)$$

From (8), we obtain

$$\begin{aligned} &P_{\text{DW}}(\neg \text{sep}(e, s), t_e = t, \text{DIF}(m\epsilon, d+1, s, t_e + v, e) | \text{dif}(\epsilon, d, s_0, s, e)) \\ &= P_{\text{DW}}(\text{DIF}(m\epsilon, d+1, s, t_e + v, e) | \text{dif}(\epsilon, d, s_0, s, e), \neg \text{sep}(e, s), t_e = t) \times P_{\text{DW}}(\neg \text{sep}(e, s), t_e = t | \text{dif}(\epsilon, d, s_0, s, e)) \\ &\geq \frac{1}{|E|^v} P_{\text{DW}}(\neg \text{sep}(e, s), t_e = t | \text{dif}(\epsilon, d, s_0, s, e) \end{aligned} \quad (9)$$

Now, let  $T \geq s$  be given. We use conditional probability and (9) to obtain the following:

$$\begin{aligned}
& P_{\mathbf{DW}}(\neg \text{sep}(e, s), t_e \leq T, \text{DIF}(m\epsilon, d+1, s, t_e+v, e) | \text{dif}(\epsilon, d, s_0, s, e)) \\
&= \sum_{t=s}^T P_{\mathbf{DW}}(\neg \text{sep}(e, s), t_e = t, \text{DIF}(m\epsilon, d+1, s, t_e+v, e) | \text{dif}(\epsilon, d, s_0, s, e)) \\
&\geq \sum_{t=s}^T \frac{1}{|E|^v} P_{\mathbf{DW}}(\neg \text{sep}(e, s), t_e = t | \text{dif}(\epsilon, d, s_0, s, e)) \\
&= \frac{1}{|E|^{v+1}} \cdot P_{\mathbf{DW}}(\neg \text{sep}(e, s), t_e \leq T | \text{dif}(\epsilon, d, s_0, s, e)). \tag{10}
\end{aligned}$$

Recall that if  $\neg \text{sep}(e, s)$  is true, then  $t_e \leq \infty$ . Therefore we know

$$\neg \text{sep}(e, s) \wedge \text{dif}(\epsilon, d, s_0, s, e) = \bigvee_{t=s}^{\infty} [\neg \text{sep}(e, s) \wedge t_e = t] \wedge \text{dif}(\epsilon, d, s_0, s, e).$$

By the lower continuity of measure, there exists some  $T \geq s$  for which

$$P_{\mathbf{DW}}\left(\bigvee_{t=s}^T [\neg \text{sep}(e, s) \wedge t_e = t] \wedge \text{dif}(\epsilon, d, s_0, s, e) | \text{dif}(\epsilon, d, s_0, s, e)\right) \geq \frac{1}{2} P_{\mathbf{DW}}(\neg \text{sep}(e, s) \wedge \text{dif}(\epsilon, d, s_0, s, e) | \text{dif}(\epsilon, d, s_0, s, e)),$$

or in other words,

$$P_{\mathbf{DW}}(\neg \text{sep}(e, s), t_e \leq T | \text{dif}(\epsilon, d, s_0, s, e)) \geq \frac{1}{2} P_{\mathbf{DW}}(\neg \text{sep}(e, s) | \text{dif}(\epsilon, d, s_0, s, e)). \tag{11}$$

Combining (10) and (11), we get that

$$P_{\mathbf{DW}}(\neg \text{sep}(e, s), t_e \leq T, \text{DIF}(m\epsilon, d+1, s, t_e+v, e) | \text{dif}(\epsilon, d, s_0, s, e)) \geq \frac{1}{2|E|^{v+1}} \cdot P_{\mathbf{DW}}(\neg \text{sep}(e, s) | \text{dif}(\epsilon, d, s_0, s, e)).$$

Finally, recall that  $\text{conn}(e) \Rightarrow \neg \text{sep}(e, s)$  by definition, and that

$$\neg \text{sep}(e, s), t_e \leq T, \text{DIF}(m\epsilon, d+1, s, t_e+v, e) \Rightarrow \text{DIF}(m\epsilon, d+1, s, T+v, e).$$

Then we have the following chain of inequalities

$$\begin{aligned}
P_{\mathbf{DW}}(\text{DIF}(m\epsilon, d+1, s, T+v, e) | \text{dif}(\epsilon, d, s_0, s, e)) &\geq P_{\mathbf{DW}}(\neg \text{sep}(e, s), t_e \leq T, \text{DIF}(m\epsilon, d+1, s, t_e+v, e) | \text{dif}(\epsilon, d, s_0, s, e)) \\
&\geq \frac{1}{2|E|^{v+1}} \cdot P_{\mathbf{DW}}(\neg \text{sep}(e, s) | \text{dif}(\epsilon, d, s_0, s, e)) \\
&\geq \frac{1}{2|E|^{v+1}} \cdot P_{\mathbf{DW}}(\text{conn}(e) | \text{dif}(\epsilon, d, s_0, s, e)),
\end{aligned}$$

so that  $T+v$  is our desired time step. This completes the proof.  $\square$

In subsequent proofs, we will denote  $q := \frac{1}{2|E|^v}$  for brevity. With some work, one can get from Lemma IV.6 the following result, whose proof we defer to Appendix B.3.

**Lemma IV.7.** *For a finite choice of possible initial opinions  $\mathbf{x}(0)$ , and a fixed  $\epsilon > 0$ , suppose  $P_{\mathbf{DW}}(\text{conn}(e)) > 0$  and that for all  $t \geq 0$ ,  $P_{\mathbf{DW}}(a(t) - n(t) \geq \epsilon | \text{conn}(e)) \geq \delta > 0$ . Then there exists some  $T \geq 0$  such that*

$$\mathbb{E}_{\mathbf{DW}}[x_{\min}(T)] > \mathbb{E}_{\mathbf{DW}}[x_{\min}(0)] + \frac{1}{8}(mq)^{N-1}\epsilon\delta \cdot P_{\mathbf{DW}}(\text{conn}(e)).$$

Our next major objective is to use Lemma IV.7 to show that the probability of  $\mathbf{DW}$  satisfying  $\text{conn}(e)$  and not coming to consensus is 0. The intuition behind Lemma IV.7 is that if a certain violation of consensus never stops occurring, then we can expect  $x_{\min}$  to increase without bound.

**Lemma IV.8.** *For initial opinion  $\mathbf{x}(0)$ , and a fixed  $\epsilon > 0$ , suppose  $P(\text{conn}(e)) > 0$ . Then we have that*

$$\lim_{t \rightarrow \infty} P_{\mathbf{DW}}(x_{\max}(t) - x_{\min}(t) \geq \epsilon | \text{conn}(e)) = 0.$$

*Proof.* Recall from Lemma IV.1 that  $x_{\max}(t) - x_{\min}(t)$  is nonincreasing with  $t$ , which implies that  $P_{\mathbf{DW}}(x_{\max}(t) - x_{\min}(t) \geq \epsilon | \text{conn}(e))$  is nonincreasing with  $t$ . Therefore,  $P_{\mathbf{DW}}(x_{\max}(t) - x_{\min}(t) \geq \epsilon | \text{conn}(e))$  has a limit at some  $\delta \geq 0$ . Suppose for sake of contradiction that  $\delta > 0$ . This implies that  $P_{\mathbf{DW}}(x_{\max}(t) - x_{\min}(t) \geq \epsilon | \text{conn}(e)) \geq \delta$  for all  $t \geq 0$ . Let  $\mathbb{E}_{\mathbf{DW}}[x_{\min}(\infty)]$  denote the limit of  $\mathbb{E}_{\mathbf{DW}}[x_{\min}(t)]$  as  $t \rightarrow \infty$ . In particular, there exists  $t^* \geq 0$  so that

$$\mathbb{E}_{\mathbf{DW}}[x_{\min}(t^*)] > \mathbb{E}_{\mathbf{DW}}[x_{\min}(\infty)] - \frac{1}{8}(mq)^{N-1}\epsilon\delta \cdot P_{\mathbf{DW}}(\text{conn}(e)).$$

Let  $\mathbf{DW}'$  denote the DW process where the initial opinion  $\mathbf{x}'(0)$  is distributed as  $\mathbf{x}(t^*)$ . We know that

$$P_{\mathbf{DW}'}(\text{conn}(e)) = P_{\mathbf{DW}}(\text{conn}(e)) > 0$$

and that for all  $t \geq 0$

$$P_{\mathbf{DW}'}(x_{\max}(t) - x_{\min}(t) \geq \epsilon | \text{conn}(e)) = P_{\mathbf{DW}}(x_{\max}(t+t^*) - x_{\min}(t+t^*) \geq \epsilon | \text{conn}(e)) \geq \delta.$$

Then by Lemma IV.7, there exists some  $T^* \geq 0$  such that

$$\mathbb{E}_{\mathbf{DW}'}[x_{\min}(T^*)] \geq \mathbb{E}_{\mathbf{DW}'}[x_{\min}(0)] + \frac{1}{8}(mq)^{N-1}\epsilon\delta \cdot P_{\mathbf{DW}}(\text{conn}(e)).$$

Therefore,

$$\begin{aligned} \mathbb{E}_{\mathbf{DW}}[x_{\min}(T^* + t^*)] &\geq \mathbb{E}_{\mathbf{DW}}[x_{\min}(t^*)] + \epsilon \cdot (mq/2)^{N-1} \cdot P_{\mathbf{DW}}(\text{conn}(e)) \\ &> \mathbb{E}_{\mathbf{DW}}[x_{\min}(\infty)] - \frac{1}{8}(mq)^{N-1}\epsilon\delta \cdot P_{\mathbf{DW}}(\text{conn}(e)) + \frac{1}{8}(mq)^{N-1}\epsilon\delta \cdot P_{\mathbf{DW}}(\text{conn}(e)) \\ &= \mathbb{E}_{\mathbf{DW}}[x_{\min}(\infty)]. \end{aligned}$$

Because  $x_{\min}(t)$  is nondecreasing with  $t$ ,  $\mathbb{E}_{\mathbf{DW}}[x_{\min}(t)]$  is nondecreasing with  $t$ . We therefore know  $\mathbb{E}_{\mathbf{DW}}[x_{\min}(\infty)] \geq \mathbb{E}_{\mathbf{DW}}[x_{\min}(t^*)]$ , which contradicts the above inequality, as desired.  $\square$

Using Lemma IV.8, we show the following corollary:

**Corollary IV.8.1.** *For any model  $\mathbf{DW}$  of the form in Definition III.1, suppose that  $P(\text{conn}(e)) > 0$ . We then have that*

$$P_{\mathbf{DW}}(\text{consensus} | \text{conn}(e)) = P_{\mathbf{DW}}(\text{stab} | \text{conn}(e)) = 1.$$

*In particular, this implies that, for any model DW of the form in Definition III.1,*

$$P_{\mathbf{DW}}(\text{stab} | \text{conn}(e))P_{\mathbf{DW}}(\text{conn}(e)) = P_{\mathbf{DW}}(\text{conn}(e)).$$

*Proof.* We have that that  $P_{\mathbf{DW}}(\text{consensus} | \text{conn}(e)) < 1$  if and only if there exists some  $\epsilon > 0$  for which

$$\limsup_{t \rightarrow \infty} P_{\mathbf{DW}}(x_{\max}(t) - x_{\min}(t) \geq \epsilon | \text{conn}(e)) > 0.$$

Because  $P_{\mathbf{DW}}(x_{\max}(t) - x_{\min}(t) \geq \epsilon | \text{conn}(e))$  is nonincreasing with  $t$ , we conclude that  $P_{\mathbf{DW}}(\text{consensus} | \text{conn}(e)) < 1$  if and only if

$$\lim_{t \rightarrow \infty} P_{\mathbf{DW}}(x_{\max}(t) - x_{\min}(t) \geq \epsilon | \text{conn}(e)) > 0.$$

Because  $P(\text{conn}(e)) > 0$ , Lemma IV.8 implies that

$$\lim_{t \rightarrow \infty} P_{\mathbf{DW}}(x_{\max}(t) - x_{\min}(t) \geq \epsilon | \text{conn}(e)) = 0,$$

so  $P_{\mathbf{DW}}(\text{consensus} | \text{conn}(e)) = 1$ , as desired.  $\square$

We have shown that the adaptive-confidence DW model comes to consensus almost surely in the cases where  $\text{conn}(e)$  holds. In particular, consensus is an example of a limit state. Now we need to study the existence of a limit state in the case in which  $\text{sep}(e)$  holds. We state the following lemma, whose proof we defer to the Appendix B.4

**Lemma IV.9.** *Let  $n_0$  be some positive integer. Suppose that any model of the form in Definition III.1, with  $N < n_0$ , converges to a limit state almost surely. Then for any model of the form in Definition III.1 with  $N = n_0$ , we further have  $P_{\text{DW}}(\text{stab}, \text{sep}) = P_{\text{DW}}(\text{sep})$ .*

We are now ready to prove almost sure existence of a limit state in general.

**Theorem IV.3.** *For a fixed  $x(0) \in [0, 1]$ , let  $c$  be such that  $c(x) \geq b > 0$  for all  $x \in [0, 1]$ . Suppose further that  $x - c(x)$  is nondecreasing with respect to  $x$ . Then our adaptive-confidence DW model in Definition III.1 converges to a limit state almost surely.*

*Proof.* Let  $\text{stab}(\{e_i\}_{i=0}^{\infty})$  denote the statement that the DW model has a limit opinion state for the edge sequence  $\{e_i\}_{i=0}^{\infty}$ . We prove this by induction on the number of nodes. Observe that, for  $c(x)$  and an adaptive-confidence DW model with 1 node, the model converges to a limit state, and thus almost surely converges to a limit state.

Now suppose that, for all  $m \in \{1, \dots, m_0\}$ , an adaptive-confidence DW model on a network of  $m$  nodes, with confidence  $c$  and convergence parameter  $\mu$ , achieves a limit state almost surely. We now consider an adaptive-confidence DW model  $\text{DW}$  with a graph topology consisting of  $m_0 + 1$  nodes. By Lemma IV.9, we know that  $P(\text{stab}, \text{conn}) = P(\text{conn})$ . Additionally, recall from Lemma IV.8.1 that  $P(\text{stab}, \text{conn}) = P(\text{conn})$ . Combining these two facts, we obtain the following:

$$\begin{aligned} P(\text{stab}) &= P(\text{stab}, \text{conn}(e)) + P(\text{stab}, \text{sep}) \\ &= P(\text{conn}(e)) + P(\text{sep}(e)) \\ &= 1. \end{aligned}$$

This completes the proof. □

**Remark IV.1.** *In Lemma IV.6, the only assumptions on the confidence-bound function  $c(x)$  is that  $\inf_{x \in [0, 1]} c(x) > 0$  and that if the confidence-bound of node  $i$  decreases if the opinion of node  $i$  decreases (that is, if  $c(x_i)$  decreases then  $x_i$  decreases). However, we need not assume every node has the same confidence function; in particular, our model in Definition III.1 could be modified so that each node  $i$  has its own confidence-bound function,  $c_i : [0, 1] \rightarrow [0, 1]$ . Lemmas IV.7– IV.9 make no further use of  $c$ . As a result, Theorem IV.3 holds for any adaptive-confidence DW model with a heterogeneous confidence-bound as long as, for all  $i$ ,  $\inf_{x \in [0, 1]} c_i > 0$  and  $x - c_i(x)$  is nondecreasing in  $x$ . This generalizes the result from Chen et al. in [10, Theorem 1, Part i].*

**Remark IV.2.** *All the results in this section also hold in the case that  $x + c(x)$  is nondecreasing in  $x$ . This case only requires small adaptations to the proofs. For Lemma IV.6 one would need to adapt the definition of  $\text{dif}(\epsilon, d, s_0, s, e)$  and  $\text{DIF}(\epsilon, d, s, T, e)$  to reflect  $x_{\max}$  rather than  $x_{\min}$ . Lemma IV.7 would be adapted to show that*

$$\mathbb{E}_{\text{DW}}[x_{\max}(T)] < \mathbb{E}_{\text{DW}}[x_{\max}(0)] + \frac{1}{8}(mq)^{N-1}\epsilon\delta \cdot P_{\text{DW}}(\text{conn}(e)).$$

*From there, the above equation can be used to adapt the proof of Lemma IV.8. Subsequent results hold without any change.*

## D. Conjectures

In regards to confidence functions that do not lead to convergence to a limit state with probability one, the only functions that we have found that lead to such behavior are those that allow for one node to always have two nodes with confidence 0 within its confidence interval. This observation leads us to the following conjectures:

**Conjecture IV.1.** *For any graph topology and for a fixed  $x(0) \in [0, 1]$ , let  $c$  be such that  $\inf_{x \in [0, 1]} c(x) > 0$ . Then our adaptive-confidence DW model in Definition III.1 converges to a limit state almost surely.*

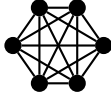
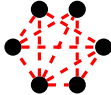
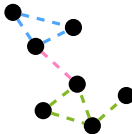
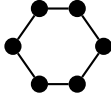
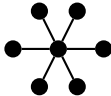
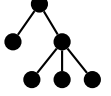
**Conjecture IV.2.** *For any graph topology and for a fixed  $x(0) \in [0, 1]$ , let  $c$  be continuous. Then our adaptive-confidence DW model in Definition III.1 converges to a limit state almost surely.*

## V. DETAILS OF AGENT-BASED SIMULATIONS

Equations (3) and (4) with three types of confidence-bound

In Section IV, we presented theoretical results for the existence of limiting behavior for our model described in

TABLE II: Summary of the definitions of the types of networks on which we study our adaptive-confidence DW model. The black solid lines represent deterministic edges, the dashed colored lines represent nondeterministic edges, where different colors indicate different probabilities. We give a more detailed definition of the SBM in Section VI B 3.

Network	Definition	Example	Parameters
$C(N)$	A complete graph $C(N)$ with $N$ pairwise adjacent nodes		$N \in \{10, 50, 100, 500, 1000\}$
$G(N, p)$	An Erdős-Rényi (ER) graph in which we choose each of the possible edges with independent, homogeneous probability $p$ [18, 19]		$N = 100, p \in \{0.1, 0.25, 0.5\}$
$G(N, \mathbf{P})$	A 2-community stochastic-block-model (SBM) graph, with nodes assigned to 2 communities with sizes $s_A, s_B$ ( $N = s_A + s_B$ ) and probability matrix $\mathbf{P} \in \mathbb{R}^{2 \times 2}$ for choosing possible edges between and within communities [20]		Specification 1: $s_A = 25, s_B = 75$ $P_{AA} = 0.7$ $P_{AB} = 0.002$ $P_{BB} = 0.5$ Specification 2: $s_A = 50, s_B = 50$ $P_{AA} = 0.5$ $P_{AB} = 0.002$ $P_{BB} = 0.5$
$C_2(N)$	A cycle graph with $N$ nodes		$N \in \{100, 500\}$
$S(N)$	A star graph with $N$ nodes; the central node has degree $N - 1$ and the other nodes are adjacent only to this central node		$N \in \{100, 500\}$
$T(N)$	A tree graph, which is connected and acyclic, chosen uniformly at random from the set of all trees with $N$ nodes		$N \in \{100, 500\}$

functions. First, on a complete graph, our model with any confidence-bound function with  $c(x) > \frac{1}{2+\mu}$  has probability 1 of reaching a limit state. Second, on any graph, when the confidence-bound function is monotone, our model is guaranteed to reach a limit state. Finally, on any graph, if the confidence-bound function has the property that  $x - c(x)$  is increasing, then the model converges to a limit state with probability 1.

With an understanding of the existence of a limit state for our model in certain cases, we now wish to understand how our model behaves at the limit state. To develop an understanding of our model's limit state behavior, we simulate our model using various graph types and confidence-bound functions. In this section, we specify the networks and confidence-bound functions we use in our experiments. In Section VI, we discuss our results and observations.

### A. Network Structures

To study the behavior at limit state of our adaptive-confidence model on different network topologies, we numerically simulate the model described by Equations (3) and (4) on complete graphs, Erdős-Rényi (ER) graphs, stochastic-block-model (SBM) graphs, star graphs, and ring graphs. We also numerically simulate our model on different confidence-bound functions; some of them have one parameter and others have two parameters. For each network on which we run simulations, we provide its definition, a graphical example, and its parameter specifications in Table II.

TABLE III: The one-parameter confidence-bound functions on which we run simulations.

Confidence-Bound Function	Description	Parameter	Example
$a \exp\left(\frac{-(x-0.5)^2}{2(0.1)^2}\right) + 0.5$	An adjusted Gaussian with mean 0.5, standard deviation 0.1, and height $a$	$a \in [-0.5, 0.5]$	
$0.5 \operatorname{sech}^2(a(x-0.5))$	A concave down bell curve with its peak at (0.5, 0.5) - where a lower $a$ corresponds to a flatter bell	$a \in [0, 10]$	

## B. Confidence-Bound Functions

We employ two categories of confidence-bound functions: one-parameter confidence-bound functions and two-parameter confidence-bound functions. In Table III, we specify the one-parameter confidence-bound functions, which include two hyperbolic-secant functions and an adjusted Gaussian function. In Table IV, we specify the two-parameter confidence-bound functions, which include a parabolic, a cosine, and a piecewise-linear function. In Tables III and IV, the ‘‘Parameter(s)’’ columns indicate the range of values tested for each parameter. For a parameter  $p \in [l, r]$ , we choose a discrete set,  $P$ , of parameter values in the range:

$$P = \{p_n : p_n = l + n\Delta s, \quad n \in \{0, 1, \dots, 29\},$$

where  $\Delta s = \frac{r-l}{29}$ . For each confidence-bound function, we run our numerical simulations using these 30 equally spaced values within the given range for each parameter.

## C. Simulation Specifics

To highlight the role of the confidence-bound function, we set the compromise parameter to  $\mu = 0.5$  throughout all of our numerical experiments. In our adaptive-confidence DW-model simulations on a network with  $N$  nodes, we terminate our simulations when the opinions of all nodes change by less than 0.02 for  $10N$  iterations in a row. That is, the simulation terminates if  $|x_i(t) - x_i(t+1)| < 0.02$  for all  $x_i \in V$  for  $t \in \{t_k, t_k + 1, \dots, t_k + 10N\}$ .

One of the major goals of our numerical simulations is to measure whether the system comes to consensus (1 opinion cluster), polarization (2 opinion clusters), or fragmentation (more than 2 opinion clusters). We calculate two quantities

to measure this. Following Li and Porter [12], we calculate the Shannon entropy of the system at termination time. Suppose that the system contains  $K$  final opinion clusters labeled  $S_r$  with  $r \in \{1, 2, 3, \dots, K\}$ . Shannon entropy is

$$H = - \sum_{r=1}^K \frac{|S_r|}{N} \ln \left( \frac{|S_r|}{N} \right). \quad (12)$$

Intuitively, a low entropy suggests consensus and high entropy indicates fragmentation. When  $H = 0$ , the model is at consensus; when  $H > \ln(2) \approx 0.6931$ , the model is guaranteed to reach fragmentation; when  $0 < H < \ln(2)$ , the model can be either be in a polarized state or fragmented state.

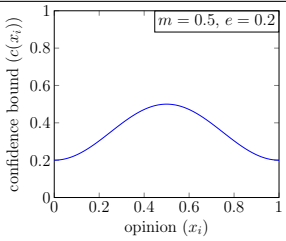
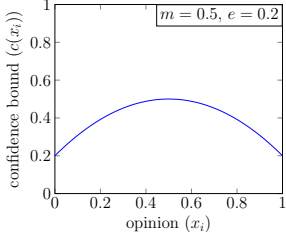
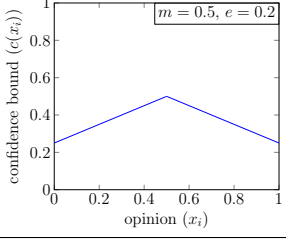
When we want to focus on whether or not a population reaches consensus, we measure the ratio of size of the largest opinion cluster to the total number of nodes:

$$R = \frac{\max_r |S_r|}{N}. \quad (13)$$

since our model is inherently stochastic, we are unable to definitively say when a simulation of our model using confidence-bound function surely comes to consensus. Rather, we say that an experiment results in likely consensus if the resulting mean value of  $R$  for an experiment is within one standard deviation of  $R = 1$ .

To determine the final opinion clusters, we develop an algorithm that accounts for both the final opinions and the underlying network structure. We account for the asymmetry in our update rule (Equations (3) and (4)) by first generating a directed graph i.e. a digraph  $G' = (V, E')$ , where we replace every edge  $\{i, j\} \in E$  with two edges  $(i, j), (j, i) \in E'$ . For each edge,  $(i, j)$ , in the digraph we remove the edge from the graph if  $|\Delta_{i,j}| < c(x_j(t_{\text{termination}}))$  where  $t_{\text{termination}}$  is the time step that we terminate the simulation at. We de-

TABLE IV: The two-parameter confidence-bound functions on which we run simulations.

Confidence-Bound Function	Description	Parameters	Example
$-\frac{m-e}{2} \cos(2\pi x) + \frac{m+e}{2}$	A cosine wave with period 1, with $c(0.5) = m$ and $c(0) = c(1) = e$	$m, e \in [0.01, 0.5]$	
$-4(m-e)x^2 + 4(m-e)x + e$	A parabola, with $c(0.5) = m$ and $c(0) = c(1) = e$	$m, e \in [0.01, 0.5]$	
$2 x - 0.5 (e - m) + m$	a piecewise-linear function, with $c(0.5) = m$ and $c(0) = c(1) = e$	$m, e \in [0.01, 0.5]$	

fine a cluster as a strongly connected component within this digraph.

## VI. AGENT-BASED SIMULATION RESULTS

### A. One-Parameter Confidence-Bound Functions

In our experiments, we restrict our attention to functions that are symmetric about  $x = 0.5$ . This restriction allows us to explore a scenario in which the opinion of the agents depends on their distance from the center of the opinion space. With this restriction in mind, we first explore confidence-bound functions whose behavior is dependent on a single parameter,  $a$ . For these one-parameter functions, we are interested in determining a region for  $a$  where consensus is guaranteed. We list the functions and their descriptions in Table III. To determine these regions of guaranteed consensus, we choose a graph structure and simulate our adaptive-confidence DW model 10 times. For the adjusted Gaussian function, we test  $a \in [-0.5, 0.5]$ ; for the hyperbolic-secant function, we test value of  $a \in [0, 10]$ . We track the mean and standard deviation of ratio,  $R$  (as defined in Equation (13)), of the size of the largest opinion cluster to the total number of nodes across these 10 runs.

We first consider the adjusted Gaussian confidence-bound

function family. For this family of functions, the parameter  $a$  corresponds to the value at the middle of the opinion space. In Figure 1a, we plot the results of our numerical experiment; the different colored curves represent the results of our experiments using different graph structures. For each curve, we display the mean value of  $R$  that we observed with a marker. We also display a shaded region that indicates one standard deviation in either direction of the mean for that experiment. For all the  $a$  values we use in our simulations, we observe likely consensus everywhere except  $a = -0.5$  for all three networks. The standard deviation for all three curves is not noticeable, implying that the likelihood of achieving a simulation achieving non-consensus using an adjusted Gaussian confidence-bound function with  $a \neq 0$  is small.

The results of the experiments on the Gaussian confidence-bound function family suggest that the ability of the system to come to consensus is not very sensitive to the value of the confidence bound toward the center of the opinion space. This outcome may have been different had the extremes of the opinion space had different confidence bounds, which is a possibility we explore in Section VI B.

To test the sensitivity of consensus formation at a limit state to the confidence bounds at the extremes of the opinion space, we explore the hyperbolic-secant confidence-bound function family. For this family of functions, we fix the confidence bound of the center of the opinion as  $c(0.5) = 0.5$ . When  $a = 0$ , the confidence-bound function is the line

$c(x) = 0.5$ . I.e., when  $a = 0$ , we are simulating the standard DW model with a confidence bound of 0.5. As we increase  $a$ , the magnitude of the slope increases and the confidence bound at the extremes of the opinion space decreases. We display the results of this experiment in Figure 1b. We observe that as the function approaches a spike at  $x = 0.5$ , the size of the largest opinion cluster decreases. Since the size of the largest opinion cluster is decreasing as  $a$  increases, but the number of agents is held constant at  $N = 100$ , we must have more opinion clusters forming as  $a$  increases. Thus we observe increased levels of fragmentation as  $a$  increases.

## B. Two-Parameter Confidence-Bound Functions

We experiment with three two-parameter confidence-bound functions in Table IV and with all six graph types in Table II. We now consider confidence-bound functions that are characterized by the confidence bound at the center of the opinion space ( $m$ ) and at the extremes of the opinion space ( $e$ ) in our simulations. Let  $S$  be a set of thirty evenly spaced points in the interval  $[0.01, 0.5]$ . For each simulation of our adaptive-confidence DW model, we generate 10 graphs; for each of these graphs, we uniformly randomly sample  $\mathbf{x}(0)$  from  $[0, 1]^{100}$ . For each point  $(m, e) \in S^2$ , we simulate our adaptive-confidence DW model until termination (see Section V C). We then calculate the mean Shannon entropy across these simulations. We indicate the observed mean entropy in a heatmap. Each cell in the heatmap shows the results of an experiment that was run using the corresponding  $m$  and  $e$  values. We also track the mean time until our simulations terminated and display them in a similar fashion to the entropy.

### 1. The Complete Graph

To explore the behavior at limit state for our adaptive DW model, we begin by performing numerical simulations on a complete graph. It has been demonstrated numerically on a complete graph that the standard DW model undergoes a transition from the limit state being in a polarized or fragmented state when  $c < 0.5$  to the limit state being at consensus when  $c \geq 0.5$  [21]. Here, we are interested in if our system undergoes a similar transition from a fragmented/polarized state to consensus for certain choices of our parameters,  $m$  and  $e$ .

In Figure 2, we show the mean Shannon entropy for 10 simulations of our adaptive-confidence DW model on a complete graph, using the two-parameter confidence-bound functions and parameter values described in Table IV. Along the diagonal of the heatmap in Figure 2 is the observed mean entropy of our numerical simulations using confidence-bound functions where  $m = e$ . All of the two-parameter confidence-bound functions that we experiment with are horizontal lines when  $m = e$ . Hence, the diagonal of our heatmaps in this

section correspond to the mean entropy that we observed for standard DW model where the confidence bound,  $c$ , is such that  $c = m = e$ .

Figure 2 shows that the mean entropy is not symmetric across the line  $m = e$ . For any of the three confidence-bound function families, we observe the highest mean entropy occurs when both  $m$  and  $e$  are less than approximately 0.09. When  $e$  is less than approximately 0.09 and  $m$  is greater than roughly 0.35, the piecewise-linear family yields a lower mean entropy than the cosine and parabolic families. We note that for the cosine confidence-bound function, the region where  $e$  is less than approximately 0.09 does not have any obvious groups of low mean entropy results (i.e., there are no groups of black cells in this region). Similarly, for the parabolic confidence-bound function, we observe no obvious groups of low entropy when  $e$  is approximately less than 0.18. We also see that for  $m$  values lower than roughly 0.26, there are no clear groups of low entropy results for experiments performed with either the cosine and piecewise-linear confidence-bound functions.

The existence of regions where we observe almost no groups of low entropy results suggests that for all of our two-parameter confidence-bound functions, there are minimum values of both  $m$  and  $e$  that are required for the our adaptive-confidence model to achieve consensus. However, the fact that the regions where we are unable to find groups of low entropy are different for different confidence-bound functions suggests that the threshold values for  $m$  and  $e$  are not the same across different confidence-bound functions.

In Figure 2, we are also able to analyze the “fronts” of consensus. Loosely, a consensus front is the boundary between zero and nonzero entropy. In Figure 2, this is the edges between a purple cell and a black cell. The fronts of consensus for both the parabolic and piecewise-linear confidence-function family appear roughly linear. We observe that the front for the piecewise-linear confidence-function family has a steeper slope than the parabolic confidence-function family. The cosine front appears to be nonlinear.

We show the mean time until we terminated our simulations for different values of  $m$  and  $e$  in Figure 3. We observe that the cosine confidence-bound function family converges in fewer steps than the piecewise-linear or parabolic confidence-bound function family. We also notice that, as was the case for the mean entropy results, the mean time until termination is not symmetric across the line  $m = e$ . For any fixed value of  $m$ , we observe a decrease in mean time until convergence as  $e$  increases. Similarly, for any fixed value of  $e$ , we observe a decrease in the mean time until convergence as  $m$  increases.

### 2. Erdős-Rényi (ER) Graphs

On Erdős-Rényi (ER) graphs, it is known that for standard DW model the transition points for the confidence bound are the same as for complete graphs, but that con-

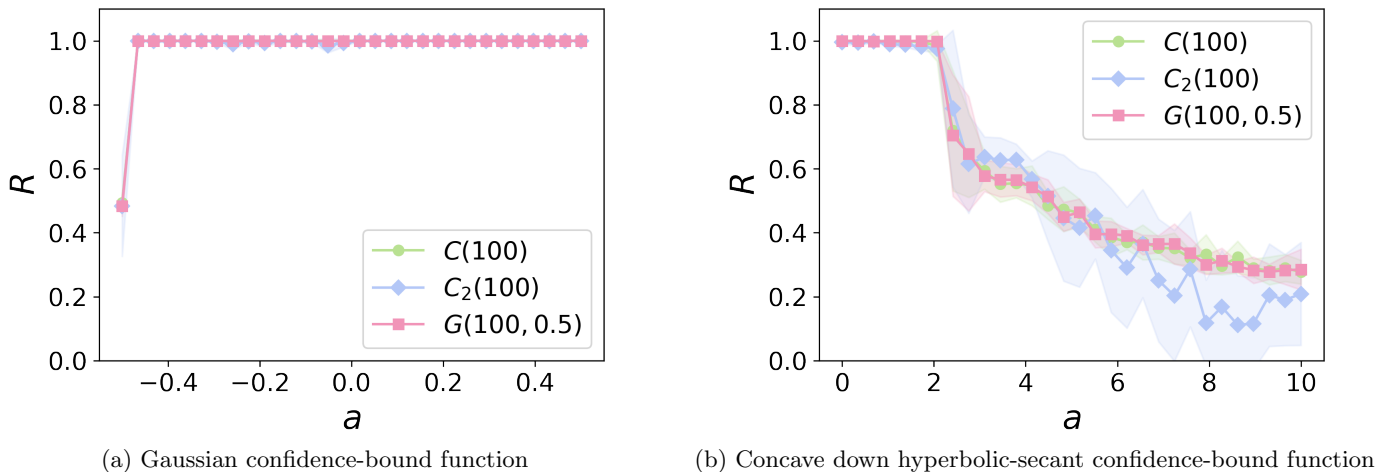


FIG. 1: The mean ratio  $R$  of the size of the largest opinion cluster and total node count versus the parameter  $a$  for the one-parameter confidence-bound functions from Table III. Each point is the mean value of  $R$  over 10 simulations. The shaded region corresponds to one standard deviation in each direction from the mean. For each confidence-bound function family, we test 30 uniformly spaced values of  $a$  within the intervals from Table III. Each curve corresponds to a different graph topology and uses the notation from Table II.

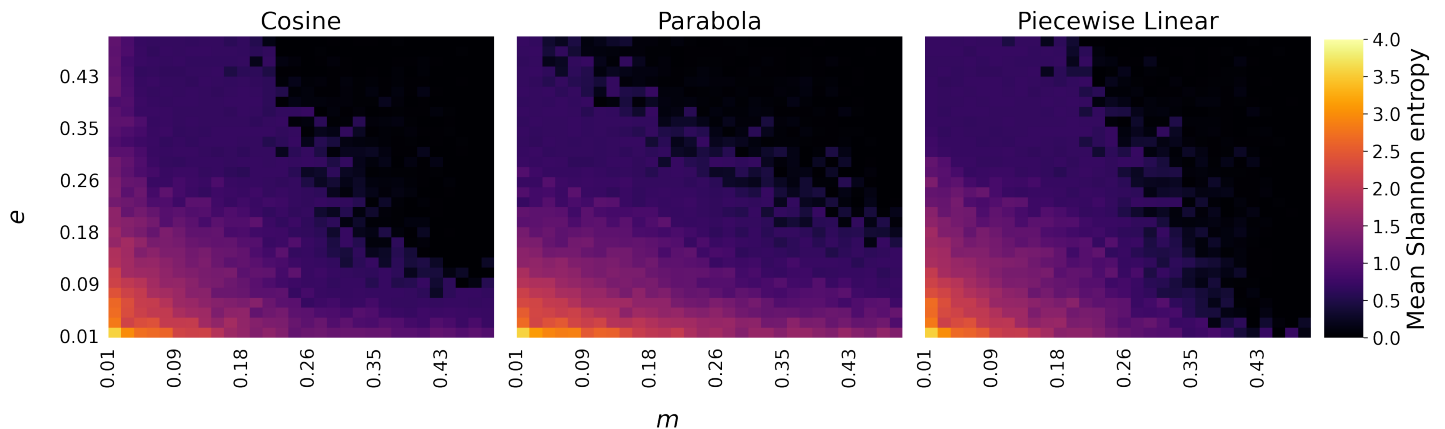


FIG. 2: Mean Shannon entropy at limit state for simulations of our adaptive-confidence DW model on a 100-node complete graph using the (left) cosine, (center) parabolic, and (right) piecewise-linear confidence-bound function families. For each confidence-bound function family, we consider 30 evenly spaced values of  $m$  and  $e$  in the interval  $[0.01, 0.5]$ . Each cell indicates the mean Shannon entropy across 10 simulations of our adaptive-confidence DW model.

vergence times of DW simulations using ER graphs are often lower than for DW simulations using the complete graph [5]. We demonstrate that similar trends exist for our adaptive DW model.

Figure 4 shows the mean Shannon entropy we observed for numerical simulations of our adaptive-confidence DW model on ER graphs using two different connection probabilities and the confidence-bound function families in Table IV. In Figure 4, we observe much larger entropy when  $p = 0.1$  than we do when  $p = 0.5$  or for the complete graph (i.e.  $p = 1$ ). We suspect that this is because of the definition of an opinion

cluster. In our definition of an opinion cluster, all nodes of an opinion cluster must be in a strongly connected component of the effective graph (described in Section III). Therefore, the number of opinion clusters is upper bounded by the number of strongly connected components in the digraph that is created by replacing all edges in the graph that we simulate our adaptive-confidence model on with two edges facing opposite directions. Since ER graphs with  $p = 0.1$  are likely to have less edges than ER graphs with a greater value of  $p$ , we also expect ER graphs with  $p = 0.1$  to have a smaller upper bound on the number of opinion clusters at the limit

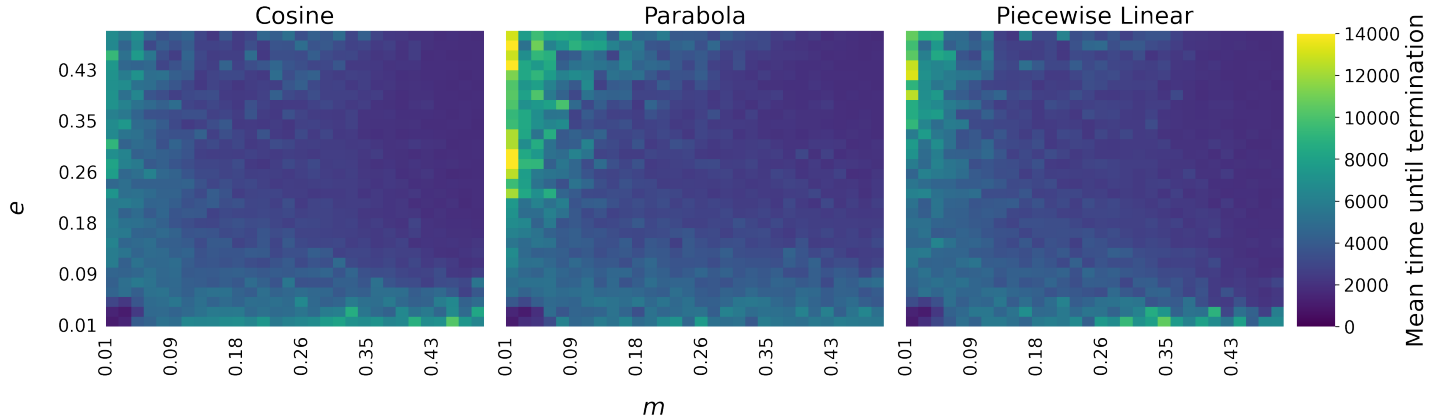


FIG. 3: Mean number of steps until termination for simulations of our adaptive-confidence DW model on a 100 node complete graph using the (left) cosine, (center) parabolic, and (right) piecewise-linear confidence-bound function families. For each confidence-bound function family, we consider 30 evenly spaced values of  $m$  and  $e$  in the interval  $[0.01, 0.5]$ . Each cell displays the mean time until termination across 10 simulations of our adaptive-confidence DW model.

state. We also note that while we observe lower mean entropy values for simulations using ER graphs than for simulations using a complete graph, we also observe that the consensus fronts across all confidence-bound families appear similar to the fronts we observed for the complete graph experiments in Figure 2. Thus, our results for the mean entropy suggest that the values of  $m$  and  $e$  required for consensus when simulating our adaptive-confidence model on an ER graph are similar to the values of  $m$  and  $e$  required for consensus when simulating our adaptive-confidence model on a complete graph.

As we did for complete graphs, we study the convergence times for our simulations using ER graphs. We show the mean time until termination for our numerical simulations in Figure 5. As is true for the standard DW model, we observe smaller convergence times for smaller choices of  $p$ . For  $p = 0.1$ , the convergence heatmaps differ from the heatmaps in Figure 3. The values of  $m$  and  $e$  that result in long convergence time are now more concentrated around regions where either  $m$  or  $e$  is small (less than approximately 0.09). When  $p = 0.5$ , the fronts follow the patterns that we observed in the complete graph experiments in Figure 3.

We observe from Figure 5 that as  $p$  decreases, we observe longer times until termination (indicated by brighter colors across each of the three heatmaps). However, we also notice for experiments that used  $e = 0.01$ , the maximum mean time until termination is smaller for the experiments using an ER graph with  $p = 0.1$  than for the experiments that use an ER graph with  $p = 0.5$ . This phenomenon is interesting because it suggests that there exists confidence-bound functions that violate the pattern observed in the standard DW model where lower values of  $p$  increases the time until our adaptive-confidence model converges.

### 3. Stochastic-Block-Models graphs

A stochastic block model (SBM) is a generative model that produces random graphs, which tend to have underlying community structures. We focus on 2-community SBMs in this paper, community  $A$  and  $B$ . Let the number of nodes in community  $A$  be  $s_A$  and the number of nodes in community  $B$  be  $s_B$ . We construct our SBM by specifying  $s_A$ ,  $s_B$ , and a probability matrix  $\mathbf{P}$ . For an undirected SBM with  $n$  communities, its probability matrix is symmetric and has size  $n \times n$ . Each element in the probability matrix defines the edge probability between a node in one community and a node in the other community. That is, the diagonal entries of the block probability matrix are the edge probabilities within communities and the rest are the edge probabilities between communities. In our experiments, we employ 2 combinations of community sizes and block probability matrices. The probability matrix is symmetric with 4 elements:

$$\mathbf{P} = \begin{pmatrix} P_{AA} & P_{AB} \\ P_{BA} & P_{BB} \end{pmatrix},$$

where  $P_{AB} = P_{BA}$ .

As we indicated in Table II, we have 2 specifications for SBM graphs and both have 100 nodes. Specification 1 has communities with  $s_A = 25$  nodes and  $s_B = 75$  nodes, with  $P_{AA} = 0.7$ ,  $P_{AB} = 0.002$ , and  $P_{BB} = 0.5$ . Let the SBM graph with the first specification be  $\text{SBM}_1$ . Specification 2 has communities with  $s_A = 50$  nodes and  $s_B = 50$  nodes, with  $P_{AA} = 0.5$ ,  $P_{AB} = 0.002$ , and  $P_{BB} = 0.5$ . Let the SBM graph with the second specification be  $\text{SBM}_2$ .

In Figure 6, we observe that the entropy heatmaps for (top)  $\text{SBM}_1$  and (bottom)  $\text{SBM}_2$  are similar to each other for each confidence-bound function. In Figure 6, we notice that there are more cells of different colors that border one another in the results of our experiments that use  $\text{SBM}_1$  than

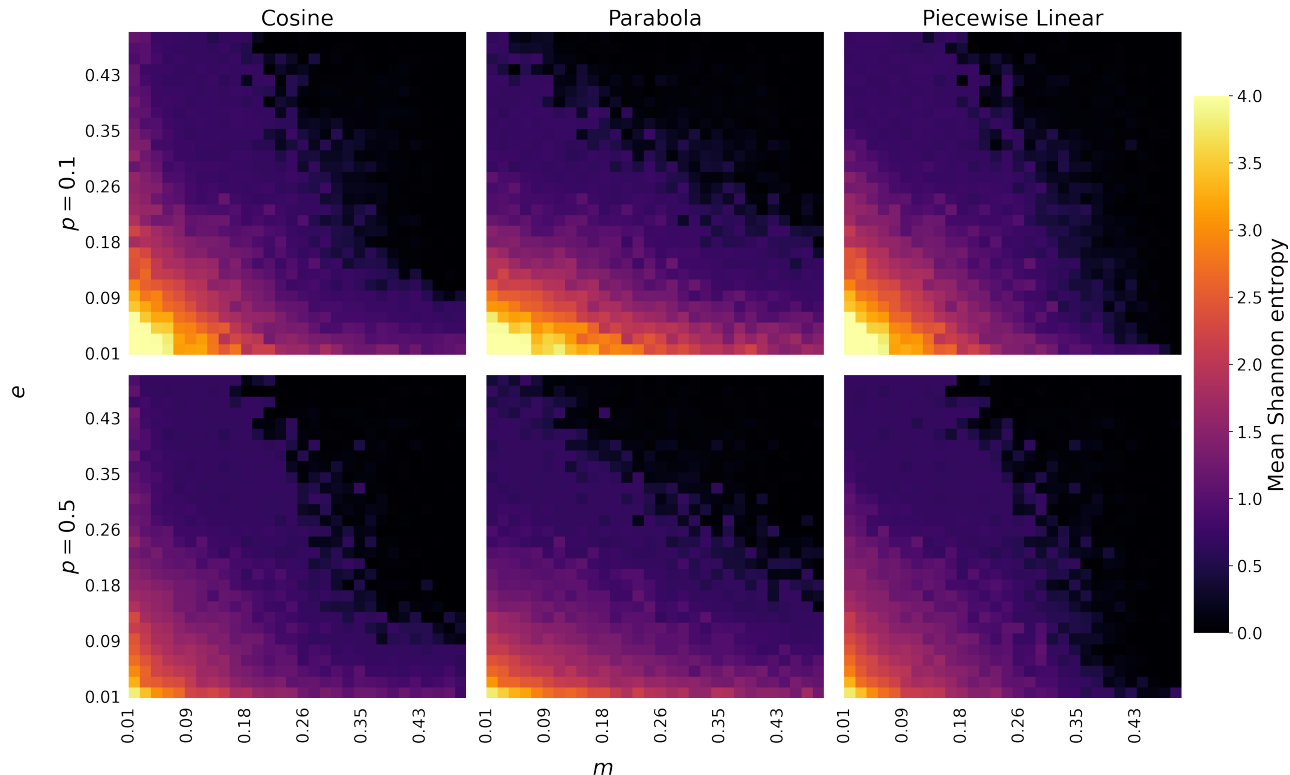


FIG. 4: Mean Shannon entropy at limit state for 10 simulations of our adaptive-confidence DW model on 100 node ER graphs. Here we test (top)  $p = 0.1$  and (bottom)  $p = 0.5$ . For confidence-bound functions, we use the (left column) cosine, the (center column) parabolic, and the (right column) piecewise-linear confidence-bound function families. We consider 30 evenly spaced values of  $m$  and  $e$  in the interval  $[0.01, 0.5]$ . Each cell indicates the mean Shannon entropy across 10 simulations of our adaptive-confidence DW model.

there are in the results of our experiments that use  $\text{SBM}_2$ . As we observed for ER graphs, entropy is generally higher for graphs where the density of edges within the graph is higher. This is supported by the observation that the mean entropy is generally lower in results using the  $\text{SBM}_1$  graph than in the results using the  $\text{SBM}_2$  graph and each entry in the probability matrix in  $\text{SBM}_1$  ( $P_{AA} = 0.7$ ,  $P_{AB} = 0.002$ , and  $P_{BB} = 0.5$ ) is greater than or equal to the entry in the probability matrix in  $\text{SBM}_2$  ( $P_{AA} = 0.5$ ,  $P_{AB} = 0.002$ , and  $P_{BB} = 0.5$ ).

Unfortunately, we cannot draw many further conclusions from this comparison because the 2 specifications not only have different number of nodes in the 2 communities, but also have different probability matrices. In the future, we plan to conduct more experiments where we only change the probability matrix or the partition of nodes.

When comparing with the complete and ER graphs, we see that the overall trend remains the same, but the mean Shannon entropy is higher overall. In the future, we plan to track the number of edges our SBM and ER graphs have so that we can have a more direct comparison of the 2 graph types and how the number of edges may affect the final mean Shannon entropies.

The convergence times for the SBM in Figure 7 do not resemble the results for convergence times of experiments that use any other of the graph types that we have examined thus far. We are unable to observe any clear pattern for the convergence times of the cosine, parabolic, or piecewise-linear functions. We do still observe higher convergence times for the SBM with lower probabilities of connection ( $\text{SBM}_2$ ). The transition of mean time until termination from low to high is also much less smooth than in past graph types. The parabolic confidence-bound function has a region of very little change in mean time until termination for small  $e$  (between roughly 0.09 and 0.18), which is not true for the cosine or piecewise-linear confidence-bound function families.

#### 4. Cycle Graph

For each type of graph thus far, we have observed the same general patterns for Shannon entropy and consensus fronts. This perhaps suggests that the confidence-bound function is more influential than the graph topology on the limit-state behavior. However, this is not always the case. One graph type where we observe different behavior is a cycle

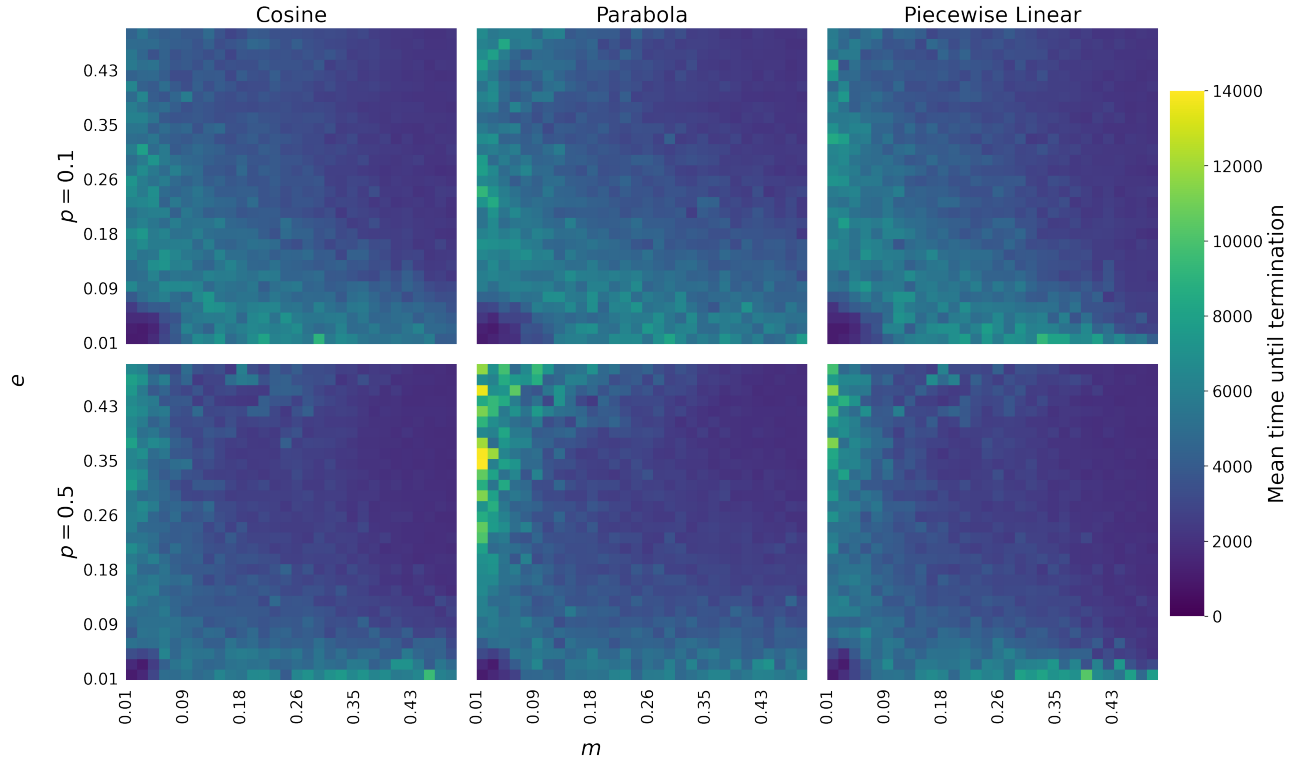


FIG. 5: Mean number of steps until termination for 10 simulations of our adaptive-confidence DW model on 100 node ER graphs. We again test (top)  $p = 0.1$  and (bottom)  $p = 0.5$  and the (left) cosine, (center) parabolic, and (right) piecewise-linear confidence-bound function families. For each confidence-bound function, we consider 30 evenly spaced values of  $m$  and  $e$  in the interval  $[0.01, 0.5]$ . Each cell indicates the mean time until termination across 10 simulations of our adaptive-confidence DW model.

graph. In Figure 8, we show the entropy at limit-state for our numerical simulations using a cycle graph and the two-parameter confidence-bound functions in Table IV.

In Figure 8, the consensus front does not at all resemble those in the previous types of graphs. We also observe much less variation in behavior across the confidence-bound function families, which suggests that graph types can significantly influence limit-state behavior. While the results using the cosine and piecewise-linear confidence-bound function families are more similar to each other than they are to the results for the parabola confidence-bound function family, the differences between all three confidence-bound families' results are more difficult to observe than they have been in the results that used the previous graph types.

The results of the termination time (see in Figure 9) for a cycle graph also does not resemble any of the converge time results seen so far. The largest convergence times for simulations using the cycle graph occur when either  $m$  or  $e$  are large, which is the opposite of the results found for experiments using the complete and ER graphs (Figures 3 and 5).

### 5. Star Graph

We now consider a star graph. In Figure 10, we demonstrate the results of our entropy experiments using a star graph and the confidence-bound functions from Table IV. We observe that the Shannon entropy at any cell is often much higher than the Shannon entropy at the cell in the same position in the heatmaps of our results of experiments using the complete or ER graphs. The behavior of the fronts also differs from the behavior of the fronts observed in our experiments on the previous graph types. While the fronts in Figure 10 do resemble the fronts in Figure 2, there are numerous differences. We observe that while the fronts in Figure 2 often exist between purple and black cells, the fronts in Figure 10 are between both purple and black cells as well as orange and black cells. Moreover, we notice that the mean entropy results for the piecewise-linear and cosine confidence-bound families show a region of purple cells protruding into a region of black cells.

We display the mean time until we terminated our simulations in Figure 11. The termination time results suggest that simulations that use a parabolic confidence-bound function take longer to converge than simulations that use either

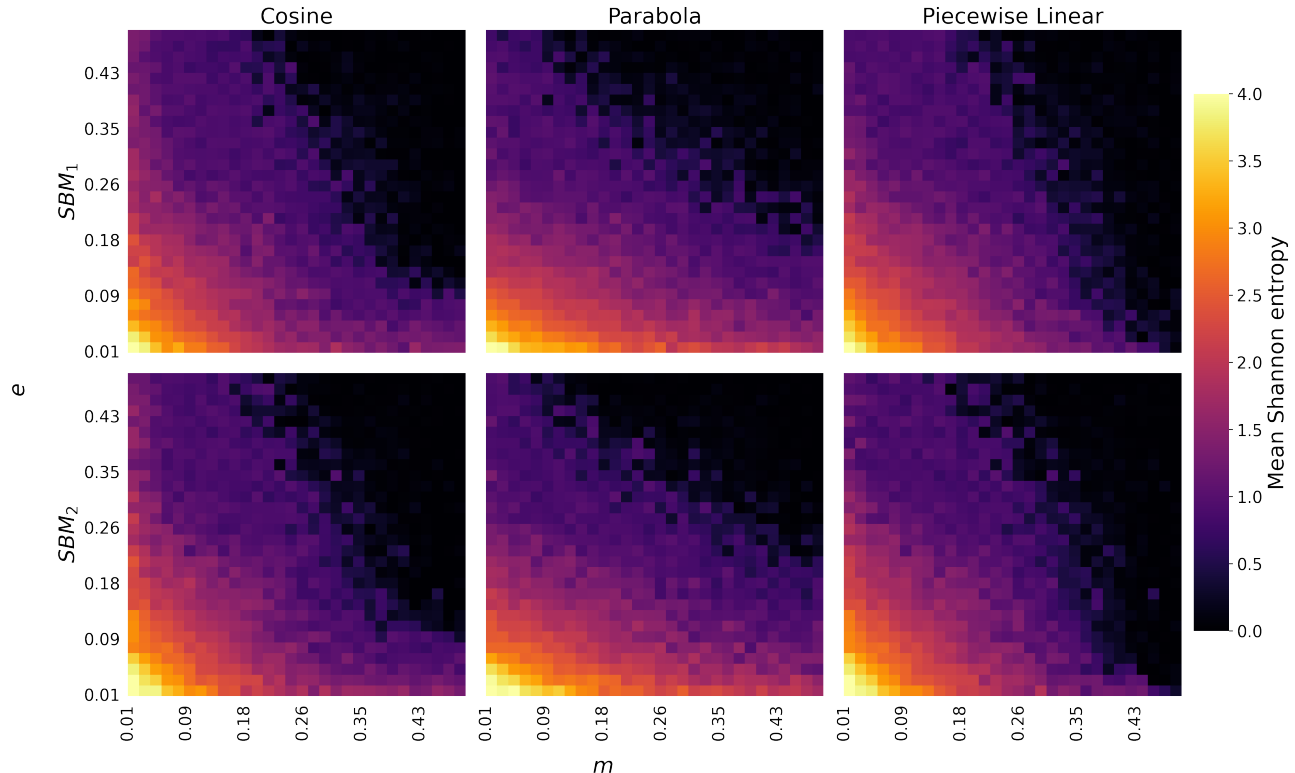


FIG. 6: Mean Shannon entropy at limit state for 10 simulations of our adaptive-confidence DW model on 100 node SBM graphs. Here we specifically test (top)  $SBM_1$  with community sizes of 25 and 75, with  $P_{AA} = 0.7$ ,  $P_{AB} = 0.002$ , and  $P_{BB} = 0.5$  and (bottom)  $SBM_2$  with community sizes of 50 and 50, with  $P_{AA} = 0.5$ ,  $P_{AB} = 0.002$ , and  $P_{BB} = 0.5$ . For confidence-bound functions we use the (left column) cosine confidence-bound function family, the (center column) parabolic confidence-bound function family, and the (right column) piecewise-linear confidence-bound function family. We consider 30 evenly spaced values of  $m$  and  $e$  in the interval 0.01 and 0.5. Each cell indicates the mean Shannon entropy across 10 simulations of our adaptive-confidence DW model.

a cosine or piecewise-linear confidence-bound function. We observe in the results of our experiments that use any of three confidence-bound function families that as  $e$  increases, the resulting termination time increases. However, for values of  $e$  that are close to 0.5, we notice that termination time tends to decrease with an increase in  $m$ . However, for  $e$  values that are close to 0, the termination time tends to increase with an increase in  $m$ .

### 6. Tree Graphs

Finally, we explore random tree graphs. In Figure 12, we plot the results of the entropy experiments for all 3 confidence-bound functions in Table IV.

In Figure 12, we increase the color bar maximum to be 4.5 instead of 4 because the limit-states of the 10 simulations on random tree graphs produce a higher mean Shannon entropy than simulations that use complete, ER, SBM, or star graphs. If we consider all 6 graph types we used in our experiments, the heatmaps for random tree graphs (Figure 12)

and cycle graphs (Figure 8) are the most similar. While the entropy gradually decreases as  $m$  and  $e$  increase, the transition to consensus does not occur until we approach high  $m$  and  $e$  values. Comparing the effect of confidence-bound functions on the mean entropy for experiments using random tree graphs, we observe that the simulations that use parabola or piecewise-linear functions have similar entropy results, where their entropies decrease to values close to 0 as  $m$  approaches 0.5 even with small  $e$  values. However, the cosine function is much more sensitive to high  $m$  values than the other 2 confidence-bound functions. Unlike our previous observations where the parabola tends to be the one standing out, our random tree graphs tell us a different story.

The confidence-bound functions affect the mean time until termination (Figure 13) similarly to the mean Shannon entropies. The heatmaps for experiments using parabolic and the piecewise-linear confidence functions resemble each other, but the cosine graph takes much longer to converge for low values of  $m$ . With low values of  $e$ , however, the parabola and the piecewise-linear take much longer to converge. For all three plots in Figure 13, we observe a slight

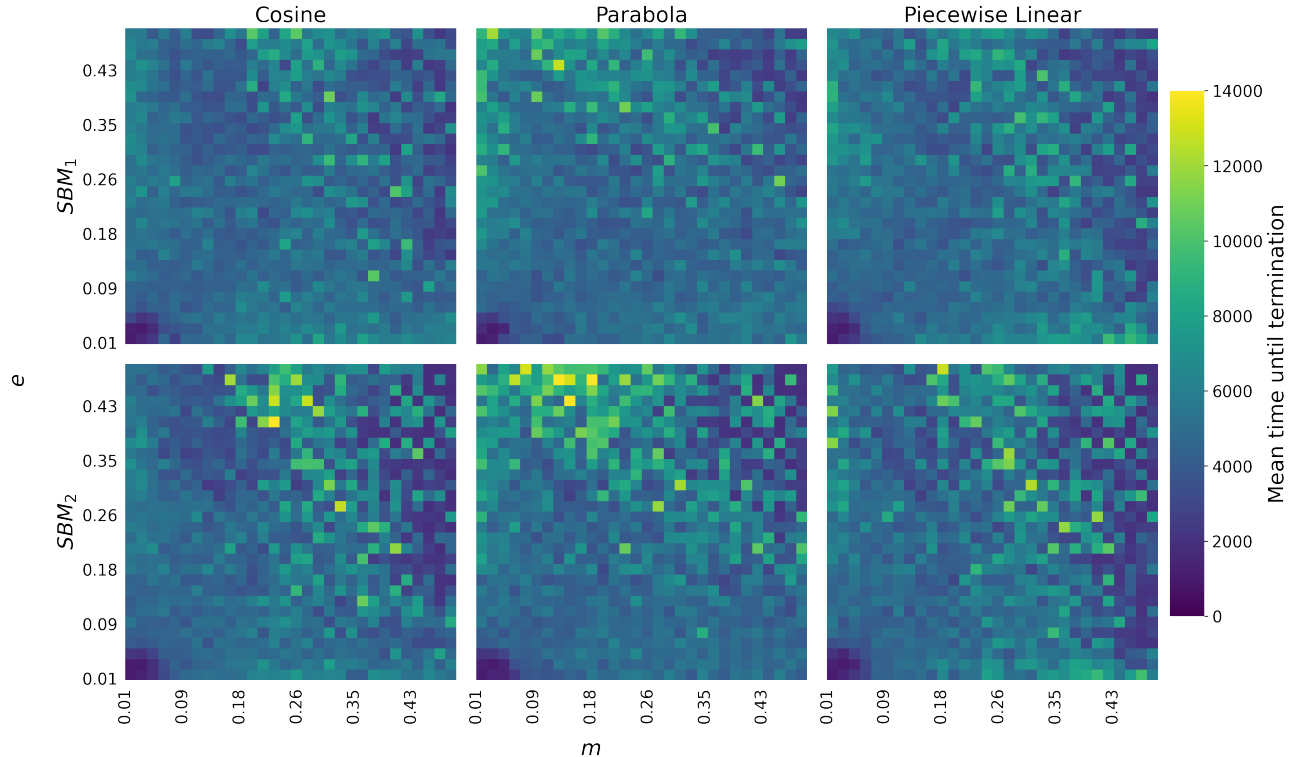


FIG. 7: Mean number of steps until termination for 10 simulations of our adaptive-confidence DW model on 100 node SBM graphs. We again test (top)  $SBM_1$  with community sizes of 25 and 75, with  $P_{AA} = 0.7$ ,  $P_{AB} = 0.002$ , and  $P_{BB} = 0.5$  and (bottom)  $SBM_2$  with community sizes of 50 and 50, with  $P_{AA} = 0.5$ ,  $P_{AB} = 0.002$ , and  $P_{BB} = 0.5$  and the (left) cosine, (center) parabolic, and (right) piecewise-linear confidence-bound function families. For each confidence-bound function, we consider 30 evenly spaced values of  $m$  and  $e$  in the interval  $[0.01, 0.5]$ . Each cell displays the mean time until termination across 10 simulations of our adaptive-confidence DW model.

decrease in mean time until convergence when  $m$  and  $e$  are both near 0.26, which is essentially the standard DW model with a constant confidence bound of 0.26. In previous graphs, even when entropy heatmaps look similar, such as the ER and SBM graphs, their convergence time look very different. However, by comparing Figure 9 and Figure 13, we see that the heatmaps for convergence also share similar features: higher  $e$  values correspond to high mean time until termination.

## VII. A MEAN-FIELD THEORY FOR THE ADAPTIVE-CONFIDENCE DW MODEL

A mean-field theory allows us to approximate a stochastic model and gain insight into the overall behavior of such a model [22]. For the DW model, instead of simulating indi-

vidual interactions at each time step with edge selections, the mean-field model considers an “average” interaction among all agents in a continuous time range [23]. The model is helpful for understanding the behavior of dynamical processes on networks as the network size tends towards infinity.

We adapt the degree-based mean-field equations of Fennell et al. [1] to our adaptive-confidence DW model. At each time step, a node’s confidence bound  $c(x)$  updates based on some function of the node’s opinion. The mean-field equation is an equation of motion for a probability density function (PDF)  $P(x, t) : [0, 1] \rightarrow \mathbb{R}$ , which maps the opinion space to  $\mathbb{R}$ . By definition, at each time step  $t$ , the area under the entire curve of the PDF is equal to 1. In this section, we discuss the master equation that governs the opinion densities; we give the full derivation in Appendix A.

The degree-class  $k$  is defined as all the nodes with degree  $k$ . For every degree-class  $k$ , we have the partial integro-differential equation

$$\frac{\partial P_k(x, t)}{\partial t} = \sum_l \frac{2q_k q_l \pi_{kl}}{\gamma} \left( \int_{|x-y| < c(y)\mu} \frac{1}{\mu} P_k(y, t) P_l \left( y + \frac{1}{\mu}(x-y), t \right) dy - \int_{|x-y| < c(x)} P_k(x, t) P_l(y, t) dy \right). \quad (14)$$

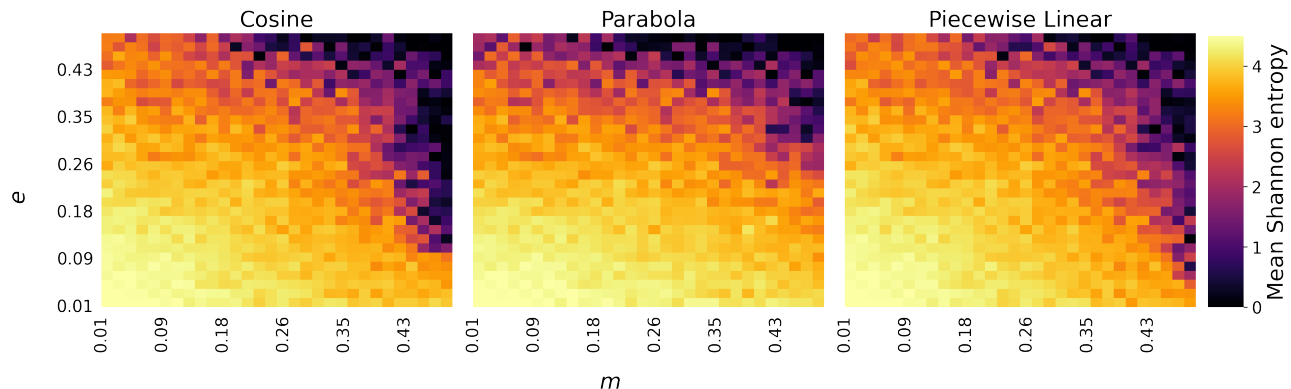


FIG. 8: Mean Shannon entropy at limit state for 10 simulations of our adaptive-confidence DW model on a 100-node cycle graph. For confidence-bound functions we use the (left) cosine, (center) parabolic, and (right) piecewise-linear confidence-bound function families. We consider 30 evenly spaced values of  $m$  and  $e$  in the interval  $[0.01, 0.5]$ . We show the mean Shannon entropy across 10 simulations in each cell. Note here that the  $y$ -limits are from 0 to 4.5 rather than the usual 0 to 4.

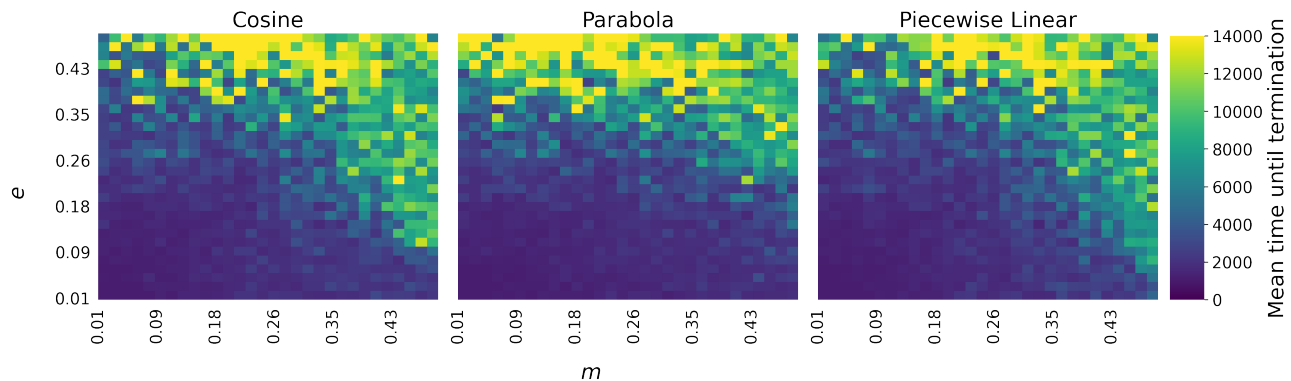


FIG. 9: Mean number of steps until termination for 10 simulations of our adaptive-confidence DW model on a 100-node cycle graph. We test the (left) cosine, (center) parabolic, and (right) piecewise-linear confidence-bound function families. For each confidence-bound function, we consider 30 evenly spaced values of  $m$  and  $e$  in the interval  $[0.01, 0.5]$ . Each cell indicates the mean Shannon entropy across 10 simulations.

Equation (14) uses the following notation:

- $P_k(x, t)$ : the density of nodes with opinion  $x$  at time  $t$  among the degree- $k$  nodes.
- $q_k$ : the probability that a node chosen uniformly at random has degree  $k$ .
- $\pi_{kl}$ : the probability that an edge exists between a node chosen uniformly at random from all degree- $k$  nodes and a node chosen uniformly at random from all degree- $l$  nodes.
- $N$ : the number of nodes.
- $E$ : the set of edges.
- $\gamma = \frac{2|E|}{N^2}$ : graph density (with  $\gamma = 1$  on a complete graph).

- $\mu$ : compromise parameter.

Suppose that a network has  $K$  degree classes. We can then write

$$P(x, t) = \sum_{k=1}^K q_k P_k(x, t). \quad (15)$$

### A. Numerical Solver

To solve the partial integro-differential equation (14) numerically, we discretize in both time  $t$  and the opinion space  $x$ . Following [1], each time step has duration  $\Delta t = \frac{2}{N}$ , where  $N$  is the number of nodes in a network. Each spatial step is  $\Delta x = 0.0001$ .

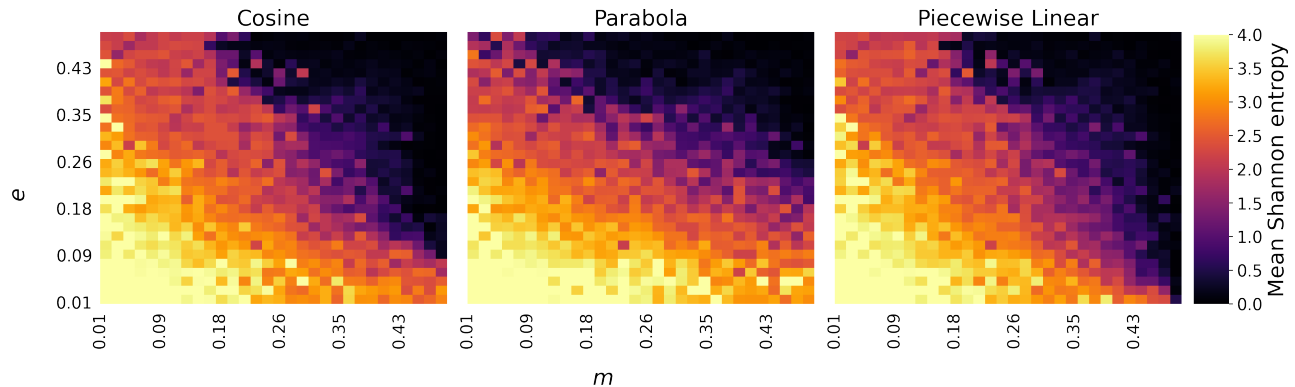


FIG. 10: Mean Shannon entropy at limit state for 10 simulations of our adaptive-confidence DW model on a 100 node star graph. For confidence-bound functions we use the (left) cosine, (center) parabolic, and (right) piecewise-linear confidence-bound function families. We consider 30  $m$  and  $e$  values evenly spaced in the interval  $[0.01, 0.5]$ . Each cell indicates the mean Shannon entropy across 10 simulations.

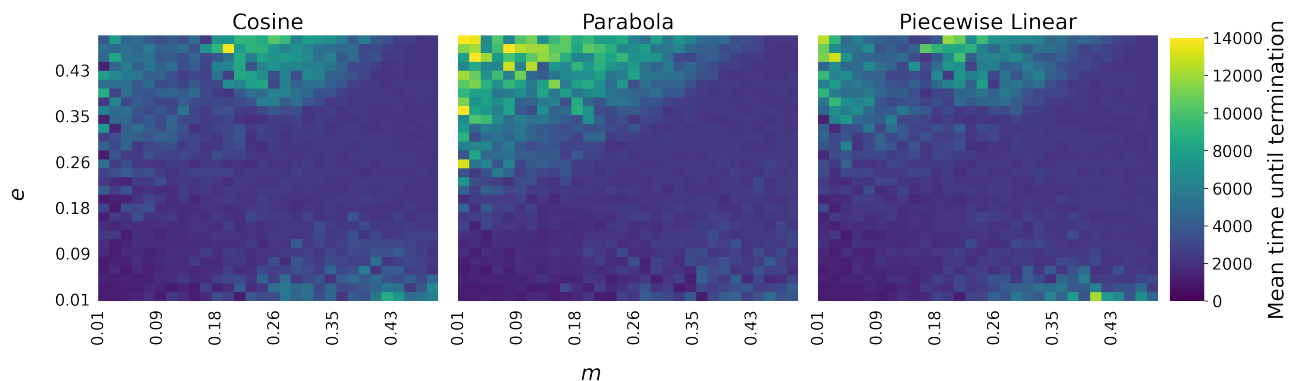


FIG. 11: Mean number of steps until termination for 10 simulations of our adaptive-confidence DW model on a 100 node star graph. We test the (left) cosine, (center) parabolic, and (right) piecewise-linear confidence-bound function families. For each confidence-bound function, we consider 30 evenly spaced values of  $m$  and  $e$  in the interval  $[0.01, 0.5]$ . Each cell indicates the mean time until termination across 10 simulations.

See Algorithm 1 for an overview of our solver algorithm. We are able to solve our partial-integro differential equation using a technique from numerical ordinary differential equations. To best match our notation with convention from numerical ordinary differential equations then, we denote  $P_k(x, t)$  as  $P_k^t(x)$ . We denote the spatial discretization as

$$X = \{x_n : x_n = n\Delta x, n \in \{0, 1, \dots, 10000\}\}.$$

(In the following explanations, we use the phrases “spatial discretization” and “mesh points” interchangeably). Using this discretization in space, we can approximate  $P^{t+1}(x_i)$  using Equation (14) and knowledge of  $P^t$ . We then use an Adams–Bashforth method [24] to yield a solution to (14). To follow convention from numerical ordinary differential equations, we then refer to the right-hand side of Equation (14) for some fixed value of  $t_n$  as  $f(t_n, P_k^{t_n})$ .

We start with a uniform density equation as the initial

---

#### Algorithm1 Numerical Solver of Equation (14)

---

```

initialize function interpolations  $P_k^t$  for all degree classes  $k$ 
while 90% of  $P_k^t(X)$  are greater than or equal to the density
threshold do
  for  $k$  in degree classes do
    try
      compute  $f(t, P_k^t)$  at mesh points
      with  $P_k^t$  and  $f(t, P_k^t)$ , get  $P_k^{t+1}$  at mesh points using
      Adams–Bashforth
    catch Overflow
      return  $\sum_k q_k P_k^t$ 
    end try
  end for
  set  $P_k^t = P_k^{t+1}$  at mesh points for all degree classes  $k$ 
  update  $P_k^t(X)$ 
end while
return  $\sum_k q_k P_k^t$ 

```

---

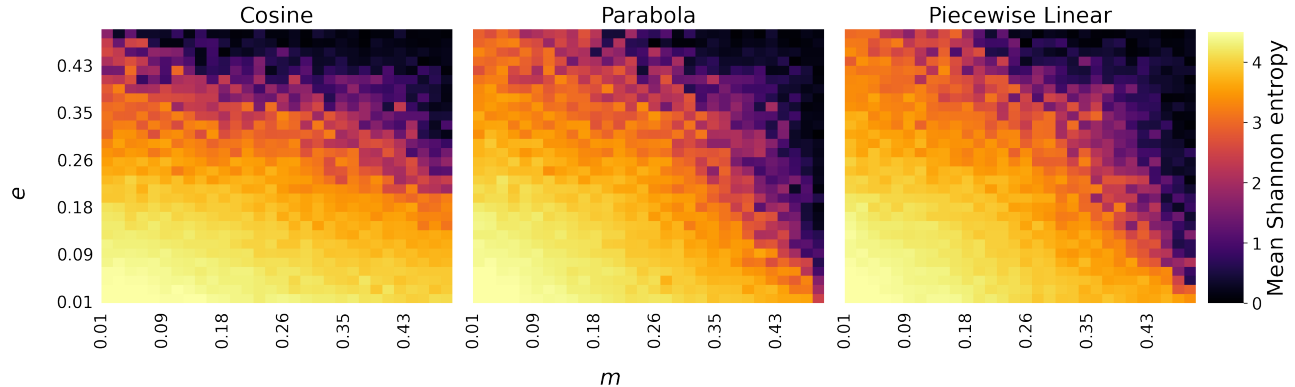


FIG. 12: Mean Shannon entropy at limit state for 10 simulations of our adaptive-confidence DW model on 100 node random tree graphs. For confidence-bound functions we use the (left) cosine, (center) parabolic, and (right) piecewise-linear confidence-bound function families. We consider 30 evenly spaced  $m$  and  $e$  values in the interval  $[0.01, 0.5]$ . Each cell indicates the mean Shannon entropy across 10 simulations. Note here that the y-limits are from 0 to 4.5 rather than the usual 0 to 4.

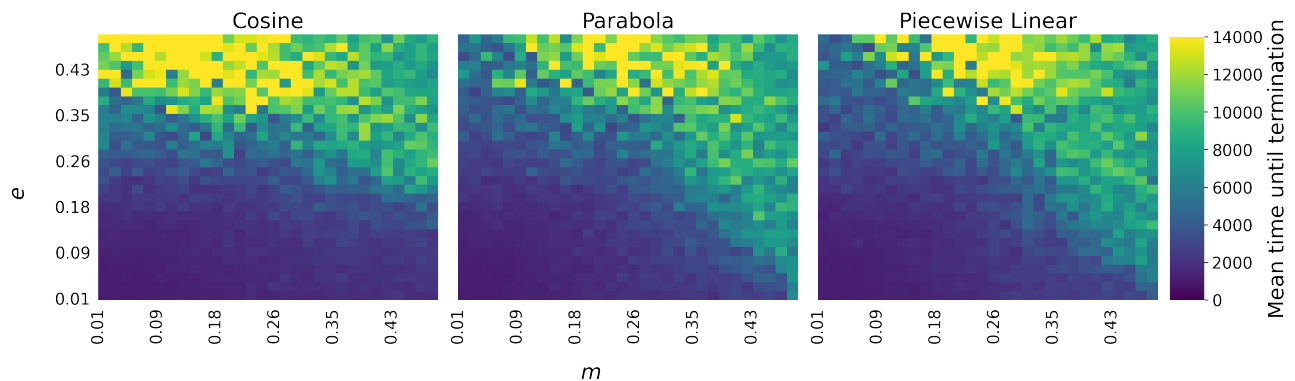


FIG. 13: Mean number of steps until termination for 10 simulations of our adaptive-confidence DW model on 100 node random tree graphs. We test the (left) cosine, (center) parabolic, and (right) piecewise-linear confidence-bound function families. For each confidence-bound function, we consider 30 evenly spaced values of  $m$  and  $e$  in the interval  $[0.01, 0.5]$ . Each cell indicates the mean time until termination across 10 simulations.

condition. That is,

$$P^0(x) = \begin{cases} 1, & x \in [0, 1] \\ 0, & \text{otherwise.} \end{cases}$$

We then use a third-order Adams–Bashforth method to determine the values of  $P^{t_{n+1}}(x_i)$  for all  $x_i \in X$ . The Adams–Bashforth method requires the following inputs:

$$y' = f(t, y), \quad y(t_0) = y_0,$$

which, when applying our notation, is

$$\frac{\partial P_k^t}{\partial t} = f(t, P_k^t), \quad P_k^0 = P_0.$$

Evaluating the value of  $f(t, P_k^t)$  requires an integration, which we perform with a modified trapezoidal rule. For each

point  $x_i$  in our spatial discretization we compute the region

$$D = X \cap \{y : |x_i - y| < c(y)\mu\}.$$

We then compute the true bounds of integration

$$a = \inf\{y : |x_i - y| < c(y)\mu\} \\ b = \sup\{y : |x_i - y| < c(y)\mu\}$$

We define  $\widetilde{P}_k^t(x)$  to be the result of linearly interpolating the set  $P_k^t(X)$ , and we let  $S$  be the result of performing the trapezoid rule on the function  $\frac{1}{\mu}\widetilde{P}_k^t(y)\widetilde{P}_l^t(y + \frac{1}{\mu}(x_i - y))$  using the points in  $D$ . Let the first integral in the parenthesis on the right-hand side of Equation (14) be  $\text{RHS}_1$ . We approximate

RHS<sub>1</sub> as

$$\begin{aligned} \text{RHS}_1 = & S + \frac{1}{\mu} \widetilde{P}_k^t(a) \widetilde{P}_l^t \left( a + \frac{1}{\mu} (x_i - a) \right) \Big|_{x \in D}^{\min x - a} \\ & + \frac{1}{\mu} \widetilde{P}_k^t(a) \widetilde{P}_l^t \left( b + \frac{1}{\mu} (x_i - b) \right) \Big|_{x \in D}^{\max x - b}. \end{aligned}$$

We compute the second integral similarly. During our integration computation, we may encounter points outside of the interval  $[0, 1]$ . Since the opinion space is  $[0, 1]$ , we know that any point outside of the interval  $[0, 1]$  must have a value of 0. Hence, we add 50 ghost points of value 0 on either side of the opinion space. After we compute the values of  $f$  at our mesh points, we note that because we are working with a density function, we require that

$$\int_0^1 f(t, P_k^t)(x) dx = 0.$$

To ensure this, we reset the values of  $f$  as

$$f(t, P_k^t)(x) := f(t, P_k^t)(x) - \frac{\sum_{x \in X} f(t, P_k^t)(x)}{|X|}$$

after we compute the value of  $f(t, P_k^t)$  at each point in the discretization. In all of our simulations, the density of each degree class converged to a sum of delta functions. Thus, we repeat this time-stepping process until a sufficiently low number of points in the set  $P_k^t(X)$  are below the density threshold. In our experiments, we set the density threshold to be 0.1 and required that 90% of the points in  $P_k^t(X)$  fall below the density threshold. That is, we terminate the mean-field simulation when

$$\frac{|\{y \in P_k^t(X) : y < 0.1\}|}{|P_k^t(X)|} \leq 0.1.$$

## B. Experiment Details and Results

We examine our mean-field model (14) on complete graphs and configuration-model graphs with the three two-parameter confidence-bound functions (see Table IV) and a constant function  $c(x) = 0.1$ , which corresponds to the standard DW model with a confidence bound of 0.1. We set  $m = 0.3$  and  $e = 0.1$  for all of the confidence-bound functions. We first run agent-based simulations on complete graphs and track the time until the simulations terminate using the termination criteria that we stated in Section V. As mentioned earlier, each time step in our simulations of our mean-field approximation is  $\Delta t = \frac{2}{N}$ . Since we approximate our mean-field equation for the density of opinions at a tenth of the time until termination, halfway to termination, and then at termination, we need the corresponding time step in agent-based simulations. To convert the time, we calculate

$$\text{density time} = \text{discrete time} \cdot \frac{2}{N}.$$

### 1. Complete Graph

For a complete graph with  $N$  nodes, all nodes have degree  $N - 1$ , which simplifies the partial integro-differential equation in Equation (14) to the following equation:

$$\begin{aligned} \frac{\partial P(x, t)}{\partial t} = & \int_{|x-y| < c(y)\mu} \frac{1}{\mu} P(y, t) P \left( y + \frac{1}{\mu} (x - y), t \right) dy \\ & - \int_{|x-y| < c(x)} P(x, t) P(y, t) dy. \end{aligned} \quad (16)$$

We use both 500-node and 1000-node complete graphs. Figure 14 we show the results for constant confidence function  $c(x) = 0.1$  which corresponds to the approximation of the standard DW model. We define the agent-based density as the number of nodes in the agent-based simulation within each interval  $\Delta t$ . At a tenth of the time to termination and halfway to termination, we observe that the mean-field model fits the actual agent-based density relatively well. At termination, we see an overestimation in density at more extreme opinion values and a mismatch in density peaks.

This overestimation occurs in almost all of our simulations at termination, regardless of confidence-bound functions. We believe this overestimation is due to a finite-size effect. One derives the mean-field model as the number  $N$  of nodes tends to infinity, whereas we consider networks with  $N = 500$  nodes in our simulations. The mismatch of peaks also appears in many of our simulations. Stochasticity plays an important role in determining the agent-based density. Therefore, we expect that the peaks do not match up perfectly in opinion. However, the number of peaks is the same in the agent-based and mean-field simulations. In Figures 15, 16, and 17, we observe that simulations with any of the three confidence-bound functions have higher densities at the halfway point and at the time of termination than in our simulations of the standard DW model. For all confidence-bound functions, the agent-based simulations have asymmetric density distributions in the opinion space while the our mean-field model generate symmetric density functions. We suspect that is also due to a finite size effect.

We also run the same set of experiments on a complete graph with 1000 nodes. Similar to the 500-node cases (see Figures 14, 15, 16, and 17), the mean-field densities approximate the agent-based density results well at a tenth of the way to termination for the 1000-node case (see Figures 18, 19, 20, and 21). For all confidence-bound functions except the cosine confidence-bound function, the mean-field approximation approximates the behavior of the agent-based at halfway to termination better than the experiments with 500-node graphs. This supports our hypothesis that the overshoot error is a result of finite size.

The mean-field approximation underestimates the number of peaks at the limit state for the parabolic and standard confidence-bound functions. However, for the other confidence-bound functions, the mean-field approximation correctly estimates the number of peaks at the limit state.

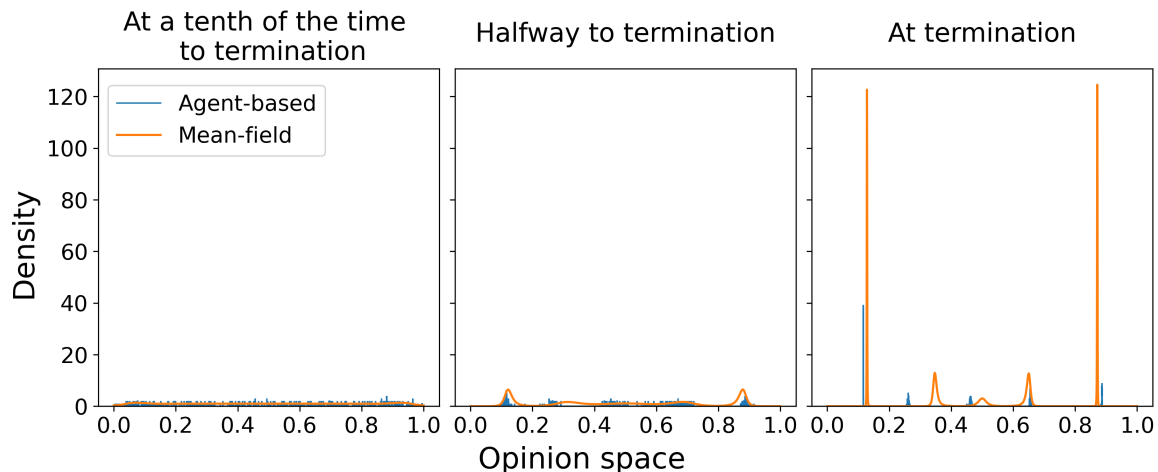


FIG. 14: Density distribution for agent-based (blue) and mean-field (orange) simulations of Equation (16) for a standard DW model with confidence bound of 0.1 on a 500-node complete graph. We run the agent-based model until no node changes their opinion by more than 0.02 for 50000 time steps. We plot our mean-field approximation and the densities of opinions observed in the agent-based simulation at (left) a tenth of the time to termination, (center) halfway to termination, and at (right) termination.

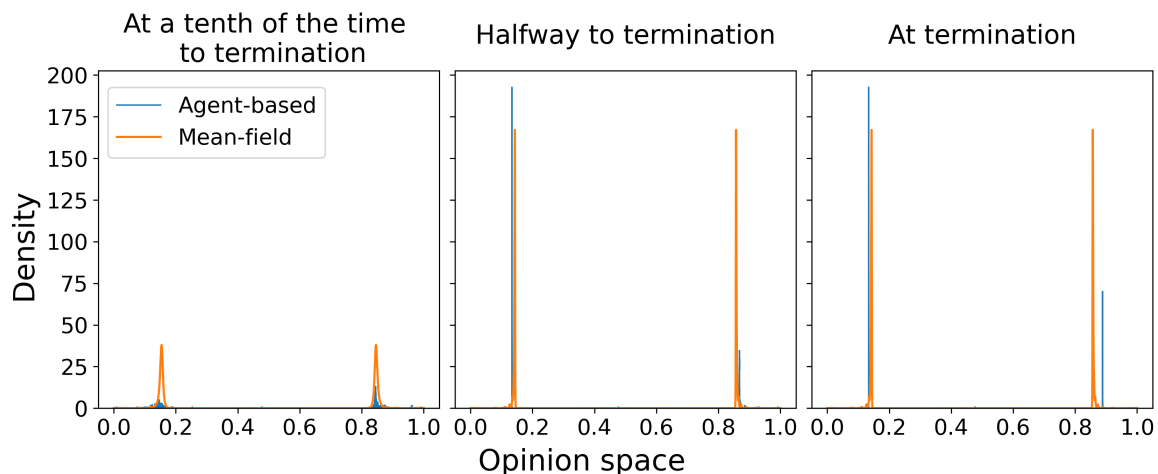


FIG. 15: Density distribution for agent-based (blue) and mean-field (orange) simulations of Equation (16) for an adaptive-confidence DW model with a cosine confidence-bound function  $c(x) = -\frac{(m-e)}{2} \cos(2\pi x) + \frac{m+e}{2}$  on a 500-node complete graph, with  $m = 0.3$  and  $e = 0.1$ . We run the agent-based model until no node changes their opinion by more than 0.02 for 50000 time steps. We plot our mean-field approximation against the densities of opinions observed in the agent-based simulation at (left) a tenth of the time to termination, (center) halfway to termination, and at (right) termination.

Interestingly, the cosine confidence-bound function is the only situation in which we observe a peak that is smaller than the agent-based simulation.

## 2. Configuration-Model Graphs

Now we study our mean-field approximation on a configuration model [25]. Here we restrict ourselves to the case of 100 node configuration models where each node is assigned a

degree from the set  $\{5, 10\}$  uniformly at random. Generating a configuration-model network often yields a multigraph for finite values of  $N$ . In our adaptive-confidence model, we consider a graph, so we must make some alterations to the configuration-model network if a multigraph is produced. If a multigraph is produced, we cut all self edges and parallel edges. This cutting procedure often creates nodes that do not have a degree from  $\{5, 10\}$ , which our mean-field approximation does not account for. Once we create our graph, we follow the experimental procedure from Section VII B 1.

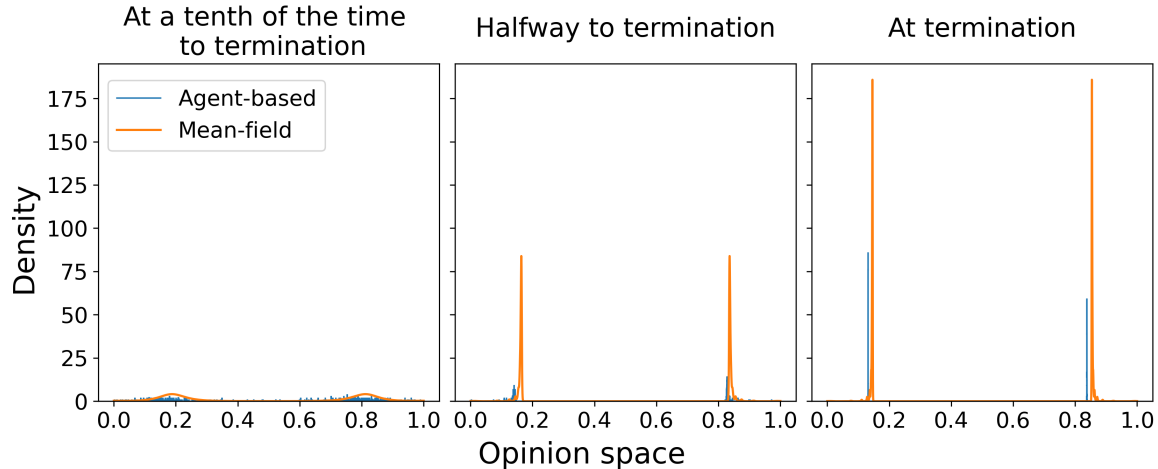


FIG. 16: Density distribution for agent-based (blue) and mean-field (orange) simulations of Equation (16) for an adaptive-confidence DW model with a parabola confidence-bound function  $c(x) = -4(m-e)x^2 + 4(m-e)x + e$  on a 500-node complete graph, with  $m = 0.3$  and  $e = 0.1$ . We run the agent-based model until no node changes their opinion by more than 0.02 for 50000 time steps. We plot our mean-field approximation against the densities of opinions observed in the agent-based simulation at (left) a tenth of the time to termination, (center) halfway to termination, and at (right) termination.

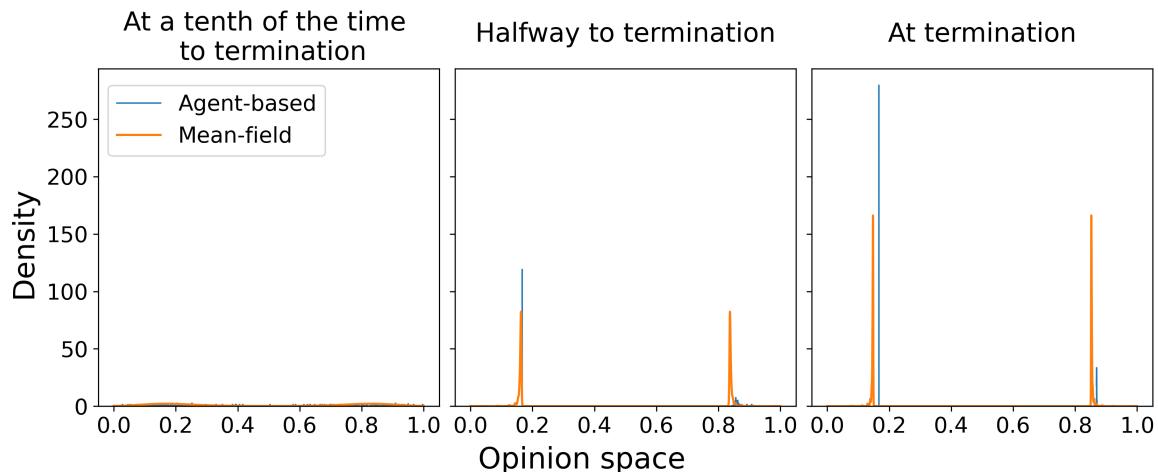


FIG. 17: Density distribution for agent-based (blue) and mean-field (orange) simulations of Equation (16) for an adaptive-confidence DW model with a piecewise-linear confidence-bound function  $c(x) = 2|x - 0.5|(e - m) + m$  on a 500-node complete graph, with  $m = 0.3$  and  $e = 0.1$ . We run the agent-based model until no node changes their opinion by more than 0.02 for 50000 time steps. We plot our mean-field approximation against the densities of opinions observed in the agent-based simulation at (left) a tenth of the time to termination, (center) halfway to termination, and at (right) termination.

We show the results of this experiment in Figure 22.

At a tenth of the way to convergence, the configuration model produces density values are less than what we observe in the agent-based simulation at some points. However, because we only use 100 nodes in this simulation, we believe this is a finite-size effect. Because there are finitely many nodes, we observe spikes in density at certain opinions and zeros at others; this is not possible for our mean-field approximation since the approximation is continuous. We also observe that at the limit state, the mean-field approxima-

tion produces the same number of peaks as the agent-based simulations.

## VIII. CONCLUSION

We studied an adaptive confidence-bound model (BCM) that we constructed by generalizing the classical DW model. Our model incorporated confidence-bound functions and asymmetric updates to the classical DW model. The

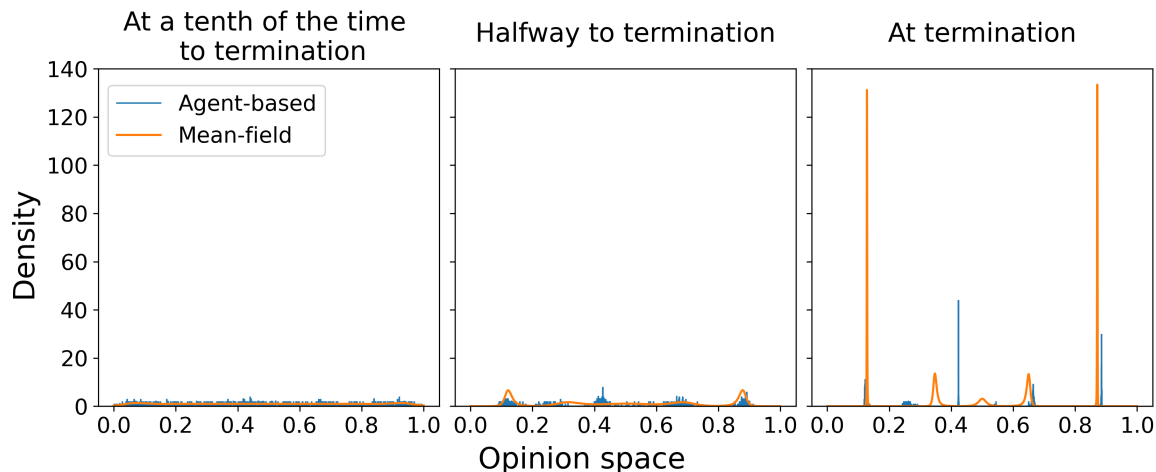


FIG. 18: Density distribution for agent-based (blue) and mean-field (orange) simulations of Equation (16) for a standard DW model with confidence bound of 0.1 on a 1000-node complete graph. We run the agent-based model until no node changes their opinion by more than 0.02 for 100000 time steps. We plot our mean-field approximation against the densities of opinions observed in the agent-based simulation at (left) a tenth of the time to termination, (center) halfway to termination, and at (right) termination.

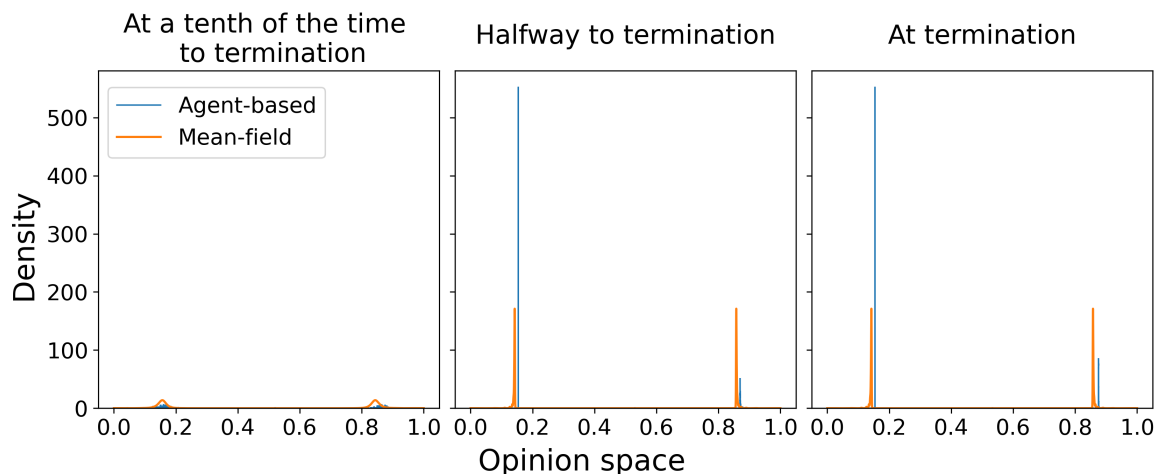


FIG. 19: Density distribution for agent-based (blue) and mean-field (orange) simulations of Equation (16) for an adaptive-confidence DW model with a cosine confidence-bound function  $c(x) = -\frac{(m-e)}{2} \cos(2\pi x) + \frac{m+e}{2}$  on a 1000-node complete graph, with  $m = 0.3$  and  $e = 0.1$ . We run the agent-based model until no node changes their opinion by more than 0.02 for 100000 time steps. We plot our mean-field approximation against the densities of opinions observed in the agent-based simulation at (left) a tenth of the time to termination, (center) halfway to termination, and at (right) termination.

confidence-bound functions take an agent's opinion at time  $t$  as input and outputs its confidence at the same time step. In real life, an individual's willingness to listen to other often depends on their opinion, and our model's adaptive confidence bound incorporates this idea. Moreover, in real-life conversations, it is not always the case that both sides compromise, as some individuals may be more open-minded than others. Our asymmetric update rule also reflects this phenomenon.

We found that in our adaptive DW model, convergence to a limit state is not guaranteed in general. We derived suffi-

cient conditions for almost sure convergence to a limit state on both complete and general graph topologies. Furthermore, we showed for any graph topology that our adaptive DW model with a monotone confidence function converges to a limit state. The methods we used to obtain these results take inspiration from the methods in [10] and [17].

We conducted numerical experiments of our agent-based adaptive-confidence DW model for 6 graph structures and 5 confidence-bound functions. We started with 2 one-parameter functions to examine how changing one parameter

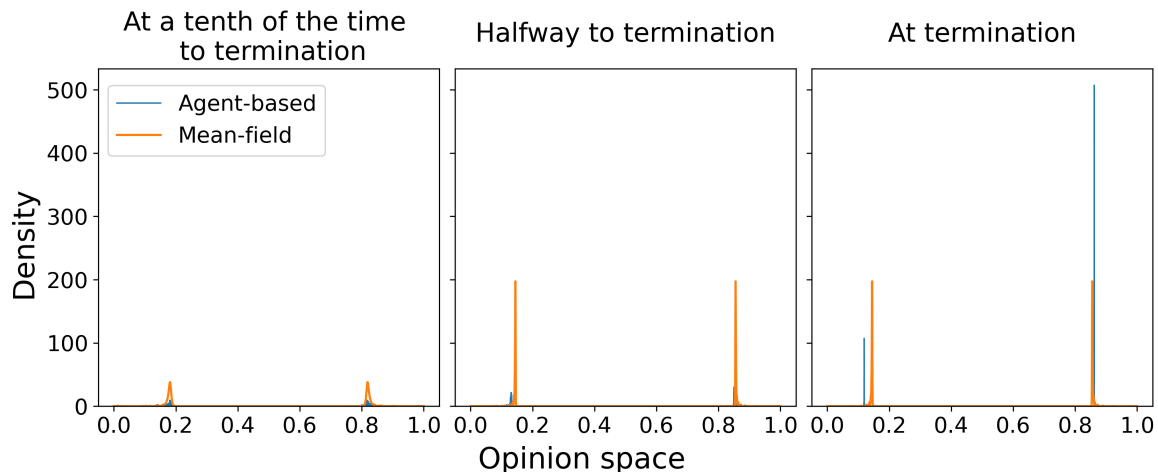


FIG. 20: Density distribution for agent-based (blue) and mean-field (orange) simulations of Equation (16) for an adaptive-confidence DW model with a parabola confidence-bound function  $c(x) = -4(m-e)x^2 + 4(m-e)x + e$  on a 1000-node complete graph, with  $m = 0.3$  and  $e = 0.1$ . We run the agent-based model until no node changes their opinion by more than 0.02 for 100000 time steps. We plot our mean-field approximation against the densities of opinions observed in the agent-based simulation at (left) a tenth of the time to termination, (center) halfway to termination, and at (right) termination.

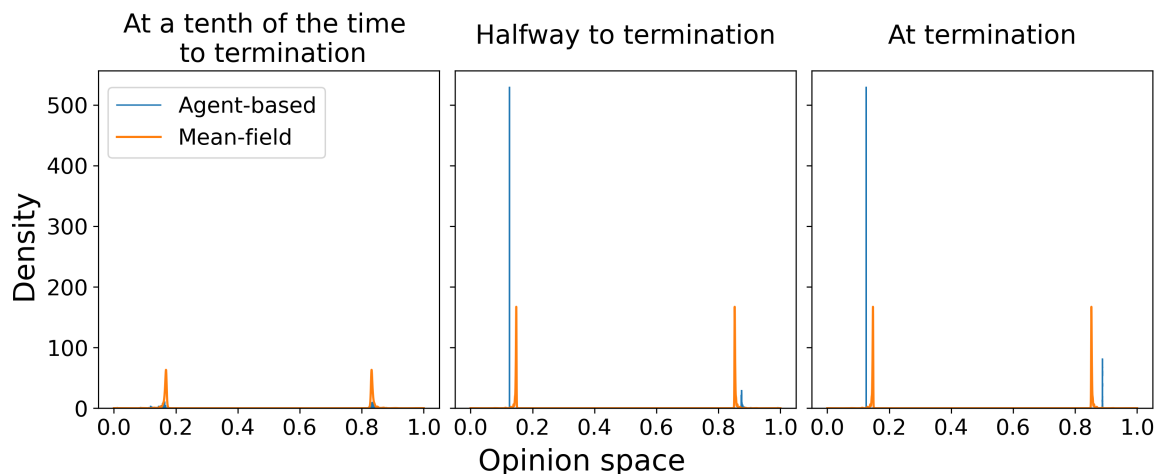


FIG. 21: Density distribution for agent-based (blue) and mean-field (orange) simulations of Equation (16) for an adaptive-confidence DW model with a piecewise-linear confidence-bound function  $c(x) = 2|x - 0.5|(e - m) + m$  on a 1000-node complete graph, with  $m = 0.3$  and  $e = 0.1$ . We run the agent-based model until no node changes their opinion by more than 0.02 for 100000 time steps and stored the total number of time steps. We plot our mean-field approximation against the densities of opinions observed in the agent-based simulation at (left) a tenth of the time to termination, (center) halfway to termination, and at (right) termination.

affects the ratio of the size of the largest opinion cluster to the number of nodes at a limit state. We also considered 3 two-parameter functions, where we calculated Shannon entropy for final states and examined the effects of varying the middle value  $m$  and the extreme values  $e$ .

We also derived and examined a mean-field approximation of our model. This approximation comes in the form of a partial integro-differential equation that approximates the density of every degree-class  $k$ . For this equation, we de-

veloped a solver that uses Adams–Bashforth to advance the density solution in time.

## IX. ACKNOWLEDGEMENTS

We thank our mentors S. Tymochko and M. A. Porter for continuous support and guidance throughout the REU program, W. Chu and A. Dubovskaya for helpful comments and

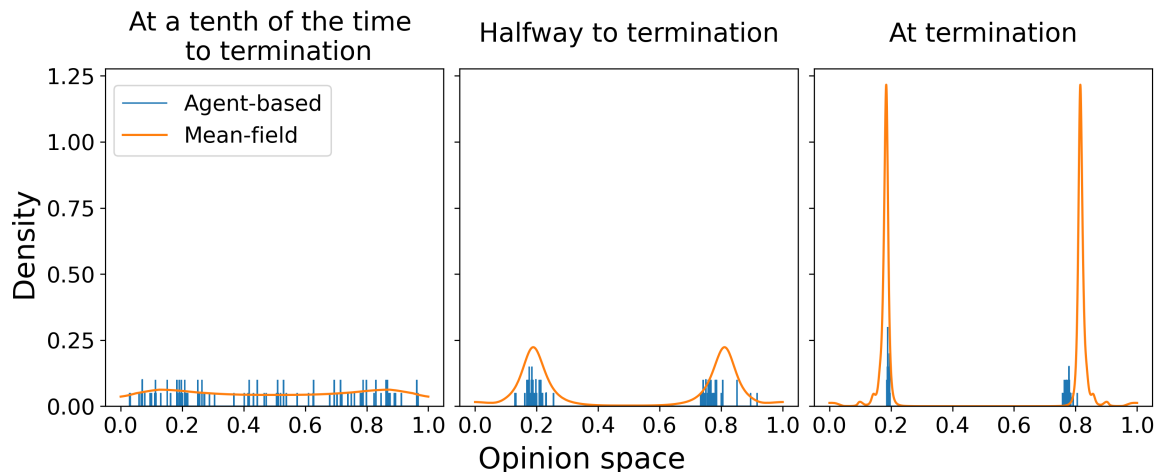


FIG. 22: Density distribution for agent-based (blue) and mean-field (orange) simulations of Equation (14) with an adaptive-confidence DW model with a parabolic confidence-bound function  $c(x) = -4(m - e)x^2 + 4(m - e)x + e$  on a 100-node configuration model, with  $m = 0.3$  and  $e = 0.1$ . We run the agent-based model until no node had changed their opinion by more than 0.02 for 10000 time steps. We plot our mean-field approximation against the densities of opinions observed in the agent-based simulation at (left) a tenth of the time to termination, (center) halfway to termination, and at (right) termination.

discussions, Bellatrix Tymochko for emotional support and joy, and A. L. Bertozzi for organizing the REU. We acknowl-

edge financial support from the National Science Foundation (grant number 1922952) through the Algorithms for Threat Detection (ATD) program.

- 
- [1] S. C. Fennell, K. Burke, M. Quayle, and J. P. Gleeson, *Physical Review E* **103**, 012314 (2021).
- [2] H. Noorazar, K. R. Vixie, A. Talebanpour, and Y. Hu, *International Journal of Modern Physics C* **31**, 2050101 (2020).
- [3] J. Lorenz, *International Journal of Modern Physics C* **18**, 1819 (2007).
- [4] H. Z. Brooks, arXiv preprint arXiv:2302.00801 (2023).
- [5] X. F. Meng, R. A. Van Gorder, and M. A. Porter, *Physical Review E* **97**, 022312 (2018).
- [6] R. Hegselmann and U. Krause, *Journal of Artificial Societies and Social Simulation* **5.3.2** (2002).
- [7] G. Deffuant, D. Neau, F. Amblard, and G. Weisbuch, *Advances in Complex Systems* **03**, 87 (2000).
- [8] J. Lorenz, *Complexity* **15**, 43 (2010).
- [9] M. Pineda and G. Buendía, *Physica A: Statistical Mechanics and its Applications* **420**, 73 (2015).
- [10] G. Chen, W. Su, W. Mei, and F. Bullo, *Automatica* **114**, 108825 (2020).
- [11] J. Zhang and Y. Hong, in *Proceedings of the 31st Chinese Control Conference* (IEEE, 2012) pp. 1124–1129.
- [12] G. J. Li, J. Luo, and M. A. Porter, *Bounded-Confidence Models of Opinion Dynamics with Adaptive Confidence Bounds* (2023), arXiv:2303.07563 [physics].
- [13] H. Z. Brooks and M. A. Porter, *Physical Review Research* **2**, 023041 (2020).
- [14] G. Deffuant, F. Amblard, G. Weisbuch, and T. Faure, *Journal of Artificial Societies and Social Simulation* **5.4.1** (2002).
- [15] B. Kozma and A. Barrat, *Physical Review E* **77**, 016102 (2008).
- [16] J. Lorenz, *Physica A: Statistical Mechanics and its Applications* **355**, 217 (2005).
- [17] W. Mei, J. M. Hendrickx, G. Chen, F. Bullo, and F. Dörfler, *Convergence, consensus and dissensus in the weighted-median opinion dynamics* (2022), arXiv:2212.08808.
- [18] P. Erdős, A. Rényi, *et al.*, *Publ. math. inst. hung. acad. sci* **5**, 17 (1960).
- [19] E. N. Gilbert, *The Annals of Mathematical Statistics* **30**, 1141 (1959).
- [20] P. W. Holland, K. B. Laskey, and S. Leinhardt, *Social networks* **5**, 109 (1983).
- [21] S. Fortunato, *International Journal of Modern Physics C* **15**, 1301 (2004).
- [22] D. Bauso, H. Tembine, and T. Basar, *SIAM Journal on Control and Optimization* **54**, 3225 (2016).
- [23] W. Chu and M. A. Porter, arXiv preprint arXiv:2203.12189 (2023), *SIAM Journal on Applied Mathematics*, in press.
- [24] J. C. Butcher, *Numerical differential equation methods*, in *Numerical Methods for Ordinary Differential Equations* (John Wiley & Sons, Ltd, 2016) Chap. 2, pp. 55–142.
- [25] M. E. Newman, *SIAM review* **45**, 167 (2003).

## Appendix A: Mean-field Derivation

### 1. Assumptions

- The graph is from a configuration model [25]. That is, the degree of each node is fixed.
- At each time step, we track the degree of each node and cut all edges in the graph. We assign  $k$  “stubs” to each node, where  $k$  is the degree of the node. For each stub, we uniformly randomly select another stub and draw an edge between these two stubs.
- The network is sufficiently dense (we are doing this in a loose way without defining asymptotic bounds).

### 2. Notation

- $P_k(x, t)$ : the density of nodes w opinion  $x$  at time  $t$  among degree- $k$  nodes.
- $P_k(x, t)dx$ : the probability that a degree- $k$  node has an opinion found in the interval  $[x, x + dx)$ .
- $q_l$ : the probability that a node chosen uniformly at random has degree  $l$ .
- $N$ : number of nodes.
- $E$ : the set of edges.
- $Nq_k$ : asymptotic expected number of degree- $k$  nodes as  $N \rightarrow \infty$ .
- $\gamma = \frac{2|E|}{N^2}$ : graph density ( $\gamma = 1$  for a complete graph).
- $\pi_{kl}$ : the probability that an edge exists between a node chosen uniformly at random from all degree- $k$  nodes and a node chosen uniformly at random from all degree- $l$  nodes.

### 3. Derivation

The expected change in  $P_k(x, t)dx$  over a time increment  $dt$  is

$$\text{Expected number of degree-}k \text{ nodes entering } [x, x + dx) - \text{Expected number of nodes leaving } [x, x + dx). \quad (\text{A1})$$

To compute the positive contribution, we follow the work of Fennell et al. [1]. Consider a degree- $k$  node  $i$  with opinion  $y$ . The probability that we choose node  $i$  for interaction with a degree- $l$  node in  $dt$  is

$$\frac{Nq_l\pi_{kl}}{|E|} = \frac{\frac{2|E|}{N\gamma} \cdot q_l\pi_{kl}}{|E|} = \frac{2q_l\pi_{kl}}{N\gamma}. \quad (\text{A2})$$

We see that  $Nq_l\pi_{kl}$  is the expected number of edges between nodes of degree- $k$  and nodes of degree- $l$ . Hence, when we divide  $Nq_l\pi_{kl}$  by  $|E|$ , we get the probability of selecting an edge between an degree- $k$  node and a degree- $l$  node. Substituting into the graph density equation (A2), we get that this probability is  $\frac{2q_l\pi_{kl}}{N\gamma}$ . Node  $i$  will change it's opinion only if the degree- $l$  node it was selected to update with has opinion  $z \in (y - c(y), y + c(y))$ . Node  $i$  will then update it's opinion to  $y + \mu(z - y)$ . The updated opinion will be in the interval  $[x, x + dx)$  only if  $z \in \left[ y + \frac{1}{\mu}(x - y), y + \frac{1}{\mu}(x - y) + \frac{dx}{\mu} \right)$ . To have  $z \in [x, x + dx)$ , this implies  $y + \mu(z - y) > x$  and  $y + \mu(z - y) < x + dx$ . Therefore,

$$\begin{aligned} y + \mu(z - y) &> x \\ \mu z &> x - y + \mu y \\ z &> y + \frac{1}{\mu}(x - y) \\ y + \mu(z - y) &< x + dx \\ \mu z &< x + dx - y + \mu y \\ z &< y + \frac{1}{\mu}(x - y) + \frac{dx}{\mu}. \end{aligned}$$

The density of degree- $l$  nodes such as  $z$  is  $P_l(y + \frac{1}{\mu}(x - y), t) \frac{dx}{\mu}$ , so the probability that node  $i$  has an opinion in  $[x, x + dx)$  after the time-step  $dt$  is

$$\sum_l \frac{2q_l \pi_{kl}}{N\gamma} \frac{1}{\mu} P_l \left( y + \frac{1}{\mu}(x - y), t \right) \frac{dx}{\mu}.$$

The expression for the probability that any degree- $k$  node has an opinion in  $[x, x + dx)$  after time step  $dt$  is analogous. Observe that we expect there to be  $Nq_k P_k(y, t) dy$  degree- $k$  nodes with opinion  $y$ . Therefore, the probability of a degree- $k$  node with opinion  $y$  updating it's opinion into  $[x, x + dx)$  is:

$$\sum_l \frac{2q_k q_l \pi_{kl}}{\gamma} \frac{1}{\mu} P_k(y, t) P_l \left( y + \frac{1}{\mu}(x - y), t \right) \frac{dx}{\mu}. \quad (\text{A3})$$

For a node  $i$  with opinion  $y$  to update its opinion to the interval  $[x, x + dx)$  after an update with a node of opinion  $z$ , we require  $z \in \left[ y + \frac{1}{\mu}(x - y), y + \frac{1}{\mu}(x - y) + \frac{dx}{\mu} \right)$ . For  $z$  to be a valid update partner for  $y$ , we require that  $z \in (y - c(y), y + c(y))$ . Therefore, we require that

$$\begin{aligned} y - c(y) &< y + \frac{1}{\mu}(x - y), \\ y + \frac{1}{\mu}(x - y) + \frac{dx}{\mu} &< y + c(y). \end{aligned}$$

These inequalities yield the bounds

$$-c(y)\mu < x - y < c(y)\mu - dx.$$

Thus, to determine the positive contribution in equation (A3), we integrate over all nodes with opinions that may update to the interval  $[x, x + dx)$  to obtain

$$\sum_l \frac{2q_k q_l \pi_{kl}}{\gamma} \int_{-c(y)\mu < x - y < c(y)\mu - dx} \frac{1}{\mu} P_k(y, t) P_l \left( y + \frac{1}{\mu}(x - y), t \right) dx dy. \quad (\text{A4})$$

We then calculate the negative contribution, which is the expected number of degree- $k$  nodes whose opinions move outside  $[x, x + dx)$  in a time step  $dt$ . Consider a node  $j$  with an opinion in  $[x, x + dx)$  with degree  $k$ . It will update its opinion if it interacts with a node within its confidence bound (i.e. when  $|x - y| < c(x)$ ). Therefore, the probability that node  $j$  updates its opinion during the time step is

$$\int_{|x - y| < c(x)} \sum_l \frac{2q_l \pi_{kl}}{N\gamma} P_l(y, t) dy.$$

We seek to get the expected number of degree- $k$  nodes whose opinions move outside  $[x, x + dx)$  in  $dt$ . Additionally, as  $dx \rightarrow 0$ , the probability that node  $j$  leaves the interval  $[x, x + dx)$  during the time step is equivalent to the probability that node  $j$  interacts during the time step. The number of degree- $k$  nodes whose opinion is in  $[x, x + dx)$  is  $Nq_k P_k(x, t) dx$ . Therefore,

$$\begin{aligned} Nq_k P_k(x, t) dx \cdot \int_{|x - y| < c(x)} \sum_l \frac{2q_l \pi_{kl}}{N\gamma} P_l(y, t) dy &= \int_{|x - y| < c(x)} \sum_l \frac{2q_l \pi_{kl}}{N\gamma} Nq_k \cdot P_l(y, t) dy \cdot P_k(x, t) dx \\ &= \sum_l \frac{2q_k q_l \pi_{kl}}{\gamma} \int_{|x - y| < c(x)} P_k(x, t) P_l(y, t) dy dx. \end{aligned} \quad (\text{A5})$$

Combing (A4) and (A5) yields

$$\begin{aligned} Nq_k P_k(x, t + dt) dx - Nq_k P_k(x, t) dx &= \sum_l \frac{2q_k q_l \pi_{kl}}{\gamma} \left( \int_{-c(y)\mu < x - y < c(y)\mu - dx} \frac{1}{\mu} P_k(y, t) P_l \left( y + \frac{1}{\mu}(x - y), t \right) dx dy \right. \\ &\quad \left. - \int_{|x - y| < c(x)} P_k(x, t) P_l(y, t) dx dy \right). \end{aligned} \quad (\text{A6})$$

Taking  $dx \rightarrow 0$  and then  $dt \rightarrow 0$ , we obtain

$$\frac{\partial P_k(x, t)}{\partial t} = \sum_l \frac{2q_k q_l \pi_{kl}}{\gamma} \left( \int_{|x - y| < c(y)\mu} \frac{1}{\mu} P_k(y, t) P_l \left( y + \frac{1}{\mu}(x - y), t \right) dy - \int_{|x - y| < c(x)} P_k(x, t) P_l(y, t) dy \right). \quad (\text{A7})$$

TABLE V: Defining notation used in Appendix B.

Notation	Definition
The <i>possible graph</i> : $G_{\text{pos}}(t_1, t_2)$	the graph containing all edges which ever appear within the effective graph between (not strictly) times $t_1$ and $t_2$ ; formally, $G_{\text{pos}}(t_1, t_2) := (V, \bigcup_{t' \geq t_1, t' \leq t_2} E_{\text{eff}}(t))$
The <i>observed graph</i> : $G_{\text{obs}}(t_1, t_2)$	the graph of all edges which are selected between (not strictly) times $t_1$ and $t_2$ ; formally, it is equal to $(V, \{e_{t'}   t_1 \leq t' \leq t_2\})$
$\text{sep}(e, t_1, t_2)$	the statement that the graph intersection $G_{\text{obs}}(t_1, t_2) \cap G_{\text{pos}}(t_1, t_2)$ is not weakly connected
$\text{sep}_S(e, t)$	for a subset $S \subset V$ , the statement that the graph intersection $G_{\text{obs}}(t) \cap G_{\text{pos}}(t)$ does not contain any edges in $S \times (V \setminus S) \cup (V \setminus S) \times S$ .
$\text{sep}_S(e)$	for a subset $S \subset V$ , the event that $\text{sep}_S(e, t)$ is true for some $t$ , i.e $\text{sep}_S(e) := \bigvee_{t \geq 0} \text{sep}(e, t)$ .
$\text{same}(A, s, e)$	for a set $A$ containing edge sequences of length $s$ , the statement that the first $s$ edge choices $\{e_t\}_{t=0}^s$ of <b>DW</b> match the edges in $f$ for some $f \in A$ .

### Appendix B: Various Lemmas and their Proofs

In this section, we use the notation from Section IV that is defined in Table I as well as some additional notation defined in Table V. First, we prove a lemma that builds upon Lemma IV.6, no longer using the the event dif. From this lemma, using recursion on  $d$ , we get Corollary B.1.1.

**Lemma B.1.** *For some  $\epsilon \in (0, mb]$ , time  $s_0, s \geq 0$  and let  $0 < d < N$ . Then there exists a time  $T \geq s$  such that*

$$P_{\text{DW}}(\text{DIF}(m\epsilon, d+1, s_0, T, e) | \text{DIF}(\epsilon, d, s_0, s, e)) \geq \frac{1}{2^{|E|^{v+1}}} \cdot P_{\text{DW}}(\text{conn}(e) | \text{DIF}(\epsilon, d, s_0, s, e)),$$

where

$$v := \left\lceil \frac{\ln b}{\ln(1-\mu)} \right\rceil.$$

Further, letting  $q := \frac{1}{2^{|E|^{v+1}}}$ , we have that

$$P_{\text{DW}}(\text{DIF}(m^{d-1}\epsilon, d, s_0, T, e)) \geq q P_{\text{DW}}(\text{DIF}(m^{d-2}\epsilon, d-1, s_0, s, e)) - q P_{\text{DW}}(\text{sep}(e)).$$

*Proof.* Recall that  $\text{DIF}(\epsilon, d, s_0, s, e)$  means that there exists  $t \leq T$  such that  $\text{dif}(m\epsilon, d+1, s, t, e)$ . Then, we can study  $P_{\text{DW}}(\text{DIF}(m\epsilon, d+1, s, T, e) | \text{DIF}(\epsilon, d, s_0, s, e))$  by doing casework on the time  $t \leq T$  such that  $\text{dif}(m\epsilon, d+1, s, t, e)$ :

$$\begin{aligned} & P_{\text{DW}}(\text{DIF}(m\epsilon, d+1, s_0, T, e) | \text{DIF}(\epsilon, d, s_0, s, e)) \\ &= \sum_{t=0}^s P_{\text{DW}}(\text{DIF}(m\epsilon, d+1, s_0, T, e) | \text{dif}(\epsilon, d, s_0, t, e)) \cdot P_{\text{DW}}(\text{dif}(\epsilon, d, s_0, t, e) | \text{DIF}(\epsilon, d, s_0, s, e)). \end{aligned} \quad (\text{B1})$$

For a given  $0 \leq t \leq s$ , by Lemma IV.6 there is a time  $T_t \geq t \geq 0$  such that

$$P_{\text{DW}}(\text{DIF}(m\epsilon, d+1, s_0, T_t, e) | \text{dif}(\epsilon, d, s_0, t, e)) \geq \frac{1}{2^{|E|^{v+1}}} \cdot P_{\text{DW}}(\text{conn}(e) | \text{dif}(\epsilon, d, s_0, t, e)).$$

In addition, observe that, for any  $T \geq T_t$ ,  $\text{DIF}(m\epsilon, d+1, s_0, T_t, e) \Rightarrow \text{DIF}(m\epsilon, d+1, s_0, T, e)$ , so

$$P_{\text{DW}}(\text{DIF}(m\epsilon, d+1, s_0, T, e) | \text{dif}(\epsilon, d, s_0, t, e)) \geq \frac{1}{2^{|E|^{v+1}}} \cdot P_{\text{DW}}(\text{conn}(e) | \text{dif}(\epsilon, d, s_0, t, e)). \quad (\text{B2})$$

Define  $T^* := \max_{0 \leq t \leq s} T_t$ . We have by (B2) that

$$\begin{aligned}
& \sum_{t=0}^s P_{\mathbf{D}\mathbf{W}}(\text{DIF}(m\epsilon, d+1, s_0, T^*, e) | \text{dif}(\epsilon, d, s_0, t, e)) \cdot P_{\mathbf{D}\mathbf{W}}(\text{dif}(\epsilon, d, s_0, t, e) | \text{DIF}(\epsilon, d, s_0, s, e)) \\
& \geq \sum_{t=0}^s \frac{1}{2|E|^{v+1}} \cdot P_{\mathbf{D}\mathbf{W}}(\text{conn}(e) | \text{dif}(\epsilon, d, s_0, t, e)) \cdot P_{\mathbf{D}\mathbf{W}}(\text{dif}(\epsilon, d, s_0, t, e) | \text{DIF}(\epsilon, d, s_0, s, e)) \\
& = \frac{1}{2|E|^{v+1}} \sum_{t=0}^s P_{\mathbf{D}\mathbf{W}}(\text{conn}(e), \text{dif}(\epsilon, d, s_0, t, e) | \text{DIF}(\epsilon, d, s_0, s, e)) \\
& = \frac{1}{2|E|^{v+1}} P_{\mathbf{D}\mathbf{W}}(\text{conn}(e), \text{DIF}(\epsilon, d, s_0, s, e) | \text{DIF}(\epsilon, d, s_0, s, e)) \\
& = \frac{1}{2|E|^{v+1}} P_{\mathbf{D}\mathbf{W}}(\text{conn}(e) | \text{DIF}(\epsilon, d, s_0, s, e)). \tag{B3}
\end{aligned}$$

Finally, combining (B1) and (B3), we get

$$P_{\mathbf{D}\mathbf{W}}(\text{DIF}(m\epsilon, d+1, s_0, T^*, e) | \text{DIF}(\epsilon, d, s_0, s, e)) \geq \frac{1}{2|E|^{v+1}} P_{\mathbf{D}\mathbf{W}}(\text{conn}(e) | \text{DIF}(\epsilon, d, s_0, s, e)), \tag{B4}$$

as desired. This proves the first part of the lemma.

To prove the second part of the lemma, observe the following:

$$\begin{aligned}
P_{\mathbf{D}\mathbf{W}}(\text{DIF}(m\epsilon, d+1, s_0, T^*, e)) & \geq P_{\mathbf{D}\mathbf{W}}(\text{DIF}(m\epsilon, d+1, s_0, T^*, e), \text{DIF}(\epsilon, d, s_0, s, e)) \\
& = P_{\mathbf{D}\mathbf{W}}(\text{DIF}(m\epsilon, d+1, s_0, T^*, e) | \text{DIF}(\epsilon, d, s_0, s, e)) \cdot P_{\mathbf{D}\mathbf{W}}(\text{DIF}(\epsilon, d, s_0, s, e)) \\
& \geq q P_{\mathbf{D}\mathbf{W}}(\text{conn}(e) | \text{DIF}(\epsilon, d, s_0, s, e)) \cdot P_{\mathbf{D}\mathbf{W}}(\text{DIF}(\epsilon, d, s_0, s, e)), \tag{B5}
\end{aligned}$$

where the last part is true by (B4). Then, since  $\text{conn}(e)$  is the negation of  $\text{sep}$ ,

$$\begin{aligned}
& q P_{\mathbf{D}\mathbf{W}}(\text{conn}(e) | \text{DIF}(\epsilon, d, s_0, s, e)) \cdot P_{\mathbf{D}\mathbf{W}}(\text{DIF}(\epsilon, d, s_0, s, e)) \\
& = q(1 - P_{\mathbf{D}\mathbf{W}}(\text{sep}(e) | \text{DIF}(\epsilon, d, s_0, s, e))) \cdot P_{\mathbf{D}\mathbf{W}}(\text{DIF}(\epsilon, d, s_0, s, e)) \\
& = q P_{\mathbf{D}\mathbf{W}}(\text{DIF}(\epsilon, d, s_0, s, e)) - q P_{\mathbf{D}\mathbf{W}}(\text{sep}(e) | \text{DIF}(\epsilon, d, s_0, s, e)) \cdot P_{\mathbf{D}\mathbf{W}}(\text{DIF}(\epsilon, d, s_0, s, e)) \\
& = q P_{\mathbf{D}\mathbf{W}}(\text{DIF}(\epsilon, d, s_0, s, e)) - q P_{\mathbf{D}\mathbf{W}}(\text{sep}(e), \text{DIF}(\epsilon, d, s_0, s, e)) \\
& \geq q P_{\mathbf{D}\mathbf{W}}(\text{DIF}(\epsilon, d, s_0, s, e)) - q P_{\mathbf{D}\mathbf{W}}(\text{sep}(e)). \tag{B6}
\end{aligned}$$

Combining (B5) and (B6) gives us

$$P_{\mathbf{D}\mathbf{W}}(\text{DIF}(m\epsilon, d+1, s_0, T^*, e)) \geq q P_{\mathbf{D}\mathbf{W}}(\text{DIF}(\epsilon, d, s_0, s, e)) - q P_{\mathbf{D}\mathbf{W}}(\text{sep}(e)),$$

which completes the proof.  $\square$

Inducting from  $d = 1$  in the above lemma, we obtain the following corollary:

**Corollary B.1.1.** *For some  $\epsilon \in (0, mb]$ , and time  $s_0 \geq 0$ , there exists a sequence of times  $s_0 = T_0 \leq T_1 \leq T_2 \leq \dots \leq T_N$  such that, for any  $0 < d \leq N$*

$$P_{\mathbf{D}\mathbf{W}}(\text{DIF}(m^{d-1}\epsilon, d, s_0, T_d, e) | \text{DIF}(\epsilon, 1, s_0, s_0, e)) \geq \left( \frac{1}{2|E|^{v+1}} \right)^{d-1} \prod_{k=1}^{d-1} P_{\mathbf{D}\mathbf{W}}(\text{conn}(e) | \text{DIF}(m^{k-1}\epsilon, k, s_0, T_k, e)),$$

where

$$v := \left\lceil \frac{\ln b}{\ln(1-\mu)} \right\rceil.$$

Further,

$$P_{\mathbf{D}\mathbf{W}}(\text{DIF}(m^{d-1}\epsilon, d, T_{d-1}, T_d, e)) \geq q^{d-1} P_{\mathbf{D}\mathbf{W}}(\text{DIF}(\epsilon, 1, s_0, s_0, e)) - P_{\mathbf{D}\mathbf{W}}(\text{sep}(e)) \left( \frac{q^d - q}{q - 1} \right).$$

Now, define  $\gamma_d(\delta, p) := q^{d-1}\delta - p \left( \frac{q^d - q}{q-1} \right)$ . This will be a useful function to keep track of in the subsequent analysis. Notably, the last line of Corollary B.1.1 becomes

$$P_{\mathbf{D}\mathbf{W}}(\text{DIF}(m^{d-1}\epsilon, d, s_0, T_d, e)) \geq \gamma_d(P_{\mathbf{D}\mathbf{W}}(\text{DIF}(\epsilon, 1, s_0, s_0, e)), P_{\mathbf{D}\mathbf{W}}(\text{sep}(e))).$$

Notice that, for a fixed choice of  $\delta > 0$ ,  $\lim_{p \rightarrow 0} \gamma_d(\delta, p) = q^{d-1}\delta$ . In addition,  $\gamma_d(\delta, p)$  is an increasing function in  $\delta$  and a decreasing function in  $p$ . Choosing  $p$  sufficiently close to 0 gives us the following observation:

**Observation B.1.** *Fix some  $d \in \{1, \dots, N\}$ . For any  $\delta > 0$ , there exists a  $p_\delta > 0$  such that, for any  $(\delta', p') \in [\delta, \infty) \times [0, p_\delta]$  we have  $\gamma_d(\delta', p') > q^{N-1}\delta/2$ .*

We now prove a result that is, at first, disconnected from the previous results in this appendix. However, it is a key component in the proofs of Lemma IV.7 and Lemma IV.9. Intuitively, the following lemma's goal is to allow us to reduce our study of stability to 2 cases: when  $\text{sep}(e)$  is extremely likely, and when  $\text{conn}(e)$  is extremely likely ..

**Lemma B.2.** *Suppose that  $P_{\mathbf{D}\mathbf{W}}(\text{conn}(e)) > 0$  and  $P_{\mathbf{D}\mathbf{W}}(\text{sep}(e)) > 0$ . At a time step  $t$ , denote by  $A_t$  the set of edge sequences of length  $t$ , or in other words*

$$A_t := \{ \{e_{t'}\}_{t'=0}^{t-1} | e_{t'} \in E \}.$$

Then for any  $q > 0$ , there exists a time  $t_q \geq 1$  and a partition  $\{B_{t_q}, F_{t_q}\}$  of  $A_{t_q}$  such that the following are true:

- $P_{\mathbf{D}\mathbf{W}}(\text{conn}(e) | \text{same}(B_{t_q}, t_q, e)) > 1 - q$ ,
- $P_{\mathbf{D}\mathbf{W}}(\text{same}(B_{t_q}, t_q, e) | \text{conn}(e)) > 1 - q$ ,
- $P_{\mathbf{D}\mathbf{W}}(\text{sep}(e, t_q) | \text{same}(F_{t_q}, t_q, e)) > 1 - q$ , and
- $P_{\mathbf{D}\mathbf{W}}(\text{same}(F_{t_q}, t_q, e) | \text{sep}(e)) > 1 - q$ .

*Proof.* Notice that if  $t'_1 \leq t_1$  and  $t_2 \leq t'_2$  then  $\text{sep}(e, t'_1, t'_2) \Rightarrow \text{sep}(e, t_1, t_2)$ . In addition,  $\text{sep}(e, t_1, \infty) = \text{sep}(e, t_1)$ . In particular, we observe that, for a fixed  $t_1$ , the sequence of events  $\{\text{sep}(e, t_1, t_2)\}_{t_2 > t_1}$  is decreasing, and the conjunction of every event in the sequence is equal to  $\text{sep}(e, t_1)$ .

Now, let  $r > 0$  be given such that  $r < P_{\mathbf{D}\mathbf{W}}(\text{sep}(e))$ . By the lower continuity of measure, there exists a  $t_1 \geq 0$  such that  $P_{\mathbf{D}\mathbf{W}}(\text{sep}(e)) - P_{\mathbf{D}\mathbf{W}}(\text{sep}(e, t_1)) < r/2$ . Additionally, by the upper continuity of finite measures, there exists a  $t_2 > t_1$  such that  $P_{\mathbf{D}\mathbf{W}}(\text{sep}(e, t_1, t_2)) - P_{\mathbf{D}\mathbf{W}}(\text{sep}(e, t_1)) < r/2$ . Notably, we have that  $P_{\mathbf{D}\mathbf{W}}(\text{sep}(e, t_1)) > P_{\mathbf{D}\mathbf{W}}(\text{sep}(e))/2 > 0$ , and in addition  $P_{\mathbf{D}\mathbf{W}}(\text{sep}(e, t_1, t_2)) \geq P_{\mathbf{D}\mathbf{W}}(\text{sep}(e, t_1)) > 0$ .

Our goal from here is to show that  $P_{\mathbf{D}\mathbf{W}}(\text{conn}(e) | \neg \text{sep}(e, t_1, t_2))$  is bounded below by a continuous function in  $r$  that tends to 1 as  $r \rightarrow 0$ . First, observe that

$$\begin{aligned} P_{\mathbf{D}\mathbf{W}}(\text{sep}(e), \text{sep}(e, t_1, t_2)) &= P_{\mathbf{D}\mathbf{W}}(\text{sep}(e), \text{sep}(e, t_1, t_2), \text{sep}(e, t_1)) + P_{\mathbf{D}\mathbf{W}}(\text{sep}(e), \text{sep}(e, t_1, t_2), \neg \text{sep}(e, t_1)) \\ &= P_{\mathbf{D}\mathbf{W}}(\text{sep}(e, t_1, t_2), \text{sep}(e, t_1)) - P_{\mathbf{D}\mathbf{W}}(\text{sep}(e, t_1, t_2), \text{sep}(e, t_1), \neg \text{sep}(e)) \\ &\quad + P_{\mathbf{D}\mathbf{W}}(\text{sep}(e), \text{sep}(e, t_1, t_2), \neg \text{sep}(e, t_1)) \\ &= P_{\mathbf{D}\mathbf{W}}(\text{sep}(e, t_1)) - P_{\mathbf{D}\mathbf{W}}(\text{sep}(e, t_1, t_2), \text{sep}(e, t_1), \neg \text{sep}(e)) \\ &\quad + P_{\mathbf{D}\mathbf{W}}(\text{sep}(e), \text{sep}(e, t_1, t_2), \neg \text{sep}(e, t_1)) \\ &\leq P_{\mathbf{D}\mathbf{W}}(\text{sep}(e, t_1)) + P_{\mathbf{D}\mathbf{W}}(\text{sep}(e, t_1, t_2), \neg \text{sep}(e, t_1)) \\ &< P_{\mathbf{D}\mathbf{W}}(\text{sep}(e)) + r/2. \end{aligned}$$

Then we have that

$$\begin{aligned} P_{\mathbf{D}\mathbf{W}}(\text{conn}(e) | \text{sep}(e, t_1, t_2)) &= P_{\mathbf{D}\mathbf{W}}(\text{conn}(e), \text{sep}(e, t_1, t_2)) / P_{\mathbf{D}\mathbf{W}}(\text{sep}(e, t_1, t_2)) \\ &= 1 - P_{\mathbf{D}\mathbf{W}}(\text{sep}(e), \text{sep}(e, t_1, t_2)) / P_{\mathbf{D}\mathbf{W}}(\text{sep}(e, t_1, t_2)) \\ &> 1 - (P_{\mathbf{D}\mathbf{W}}(\text{sep}(e)) + r/2) / P_{\mathbf{D}\mathbf{W}}(\text{sep}(e, t_1)) \\ &> 1 - (P_{\mathbf{D}\mathbf{W}}(\text{sep}(e)) + r/2) / P_{\mathbf{D}\mathbf{W}}(\text{sep}(e) - r/2). \end{aligned}$$

In addition,

$$\begin{aligned}
P_{\mathbf{D}\mathbf{W}}(\text{conn}(e)|\neg\text{sep}(e, t_1, t_2)) &= P_{\mathbf{D}\mathbf{W}}(\text{conn}(e), \neg\text{sep}(e, t_1, t_2))/P_{\mathbf{D}\mathbf{W}}(\neg\text{sep}(e, t_1, t_2)) \\
&= (P_{\mathbf{D}\mathbf{W}}(\text{conn}(e)) - P_{\mathbf{D}\mathbf{W}}(\text{conn}(e), \text{sep}(e, t_1, t_2)))/P_{\mathbf{D}\mathbf{W}}(\neg\text{sep}(e, t_1, t_2)) \\
&> \frac{P_{\mathbf{D}\mathbf{W}}(\text{conn}(e)) - P_{\mathbf{D}\mathbf{W}}(\text{sep}(e, t_1, t_2))(1 - (P_{\mathbf{D}\mathbf{W}}(\text{sep}(e)) + r/2)/P_{\mathbf{D}\mathbf{W}}(\text{sep}(e) - r/2))}{1 - P_{\mathbf{D}\mathbf{W}}(\text{sep}(e, t_1, t_2))} \\
&= 1 - \frac{P_{\mathbf{D}\mathbf{W}}(\text{sep}(e)) + r/2}{P_{\mathbf{D}\mathbf{W}}(\text{sep}(e) - r/2)} + \frac{P_{\mathbf{D}\mathbf{W}}(\text{conn}(e)) - 1 + (P_{\mathbf{D}\mathbf{W}}(\text{sep}(e)) + r/2)/P_{\mathbf{D}\mathbf{W}}(\text{sep}(e) - r/2)}{1 - P_{\mathbf{D}\mathbf{W}}(\text{sep}(e, t_1, t_2))} \\
&> 1 - \frac{P_{\mathbf{D}\mathbf{W}}(\text{sep}(e)) + r/2}{P_{\mathbf{D}\mathbf{W}}(\text{sep}(e) - r/2)} + \frac{P_{\mathbf{D}\mathbf{W}}(\text{conn}(e)) - 1 + (P_{\mathbf{D}\mathbf{W}}(\text{sep}(e)) + r/2)/P_{\mathbf{D}\mathbf{W}}(\text{sep}(e) - r/2)}{1 - P_{\mathbf{D}\mathbf{W}}(\text{sep}(e)) + r/2}.
\end{aligned}$$

The right hand side of the final line is a continuous function in  $r$  when  $r \in [0, \infty)$ . In addition, when  $r = 0$ , the right hand side is equal to 1. Thus, as  $r \rightarrow 0$ ,  $P_{\mathbf{D}\mathbf{W}}(\text{conn}(e)|\neg\text{sep}(e, t_1, t_2)) \rightarrow 1$ . Second, notice that

$$\begin{aligned}
P_{\mathbf{D}\mathbf{W}}(\text{sep}(e), \text{sep}(e, t_1, t_2)) &= P_{\mathbf{D}\mathbf{W}}(\text{sep}(e), \text{sep}(e, t_1, t_2), \text{sep}(e, t_1)) + P_{\mathbf{D}\mathbf{W}}(\text{sep}(e), \text{sep}(e, t_1, t_2), \neg\text{sep}(e, t_1)) \\
&= P_{\mathbf{D}\mathbf{W}}(\text{sep}(e, t_1, t_2), \text{sep}(e, t_1)) + P_{\mathbf{D}\mathbf{W}}(\text{sep}(e), \text{sep}(e, t_1, t_2), \neg\text{sep}(e, t_1)) \\
&= P_{\mathbf{D}\mathbf{W}}(\text{sep}(e, t_1)) - P_{\mathbf{D}\mathbf{W}}(\text{sep}(e, t_1, t_2), \text{sep}(e, t_1), \neg\text{sep}(e)) \\
&\quad + P_{\mathbf{D}\mathbf{W}}(\text{sep}(e), \text{sep}(e, t_1, t_2), \neg\text{sep}(e, t_1)) \\
&\geq P_{\mathbf{D}\mathbf{W}}(\text{sep}(e, t_1)) - P_{\mathbf{D}\mathbf{W}}(\text{sep}(e, t_1), \neg\text{sep}(e)) \\
&> P_{\mathbf{D}\mathbf{W}}(\text{sep}(e)) - r/2.
\end{aligned}$$

Therefore,

$$\begin{aligned}
P_{\mathbf{D}\mathbf{W}}(\text{sep}(e, t_1, t_2)|\text{conn}(e)) &= P_{\mathbf{D}\mathbf{W}}(\text{conn}(e), \text{sep}(e, t_1, t_2))/P_{\mathbf{D}\mathbf{W}}(\text{conn}(e)) \\
&= P_{\mathbf{D}\mathbf{W}}(\text{sep}(e, t_1, t_2))/P_{\mathbf{D}\mathbf{W}}(\text{conn}(e)) - P_{\mathbf{D}\mathbf{W}}(\text{sep}(e), \text{sep}(e, t_1, t_2))/P_{\mathbf{D}\mathbf{W}}(\text{conn}(e)) \\
&< (P_{\mathbf{D}\mathbf{W}}(\text{sep}(e)) + r/2)/P_{\mathbf{D}\mathbf{W}}(\text{conn}(e)) - (P_{\mathbf{D}\mathbf{W}}(\text{sep}(e)) - r/2)/P_{\mathbf{D}\mathbf{W}}(\text{conn}(e)) \\
&= r/P_{\mathbf{D}\mathbf{W}}(\text{conn}(e)).
\end{aligned}$$

In addition,

$$\begin{aligned}
P_{\mathbf{D}\mathbf{W}}(\neg\text{sep}(e, t_1, t_2)|\text{conn}(e)) &= 1 - P_{\mathbf{D}\mathbf{W}}(\text{sep}(e, t_1, t_2)|\text{conn}(e)) \\
&> 1 - r/P_{\mathbf{D}\mathbf{W}}(\text{conn}(e)).
\end{aligned}$$

Observe that the right hand side of the final line is continuous for  $r \in [0, \infty)$ . In addition, when  $r = 0$ , the right hand side equals 1. Thus, as  $r \rightarrow 0$ ,  $P_{\mathbf{D}\mathbf{W}}(\text{conn}(e)|\neg\text{sep}(e, t_1, t_2)) \rightarrow 1$ . Third, notice that

$$\begin{aligned}
P_{\mathbf{D}\mathbf{W}}(\text{sep}(e, t_2)|\text{sep}(e, t_1, t_2)) &= \frac{P_{\mathbf{D}\mathbf{W}}(\text{sep}(e, t_2), \text{sep}(e, t_1, t_2))}{P_{\mathbf{D}\mathbf{W}}(\text{sep}(e, t_1, t_2))} \\
&= \frac{P_{\mathbf{D}\mathbf{W}}(\text{sep}(e, t_1))}{P_{\mathbf{D}\mathbf{W}}(\text{sep}(e, t_1, t_2))} \\
&> \frac{P_{\mathbf{D}\mathbf{W}}(\text{sep}(e)) - r/2}{P_{\mathbf{D}\mathbf{W}}(\text{sep}(e)) + r/2}.
\end{aligned}$$

Observe that the right hand side of the final line is continuous for  $r \in [0, 2 \cdot P_{\mathbf{D}\mathbf{W}}(\text{sep}(e))]$ . In addition, when  $r = 0$ , the right hand side equals 1. Thus, as  $r \rightarrow 0$ ,  $P_{\mathbf{D}\mathbf{W}}(\text{sep}(e, t_2)|\text{sep}(e, t_1, t_2)) \rightarrow 1$ . Fourth, observe that

$$\begin{aligned}
P_{\mathbf{D}\mathbf{W}}(\text{sep}(e, t_1, t_2)|\text{sep}(e)) &= \frac{P_{\mathbf{D}\mathbf{W}}(\text{sep}(e), \text{sep}(e, t_1, t_2))}{P_{\mathbf{D}\mathbf{W}}(\text{sep}(e))} \\
&> \frac{P_{\mathbf{D}\mathbf{W}}(\text{sep}(e)) - r/2}{P_{\mathbf{D}\mathbf{W}}(\text{sep}(e))}.
\end{aligned}$$

Observe that the right hand side of the final line is continuous for  $r \in [0, \infty)$ . In addition, when  $r = 0$ , the right hand side equals 1. Thus, as  $r \rightarrow 0$ ,  $P_{\mathbf{D}\mathbf{W}}(\text{sep}(e)|\text{sep}(e, t_1, t_2)) \rightarrow 1$ . Thus, there exists some  $r$  and corresponding  $t_1, t_2$  such that the following statements are true:

- $P_{\mathbf{DW}}(\text{conn}(e) | \neg \text{sep}(e, t_1, t_2)) > 1 - q$ ,
- $P_{\mathbf{DW}}(\neg \text{sep}(e, t_1, t_2) | \text{conn}(e)) > 1 - q$ ,
- $P_{\mathbf{DW}}(\text{sep}(e, t_2) | \text{sep}(e, t_1, t_2)) > 1 - q$ , and
- $P_{\mathbf{DW}}(\text{sep}(e, t_1, t_2) | \text{sep}(e)) > 1 - q$ .

Then define  $t_q := t_2$  and define  $B_{t_q}$  as the set of edge sequences  $\{f_t\}_{t=0}^{t_2-1}$  which satisfy  $\neg \text{sep}(f, t_1, t_2)$ . Then  $\text{same}(B_{t_q}, t_q, e) \Leftrightarrow \neg \text{sep}(e, t_1, t_2)$ . Additionally, define  $F_{t_q} := A_{t_q} \setminus B_{t_q}$ , so that  $A_{t_q}$  is partitioned by  $\{B_{t_q}, F_{t_q}\}$ . Observe that, since  $\text{same}(B_{t_q}, t_q, e) \Leftrightarrow \neg \text{sep}(e, t_1, t_2)$ , we have  $\text{same}(C_{t_q}, t_q, e) \Leftrightarrow \text{sep}(e, t_1, t_2)$ . Thus, the following are all true:

- $P_{\mathbf{DW}}(\text{conn}(e) | \text{same}(B_{t_q}, t_q, e)) > 1 - q$ ,
- $P_{\mathbf{DW}}(\text{same}(B_{t_q}, t_q, e) | \text{conn}(e)) > 1 - q$ ,
- $P_{\mathbf{DW}}(\text{sep}(e, t_q) | \text{same}(F_{t_q}, t_q, e)) > 1 - q$ , and
- $P_{\mathbf{DW}}(\text{same}(F_{t_q}, t_q, e) | \text{sep}(e)) > 1 - q$ .

This completes the proof.  $\square$

We are now ready to prove Lemma IV.7, which we first restate here:

**Lemma B.3.** *For a finite choice of possible initial opinions  $\mathbf{x}(0)$ , and a fixed  $\epsilon > 0$ , suppose  $P_{\mathbf{DW}}(\text{conn}(e)) > 0$  and that for all  $t \geq 0$ ,  $P_{\mathbf{DW}}(x_{\max}(t) - x_{\min}(t) \geq \epsilon | \text{conn}(e)) \geq \delta > 0$ . Then there exists some  $T \geq 0$  such that*

$$\mathbb{E}_{\mathbf{DW}}[x_{\min}(T)] > \mathbb{E}_{\mathbf{DW}}[x_{\min}(0)] + \frac{1}{8}(mq)^{N-1}\epsilon\delta \cdot P_{\mathbf{DW}}(\text{conn}(e)).$$

*Proof.* For  $r > 0$ , let  $T(r)$  denote a time where, according to Lemma B.2, we can partition  $A_{T(r)}$  into  $\{B_{T(r)}, F_{T(r)}\}$  such that

$$P_{\mathbf{DW}}(\text{conn}(e) | \text{same}(B_{T(r)}, T(r), e)) > 1 - r$$

and

$$P_{\mathbf{DW}}(\text{same}(B_{T(r)}, T(r), e) | \text{conn}(e)) > 1 - r.$$

For brevity, we will write the event  $\text{same}(B_{T(r)}, T(r), e)$  as  $B_{T(r)}$  in the rest of this proof.

Now, we restrict our attention to the event space given by  $B_{T(r)}$ . Notice that each edge in the sequence  $\{e_t\}_{t=T(r)}^{\infty} | B_{T(r)}$  is distributed uniformly across  $E$ . In addition,  $\{\mathbf{x}(t)\}_{t=T(r)}^{\infty} | B_{T(r)}$  is determined by  $\{e_t\}_{t=T(r)}^{\infty} | B_{T(r)}$  in accordance with the update rules in Definition III.1. Hence,

$$(\{\mathbf{x}(t)\}_{t=T(r)}^{\infty} | B_{T(r)}, \{e_t\}_{t=T(r)}^{\infty} | B_{T(r)}, G, c, \mu)$$

is an adaptive-confidence DW model. We denote this model by  $\mathbf{DW}_1$ . Observe that

$$\text{DIF}(\epsilon, 1, t, t, e) \Leftrightarrow x_{\max}(t) - x_{\min}(t) \geq \epsilon,$$

so  $P_{\mathbf{DW}}(\text{DIF}(\epsilon, 1, t, t, e) | \text{conn}(e)) \geq \delta$  for all  $t \geq 0$ . Next, we have that for all  $t \geq 0$ ,

$$\begin{aligned} P_{\mathbf{DW}_1}(\text{DIF}(\epsilon, 1, t, t, e) | \text{conn}(e)) &:= P_{\mathbf{DW}}(\text{DIF}(\epsilon, 1, t + T(r), t + T(r), e) | \text{conn}(e), B_{T(r)}) \\ &\geq P_{\mathbf{DW}}(\text{DIF}(\epsilon, 1, t + T(r), t + T(r), e), B_{T(r)} | \text{conn}(e)) \\ &\geq P_{\mathbf{DW}}(\text{DIF}(\epsilon, 1, t + T(r), t + T(r), e) | \text{conn}(e)) + P_{\mathbf{DW}}(B_{T(r)} | \text{conn}(e)) - 1 \\ &> \delta - r. \end{aligned}$$

Additionally, by construction, we have  $P_{\mathbf{DW}_1}(\text{conn}(e)) > 1 - r$ . so combining the above 2 statements we obtain

$$\begin{aligned} P_{\mathbf{DW}_1}(\text{DIF}(\epsilon, 1, t, t, e)) &= P_{\mathbf{DW}_1}(\text{DIF}(\epsilon, 1, t, t, e) | \text{conn}(e)) \times P_{\mathbf{DW}_1}(\text{conn}(e)) \\ &> (\delta - r)(1 - r). \end{aligned}$$

Recall from Observation B.1 that there exists a  $p_{\delta/2} > 0$  such that, for any  $(\delta', p') \in [\delta/2, \infty) \times [0, p_{\delta/2}]$ ,  $\gamma(\delta', p') \geq q^{N-1}(\delta/2)/2$ . Now fix some  $r \leq \min\{p_{\delta/2}, 1/2\}$  such that  $(\delta - r_0)(1 - r_0) \geq \delta/2$ . Since  $r_0 < p_{\delta/2}$ , we know

$$P_{\mathbf{DW}_1}(\text{sep}) = 1 - P_{\mathbf{DW}_1}(\text{conn}(e)) < r_0 \leq p_{\delta/2}.$$

Since  $(\delta - r_0)(1 - r_0) \geq \delta/2$  we also know that  $P_{\mathbf{DW}_1}(\text{DIF}(\epsilon, 1, t, t, e)) \geq \delta/2$  for all  $t \geq 0$ . Then we conclude

$$(P_{\mathbf{DW}_1}(\text{DIF}(\epsilon, 1, 0, 0, e)), P_{\mathbf{DW}_1}(\text{sep}(e))) \in [\delta/2, \infty) \times [0, p_{\delta/2}],$$

and by corollary B.1.1, there is a time  $T_N \geq 0$  such that

$$P_{\mathbf{DW}_1}(\text{DIF}(m^{N-1}\epsilon, N, 0, T_N, e)) \geq \gamma_N(P_{\mathbf{DW}_1}(\text{DIF}(\epsilon, 1, 0, 0, e)), P_{\mathbf{DW}_1}(\text{sep}(e))).$$

This implies that

$$P_{\mathbf{DW}_1}(\text{DIF}(m^{N-1}\epsilon, N, 0, T_N, e)) \geq \frac{1}{4}q^{N-1}\delta.$$

Observe that if  $\text{DIF}(m^{N-1}\epsilon, N, 0, T_N, e)$  is true then every node  $i$  satisfies  $x_i(T_N) \geq x_{\min}(0) + m^{N-1}\epsilon$ . Therefore if  $\text{DIF}(m^{N-1}\epsilon, N, 0, T_N, e)$  is true then  $x_{\min}(T_N) \geq x_{\min}(0) + m^{N-1}\epsilon$ . Thus,

$$P_{\mathbf{DW}_1}(x_{\min}(T_N) \geq x_{\min}(0) + m^{N-1}\epsilon) \geq \frac{1}{4}q^{N-1}\delta.$$

Recall that in all cases,  $x_{\min}(T_N) \geq x_{\min}(0)$ . Now, taking expectation, we have that

$$\begin{aligned} \mathbb{E}_{\mathbf{DW}_1}(x_{\min}(T_N)) &= \mathbb{E}_{\mathbf{DW}_1}(x_{\min}(T_N) | x_{\min}(T_N) \geq x_{\min}(0) + m^{N-1}\epsilon) \times P_{\mathbf{DW}_1}(x_{\min}(T_N) \geq x_{\min}(0) + m^{N-1}\epsilon) \\ &\quad + \mathbb{E}_{\mathbf{DW}_1}(x_{\min}(T_N) | \neg x_{\min}(T_N) \geq x_{\min}(0) + m^{N-1}\epsilon) \times P_{\mathbf{DW}_1}(\neg x_{\min}(T_N) \geq x_{\min}(0) + m^{N-1}\epsilon) \\ &\geq (\mathbb{E}_{\mathbf{DW}_1}(x_{\min}(0)) + m^{N-1}\epsilon) \times P_{\mathbf{DW}_1}(x_{\min}(T_N) \geq x_{\min}(0) + m^{N-1}\epsilon) \\ &\quad + \mathbb{E}_{\mathbf{DW}_1}(x_{\min}(0)) \times P_{\mathbf{DW}_1}(\neg x_{\min}(T_N) \geq x_{\min}(0) + m^{N-1}\epsilon) \\ &= \mathbb{E}_{\mathbf{DW}_1}(x_{\min}(0)) + m^{N-1}\epsilon \cdot P_{\mathbf{DW}_1}(x_{\min}(T_N) \geq x_{\min}(0) + m^{N-1}\epsilon) \\ &\geq \mathbb{E}_{\mathbf{DW}_1}(x_{\min}(0)) + \frac{1}{4}(mq)^{N-1}\epsilon\delta. \end{aligned}$$

Equivalently, the above statement reads as  $\mathbb{E}_{\mathbf{DW}}(x_{\min}(T_N) | B_{T(r)}) \geq \mathbb{E}_{\mathbf{DW}}(x_{\min}(0) | B_{T(r)}) + \frac{1}{4}(mq)^{N-1}\epsilon\delta$ . Now, taking expectation in  $\mathbf{DW}$ , we get

$$\begin{aligned} \mathbb{E}_{\mathbf{DW}}(x_{\min}(T_N)) &= \mathbb{E}_{\mathbf{DW}}(x_{\min}(T_N) | B_{T(r)})P_{\mathbf{DW}}(B_{T(r)}) + \mathbb{E}_{\mathbf{DW}}(x_{\min}(T_N) | \neg B_{T(r)})P_{\mathbf{DW}}(\neg B_{T(r)}) \\ &\geq (\mathbb{E}_{\mathbf{DW}}(x_{\min}(0) | B_{T(r)}) + \frac{1}{4}(mq)^{N-1}\epsilon\delta)P_{\mathbf{DW}}(B_{T(r)}) + \mathbb{E}_{\mathbf{DW}}(x_{\min}(0) | \neg B_{T(r)})P_{\mathbf{DW}}(\neg B_{T(r)}) \\ &= \mathbb{E}_{\mathbf{DW}}(x_{\min}(0)) + \frac{1}{4}(mq)^{N-1}\epsilon\delta \cdot P_{\mathbf{DW}}(B_{T(r)}). \end{aligned}$$

Now we will compute a lower bound on  $P_{\mathbf{DW}}(B_{T(r)})$ :

$$\begin{aligned} P_{\mathbf{DW}}(B_{T(r)}) &\geq P_{\mathbf{DW}}(B_{T(r)}, \text{conn}(e)) = P_{\mathbf{DW}}(B_{T(r)} | \text{conn}(e)) \times P_{\mathbf{DW}}(\text{conn}(e)) \\ &> (1 - r)P_{\mathbf{DW}}(\text{conn}(e)) \\ &\geq \frac{1}{2}P_{\mathbf{DW}}(\text{conn}(e)), \end{aligned}$$

where the last step is true because  $r \leq 1/2$  by construction. Finally, we may conclude

$$\begin{aligned} \mathbb{E}_{\mathbf{DW}}(x_{\min}(T_N)) &\geq \mathbb{E}_{\mathbf{DW}}(x_{\min}(0)) + \frac{1}{4}(mq)^{N-1}\epsilon\delta \cdot (\frac{1}{2}P_{\mathbf{DW}}(\text{conn}(e))) \\ &= \mathbb{E}_{\mathbf{DW}}(x_{\min}(0)) + \frac{1}{8}(mq)^{N-1}\epsilon\delta \cdot P_{\mathbf{DW}}(\text{conn}(e)), \end{aligned}$$

as desired.  $\square$

We are almost ready to prove Lemma IV.9, but we first make the following observation:

**Observation B.2.** *We have that  $\text{sep}(e, t) = \bigvee_{S \subset V, S \neq \emptyset} \text{sep}_S(e, t)$ .*

*Proof.* By definition,  $G_{\text{obs}}(t) \cap G_{\text{pos}}(t)$  is not weakly connected if and only if there exists some nonempty proper subset  $S$  of  $V$  for which  $G_{\text{obs}}(t) \cap G_{\text{pos}}(t)$  does not contain any edges in  $S \times (V \setminus S) \cup (V \setminus S) \times S$ . Thus,  $\text{sep}(e, t) = \bigvee_{S \subset V, S \neq \emptyset} \text{sep}_S(e, t)$ .  $\square$

We are now ready to prove Lemma IV.9. We first restate the Lemma here as B.4, and then show the proof.

**Lemma B.4.** *Let  $n_0$  be some positive integer. Suppose that any model of the form in Definition III.1, with  $N < n_0$ , converges to a limit state almost surely. Then for any model of the form in Definition III.1 with  $N = n_0$ , we further have  $P_{\text{DW}}(\text{stab}, \text{sep}) = P_{\text{DW}}(\text{sep})$ .*

*Proof.* Suppose that  $P_{\text{DW}}(\text{sep}) = 0$ . Then  $P_{\text{DW}}(\text{stab}, \text{sep}) = 0 = P_{\text{DW}}(\text{sep})$  and we have our result.

Otherwise, we have  $P_{\text{DW}}(\text{sep}) > 0$ . Let  $q \in (0, 1)$  given. We will show  $P_{\text{DW}}(\text{stab}|\text{sep}) > 1 - q$ . By Lemma B.2, there exists a time  $t_q \geq 0$  and a subset  $C_{t_q}$  of  $A_{t_q}$  such that

$$P_{\text{DW}}(\text{sep}(e, t_q) | \text{same}(C_{t_q}, t_q, e)) > 1 - q, \quad (\text{B7})$$

and

$$P_{\text{DW}}(\text{same}(C_{t_q}, t_q, e) | \text{sep}) > 1 - q. \quad (\text{B8})$$

Now let  $e$  be an edge sequence that satisfies  $\text{same}(C_{t_q}, t_q, e)$ . In addition, let  $S$  be a nonempty and proper subset of  $V$ . Let  $G_S$  denote the induced subgraph of  $G$  corresponding to  $S$ . In other words,  $G_S := (S, S^2 \cap E)$ . Let  $l_S \in \mathbb{Z}_{\geq 0} \cup \infty$  denote the number of times  $t \geq t_q$  such that  $e_t \in S^2$ . In particular,  $P_{\text{DW}}(l_S = \infty | \text{same}(C_{t_q}, t_q, e)) = 1$  because each edge independently lies in  $S^2$  with some fixed nonzero probability. Let  $e_S$  denote the subsequence of  $\{e_t\}_{t=t_q}^{\infty}$  only containing edges in  $S^2$ , and let  $\{t_l\}_{l=1}^{l_S}$ . Denote by  $\text{DW}_S$  the adaptive-confidence DW model on  $G_S$  with initial opinion distribution  $\mathbf{x}(t_q) | \text{same}(C_{t_q}, t_q, e)$  and edge choice  $e$ . In other words,

$$\text{DW}_S = (G_S, c, \mu, \mathbf{x}(t_q) | \text{same}(C_{t_q}, t_q, e), e_S).$$

In what follows, we will refer to both the opinions in  $\text{DW}_S$  and  $\text{DW}$ . For clarity, we denote  $\mathbf{x}^{\text{DW}}(t)$  as the opinion vector at time  $t$  in  $\text{DW}$ , and denote  $\mathbf{x}^{\text{DW}_S}(t)$  as the opinion vector at time  $t$  in  $\text{DW}_S$ .

Now suppose that  $\text{sep}_S(e, t_q)$  is true for  $\text{DW}$ , so the opinions of nodes in  $S$  only change in  $\text{DW}$  at time  $t_l$  for  $0 \leq l \leq l_S$ . In particular, for any  $t \geq t_q$  we get that  $\mathbf{x}_S^{\text{DW}}(t) = \mathbf{x}_S^{\text{DW}}(t_l)$  for some  $0 \leq l \leq l_S$ . In addition, the sequence  $\{\mathbf{x}_S^{\text{DW}}(t_l)\}_{l=0}^{\infty}$  is equal to  $\{\mathbf{x}^{\text{DW}_S}(t)\}_{t=0}^{\infty}$ ; this is because  $\mathbf{x}_S^{\text{DW}}(t_{l+1})$  is obtained from  $\mathbf{x}_S^{\text{DW}}(t_l - 1) = \mathbf{x}_S^{\text{DW}}(t_l)$  by updating opinions along edge  $e_{t_l}$ .

We know that  $\text{DW}_S$  has a limit state with probability 1. This is because  $S$  is a proper subset of  $V$ , so the number of nodes in  $G_S$  is strictly less than in  $G$  and we may apply our initial assumptions from the Lemma statement. Thus,  $\{\mathbf{x}^{\text{DW}_S}(t)\}_{t=0}^{\infty}$  has a limit, so  $\{\mathbf{x}_S^{\text{DW}}(t_l)\}_{l=0}^{\infty}$  has a limit. Finally, this implies  $\{\mathbf{x}_S^{\text{DW}}(t)\}_{t=0}^{\infty}$  has a limit.

In summary,  $\{\mathbf{x}_S^{\text{DW}}(t)\}_{t=0}^{\infty}$  has a limit with probability 1 if  $\text{same}(C_{t_q}, t_q, e)$ ,  $\text{sep}_S(e, t_q)$ , and  $l_S = \infty$  all hold. This implies that

$$\begin{aligned} & P_{\text{DW}}(\lim_{t \rightarrow \infty} \mathbf{x}_S^{\text{DW}}(t) \text{ exists}, \text{sep}_S(e, t_q) | \text{same}(C_{t_q}, t_q, e), l_S = \infty) \\ &= P_{\text{DW}}(\text{sep}_S(e, t_q) | \text{same}(C_{t_q}, t_q, e), l_S = \infty) \times P_{\text{DW}}(\lim_{t \rightarrow \infty} \mathbf{x}_S^{\text{DW}}(t) \text{ exists} | \text{sep}_S(e, t_q), \text{same}(C_{t_q}, t_q, e), l_S = \infty) \\ &= P_{\text{DW}}(\text{sep}_S(e, t_q) | \text{same}(C_{t_q}, t_q, e), l_S = \infty). \end{aligned} \quad (\text{B9})$$

Using this, we are able to obtain the following result:

$$\begin{aligned} & P_{\text{DW}}(\lim_{t \rightarrow \infty} \mathbf{x}_S^{\text{DW}}(t) \text{ exists}, \text{sep}_S(e, t_q) | \text{same}(C_{t_q}, t_q, e)) \\ & \geq P_{\text{DW}}(l_S = \infty, \lim_{t \rightarrow \infty} \mathbf{x}_S^{\text{DW}}(t) \text{ exists}, \text{sep}_S(e, t_q) | \text{same}(C_{t_q}, t_q, e)) \\ &= P_{\text{DW}}(\lim_{t \rightarrow \infty} \mathbf{x}_S^{\text{DW}}(t) \text{ exists}, \text{sep}_S(e, t_q) | \text{same}(C_{t_q}, t_q, e), l_S = \infty) \times P_{\text{DW}}(l_S = \infty | \text{same}(C_{t_q}, t_q, e)) \\ &= P_{\text{DW}}(\text{sep}_S(e, t_q) | \text{same}(C_{t_q}, t_q, e), l_S = \infty) \times P_{\text{DW}}(l_S = \infty | \text{same}(C_{t_q}, t_q, e)) \\ &= P_{\text{DW}}(\text{sep}_S(e, t_q), l_S = \infty | \text{same}(C_{t_q}, t_q, e)) \quad \text{by (B9)} \\ &= P_{\text{DW}}(\text{sep}_S(e, t_q) | \text{same}(C_{t_q}, t_q, e)) \end{aligned} \quad (\text{B10})$$

where the last step comes from the fact that  $P_{\mathbf{DW}}(l_S = \infty | \text{same}(C_{t_q}, t_q, e)) = 1$ .

Additionally, by applying the above logic to  $V \setminus S$ , which is also a nonempty and proper subset of  $V$ , we obtain

$$P_{\mathbf{DW}}(\lim_{t \rightarrow \infty} \mathbf{x}_{V \setminus S}^{\mathbf{DW}}(t) \text{ exists, } \text{sep}_{V \setminus S}(e, t_q) | \text{same}(C_{t_q}, t_q, e)) = P_{\mathbf{DW}}(\text{sep}_{V \setminus S}(e, t_q) | \text{same}(C_{t_q}, t_q, e)). \quad (\text{B11})$$

Notice that  $\text{sep}_{V \setminus S}(e, t_q) \Leftrightarrow \text{sep}_S(e, t_q)$ . Therefore (B11) can be rewritten as

$$P_{\mathbf{DW}}(\lim_{t \rightarrow \infty} \mathbf{x}_{V \setminus S}^{\mathbf{DW}}(t) \text{ exists, } \text{sep}_S(e, t_q) | \text{same}(C_{t_q}, t_q, e)) = P_{\mathbf{DW}}(\text{sep}_S(e, t_q) | \text{same}(C_{t_q}, t_q, e)). \quad (\text{B12})$$

Combining (B10) and (B12), we obtain

$$P_{\mathbf{DW}}(\lim_{t \rightarrow \infty} \mathbf{x}_S^{\mathbf{DW}}(t) \text{ exists, } \lim_{t \rightarrow \infty} \mathbf{x}_{V \setminus S}^{\mathbf{DW}}(t) \text{ exists, } \text{sep}_S(e, t_q) | \text{same}(C_{t_q}, t_q, e)) = P_{\mathbf{DW}}(\text{sep}_S(e, t_q) | \text{same}(C_{t_q}, t_q, e)). \quad (\text{B13})$$

Notice that  $\lim_{t \rightarrow \infty} \mathbf{x}_S^{\mathbf{DW}}(t)$  exists and  $\lim_{t \rightarrow \infty} \mathbf{x}_{V \setminus S}^{\mathbf{DW}}(t)$  exists if and only if  $\lim_{t \rightarrow \infty} \mathbf{x}^{\mathbf{DW}}(t)$  exists, or equivalently  $\text{stab}(e)$  holds. Thus,

$$P_{\mathbf{DW}}(\text{stab}(e), \text{sep}_S(e, t_q) | \text{same}(C_{t_q}, t_q, e)) = P_{\mathbf{DW}}(\text{sep}_S(e, t_q) | \text{same}(C_{t_q}, t_q, e)). \quad (\text{B14})$$

This also implies that

$$P_{\mathbf{DW}}(\neg \text{stab}(e), \text{sep}_S(e, t_q) | \text{same}(C_{t_q}, t_q, e)) = 0. \quad (\text{B15})$$

Now recall from Observation B.2 that  $\text{sep}(e) = \bigvee_{S \subset V, S \neq \emptyset} \text{sep}_S(e)$ . Therefore

$$\begin{aligned} P_{\mathbf{DW}}(\neg \text{stab}(e), \text{sep}(e, t_q) | \text{same}(C_{t_q}, t_q, e)) &\leq \sum_{S \subset V, S \neq \emptyset} P_{\mathbf{DW}}(\neg \text{stab}(e), \text{sep}_S(e, t_q) | \text{same}(C_{t_q}, t_q, e)) \\ &= \sum_{S \subset V, S \neq \emptyset} 0 = 0. \end{aligned} \quad (\text{B16})$$

This implies that

$$P_{\mathbf{DW}}(\text{stab}(e), \text{sep}(e, t_q) | \text{same}(C_{t_q}, t_q, e)) = P_{\mathbf{DW}}(\text{sep}(e, t_q) | \text{same}(C_{t_q}, t_q, e)). \quad (\text{B17})$$

Combining (B17) and (B7), we get

$$P_{\mathbf{DW}}(\text{stab}(e), \text{sep}(e, t_q) | \text{same}(C_{t_q}, t_q, e)) > 1 - q. \quad (\text{B18})$$

Using the fact that  $\text{sep}(e, t_q)$  implies  $\text{sep}(e)$  we obtain

$$P_{\mathbf{DW}}(\text{stab}(e), \text{sep}(e) | \text{same}(C_{t_q}, t_q, e)) > 1 - q. \quad (\text{B19})$$

Finally, combining (B19) and (B8), we obtain

$$\begin{aligned} P_{\mathbf{DW}}(\text{stab}(e) | \text{sep}(e)) &\geq P_{\mathbf{DW}}(\text{stab}(e), \text{same}(C_{t_q}, t_q, e) | \text{sep}(e)) \\ &= \frac{P_{\mathbf{DW}}(\text{stab}(e), \text{same}(C_{t_q}, t_q, e), \text{sep}(e))}{P_{\mathbf{DW}}(\text{sep}(e))} \\ &= \frac{P_{\mathbf{DW}}(\text{stab}(e), \text{sep}(e) | \text{same}(C_{t_q}, t_q, e)) \times P_{\mathbf{DW}}(\text{same}(C_{t_q}, t_q, e))}{P_{\mathbf{DW}}(\text{sep}(e))} \\ &> (1 - q) \frac{P_{\mathbf{DW}}(\text{same}(C_{t_q}, t_q, e))}{P_{\mathbf{DW}}(\text{sep}(e))} \\ &\geq (1 - q) \frac{P_{\mathbf{DW}}(\text{same}(C_{t_q}, t_q, e), \text{sep}(e))}{P_{\mathbf{DW}}(\text{sep}(e))} \\ &= (1 - q) P_{\mathbf{DW}}(\text{same}(C_{t_q}, t_q, e) | \text{sep}(e)) \\ &> (1 - q)^2. \end{aligned}$$

Notably, the last step holds because  $q \in (0, 1)$  so  $1 - q > 0$ . Thus, for any  $0 < q < 1$ ,  $P_{\mathbf{DW}}(\text{stab}(e) | \text{sep}(e)) > (1 - q)^2$ . Because  $(1 - q)^2 \rightarrow 1$  as  $q \rightarrow 0$ , we conclude that  $P_{\mathbf{DW}}(\text{stab}(e) | \text{sep}(e)) \geq 1$ , so  $P_{\mathbf{DW}}(\text{stab}(e) | \text{sep}(e)) = 1$ , and  $P_{\mathbf{DW}}(\text{stab}(e), \text{sep}(e)) = P_{\mathbf{DW}}(\text{sep}(e))$ . This completes the proof.  $\square$